Beurteilung der Grundwasser-Vulnerabilität in Karstgebieten anhand 3D geologischer und numerischer Modelle

Inauguraldissertation

zur

Erlangung der Würde eines Doktors der Philosophie

vorgelegt der

Philosophisch-Naturwissenschaftlichen Fakultät

der Universität Basel

von

Christoph Butscher

aus Tettnang (Deutschland)

Basel, 2007

Genehmigt von der Philosophisch-Naturwissenschaftlichen Fakultät
auf Antrag von

Prof. Dr. Peter Huggenberger
Departement Umwelt, Abteilung Angewandte und Umweltgeologie
Universität Basel, Schweiz

Prof. Dr. Martin Sauter
Fakultät für Geowissenschaften und Geographie, Abteilung Angewandte Geologie
Universität Göttingen, Deutschland

Basel, den 11. Dezember 2007

Prof. Dr. Hans-Peter Hauri
Dekan

Inhaltsverzeichnis

Kurzfassung

Grundwasser ist eine der wichtigsten Ressourcen für die Menschheit. Karstgrundwasser spielt dabei eine bedeutende Rolle. Rund ein Viertel der Weltbevölkerung ist von Karstgrundwasser abhängig. Auch in zahlreichen Regionen der Schweiz ist Karstgrundwasser für die Trinkwasserversorgung unverzichtbar. Zunehmend wird auch die ökologische Bedeutung von Karstgrundwasser als Grundlage empfindlicher Lebensräume, wie zum Beispiel Quellen und Quellbäche, erkannt. Dabei ist Karstgrundwasser aufgrund der oftmals geringen Bodenüberdeckung, konzentrierter Infiltration und kurzer Aufenthaltszeiten im Untergrund besonders anfällig für Verschmutzungen. Deshalb sollten in dieser Dissertation die Kenntnisse über karstspezifische hydrologisch-hydrogeologische Prozesse verbessert und Methoden zur Beurteilung der Vulnerabilität (Verletzlichkeit des Grundwassers bzgl. Verschmutzung) weiterentwickelt werden. Übergeordnetes Ziel war es, zur Erhaltung oder Verbesserung der Grundwasserqualität in Karstgebieten beizutragen.

Die angewandte Methodik beinhaltet eine 3D geologische Modellierung des Untergrunds einerseits und eine numerische Simulation des Fliessgeschehens basierend auf volumetrischen Modellen („Box-Modelle") andererseits. Für die numerische Modellierung wurden zuvor hydrologische und meteorologische Daten über einen längeren Zeitraum aufgezeichnet. Basierend auf dem 3D geologischen Modell wurde ein Ansatz zur Lokalisierung von Quell- und Einzugsgebieten in Karstgebieten und zur Charakterisierung der unterirdischen Fliesspfade entwickelt („ABG approach"). Daraus ergab sich der strukturelle Rahmen für die Hydrologie des Gebiets. Gleichzeitig wurde mit Hilfe der numerischen Modelle die Reaktion einer Karstquelle auf Niederschlagsereignisse simuliert. Die Simulationen dienten der Quantifizierung der Vulnerabilität und ihrer zeitlichen Variabilität. Dabei wurden neue Kriterien zur Beurteilung der Vulnerabilität herangezogen: der Vulnerabilitätsindex VI, welcher die Beiträge von schnellen und langsamen Fliesssystemen zur Quellschüttung beschreibt, und die Vulnerabilitätskonzentration C_V, welche die Belastung des Quellwassers mit Schadstoffen repräsentiert. Neben der Beurteilung zeitlicher Aspekte der Vulnerabilität ermöglicht der Ansatz ausserdem, verschiedene Quellen in Bezug auf ihre Gefährdung quantitativ zu vergleichen. Zuletzt wurden die Ergebnisse aus der 3D geologischen Modellierung mit den Ergebnissen aus der numerischen Modellierung kombiniert und durch eine Kartierung der Vulnerabilität in Quelleinzugsgebieten ergänzt. Daraus ergaben sich als Endprodukt kombinierte Vulnerabilitätskarten und –zeitreihen.

Der vorgestellte Ansatz wurde in einem Untersuchungsgebiet des Schweizer Tafeljuras (Gempenplateau) getestet. Durch seine Anwendung konnte ein neuer Weg aufgezeigt werden, wie man zu einer nachvollziehbaren Ausscheidung von Schutzzonen gelangen kann. Dabei wurden mehrere Verbesserungen bestehender Kartiermethoden erreicht: Die räumliche Verteilung der Vulnerabilität wurde nicht nur für Einzugsgebiete, sondern auch für Quellgebiete angegeben; Die zeitliche Änderung der Vulnerabilität wurde ermittelt; Verschiedene Quellen konnten bezüglich ihrer Vulnerabilität quantitativ verglichen werden. Die Berücksichtigung zeitlicher Aspekte erweitert Strategien zum Grundwasserschutz um eine Dimension und eröffnet dadurch neue Wege beim Auftreten von Nutzungskonflikten in den Quelleinzugsgebieten. Beispielsweise können Auflagen in den Schutzzonen für die Landnutzer zu Zeiten geringer Vulnerabilität gelockert werden (Bewirtschaftungs-Management) oder das Trinkwasser kann zu Zeiten erhöhter Vulnerabilität an den Quellfassungen verworfen werden (Entnahme-Management). Die Möglichkeit, die Vulnerabilität an verschiedenen Quellen quantitativ zu vergleichen, schafft eine objektive Basis für die Regionalplanung. Zum Beispiel kann eine mögliche Aufgabe besonders gefährdeter Trinkwasserquellen neue Spielräume bei der Abwägung von Schutzmassnahmen in den Einzugsgebieten eröffnen. Ausserdem ergibt sich ein Potenzial für eine mögliche Revitalisierung von Quellen, die eine geringere Bedeutung für die Wasserversorgung haben.

Abstract

Groundwater is a major resource for mankind. Among groundwater resources, karst groundwater plays an important role. Approximately a quarter of the world's population depends on karst groundwater. Also in numerous regions of Switzerland, karst groundwater is indispensable for the drinking water supply. The ecological importance of karst groundwater as a prerequisite of sensitive habitats, like natural springs and spring brooks, is also increasingly recognized. However, karst aquifers are particularly vulnerable to contamination due to the often thin soil cover, concentrated infiltration and short groundwater residence times. Therefore, this thesis aimed at an improvement of the knowledge about karst specific hydrologic-hydrogeological processes and of methods for the evaluation of groundwater vulnerability. The super-ordinate goal was to contribute to the preservation or advancement of groundwater quality in karst areas.

The applied methodology includes a 3D geological modeling of the subsurface on the one hand, and a numeric simulation of the flow processes, based on volumetric models ("box models"), on the other hand. For the numeric modeling, hydrological and meteorological data were recorded for more than one year. Based on the 3D geological model, an approach was developed for the localization of discharge and catchment areas and for the characterization of the underground flow paths in karst areas ("ABG approach"). From this, the structural framework for the hydrology of the area was established. At the same time, the response of a karst spring to rainfall events was simulated with the help of the numerical models. The simulations served to quantify the vulnerability and its temporal variation. New criteria were established for the evaluation of the vulnerability: the vulnerability index VI, which specifies the contributions from fast and slowly circulating flow systems to the spring discharge, and the vulnerability concentration C_V, which represents a potential contaminant load of the spring water. Apart from the evaluation of temporal aspects of vulnerability, the approach additionally allows comparing different springs quantitatively with regard to their contamination risk. Finally, the results from the 3D geological modeling were combined with the results from the numerical modeling and contemplated by vulnerability mapping in the catchment areas. From this, combined vulnerability maps and time series resulted as the final product.

The proposed approach was tested at a field site situated in the Swiss Tabular Jura (Gempen plateau). Its application illustrated a new methodology how to accomplish a comprehensible and transparent delineation of protection zones. Several improvements of existing mapping methods were obtained: The spatial vulnerability distribution could be indicated not only for catchment areas but also for discharge areas, the temporal variation of vulnerability could be determined, and different springs could be quantitatively compared with regard to their vulnerability. The consideration of temporal aspects of vulnerability extends groundwater protection strategies by one dimension and facilitates differentiated solutions of problems when land use conflicts in the catchment areas occur. Restrictions for the land users in the protection zones, for instance, can be eased at times of low vulnerability (land use management) or the drinking water can be rejected at the spring captures at times of increased vulnerability (withdrawal management). The possibility of comparing the vulnerability of different springs quantitatively establishes an objective basis for regional planning. For example, an abandonment of particularly endangered springs can lead to new possibilities for regulations in the catchment areas. In addition, the presented approach encourages a potential revitalization of springs by evaluating springs that have a minor importance for drinking water supply.

Dank

Die vorliegende Arbeit entstand am Geologischen Institut der Universität Basel, Abteilung Angewandte und Umweltgeologie. Zum Gelingen haben viele beigetragen, in erster Linie jedoch mein Betreuer Prof. Peter Huggenberger. Ihm möchte ich ganz besonders danken, speziell für

- Ideen, die mir wertvolle Impulse gaben,
- Fachwissen, das er mir weitergab,
- Diskussionen, die immer hilfreich waren und
- Freiheiten, von denen ich in vielerlei Hinsicht profitiert habe.

Ebenfalls möchte ich Prof. Martin Sauter (Universität Göttingen) danken, der so freundlich war, das Koreferat dieser Arbeit zu übernehmen.

Diese Dissertation entstand im Rahmen des MGU-Projekts F/03 „Quellen – Trinkwasserspender und Lebensraum". Bedanken möchte ich mich bei Projektleiter Prof. Peter Nagel, Projektkoordinatorin Dr. Brigitte Baltes und allen weiteren Beteiligten, besonders Stefanie von Fumetti, Daniel Suter, Dr. Adrian Auckenthaler und Dr. Daniel Küry.

Meinen Kollegen von der Angewandten Geologie möchte ich ganz herzlich danken für die gute Zusammenarbeit und das Interesse an meiner Arbeit.

Bei der Durchführung der Experimente haben mir viele durch Rat und Tat geholfen. Ihnen allen ein herzliches Dankeschön, insbesondere Claude Schneider (Geologisches Institut) und den Brunnenmeistern Christian Schäublin (Frenkendorf) und Rolando Palladino (Liestal). Dem Institut für Meteorologie, Klimatologie und Fernerkundung der Universität Basel, insbesondere Dr. Roland Vogt, danke ich für die Bereitstellung von Klimadaten.

Mein Dank gilt auch

- Programm MGU (Mensch Gesellschaft Umwelt) der Universität Basel für die Finanzierung des „Quellen-Projekts",
- dem Amt für Umweltschutz und Energie, dort besonders Herrn Erich Eglin, für die finanzielle Unterstützung bei der Durchführung der Experimente und
- der Freiwilligen Akademischen Gesellschaft (FAG) Basel für die finanzielle Unterstützung bei den Publikationen.

Christoph Butscher

Basel, im Dezember 2007

I. Einleitung

I-1. MGU-Projekt „Quellen – Trinkwasserspender und Lebensraum"

Die vorliegende Arbeit entstand als Teilprojekt Hydrologie im Rahmen des MGU-Forschungsprojekts F /03 „Quellen: Trinkwasserspender und Lebensraum" (Baltes et al., 2005). Quellen sind seit alters her eine wichtige Trinkwasserressource für die menschliche Bevölkerung. Jedoch erst am Ende des 20. Jahrhunderts wurden Quellen als Lebensräume einer einzigartigen Tier- und Pflanzenwelt erkannt und erforscht (z. B. Thienemann, 1924). Verschiedene Randbedingungen haben sich in der Zwischenzeit verändert: Einerseits sind natürliche Quellhabitate für Lebewesen durch den Nutzungsdruck äusserst selten geworden. Entweder wurden Quellen zur Trink- und Brauchwassernutzung gefasst, oder aus siedlungshydrologischen Gründen (z. B. Drainage von landwirtschaftlich genutzten Gebieten) vom natürlichen Entwässerungssystem entkoppelt und über Rohrleitungen direkt der Kanalisation oder einem Vorfluter zugeführt. Andererseits mussten viele Quellen aus Qualitätsgründen vom Wasserversorgungsnetz abgehängt werden. Quellen sind somit in ihren verschiedenen Funktionen gefährdet und bedürfen spezifischer Schutzkonzepte. Das Projekt wollte zur Problemlösung beitragen, indem die heutige gesellschaftliche und naturwissenschaftliche Bedeutung der Quellen erfasst wird und Quellen nachhaltig in ihren Funktionen z. B. als Trinkwasserspender oder als Lebensraum erhalten und gegebenenfalls saniert oder revitalisiert werden. Bisher wurden Quellen in der Wissenschaft lediglich fachspezifisch untersucht. Für dieses Projekt wurde erstmals ein interdisziplinärer Ansatz gewählt, der biologische, hydrologische und soziologische Aspekte integriert.

I-2. Ziel der Untersuchung

Zu 39 % erfolgt die Trinkwasserversorgung in der Schweiz durch Quellen. In der Region Basel ist der Anteil des Quellwassers in den ländlichen Gebieten der Region von grösserer Bedeutung als in der Agglomeration Basel, die vorwiegend durch Grundwasser versorgt wird. Während in der Stadt Basel generell ein Rückgang des Wasserverbrauchs beobachtet werden kann, steigt er in einzelnen Gemeinden der Region - z. B. auch in solchen mit Quellwasserversorgung. Der Grund ist die Bevölkerungszunahme in ländlichen Gebieten. Die Rohwasserqualität der Quellen variiert beträchtlich. Wesentlich für die Beurteilung des Aufwandes an Aufbereitung ist insbesondere die mikrobiologische Belastung des Quellwassers. Im Jahr 2000 mussten allein im Kanton Basellandschaft bei routinemässigen Trinkwasserkontrollen 28 Beanstandungen verzeichnet werden. Neue Untersuchungen zeigen,

dass das Belastungsmuster stark mit der Abflusscharakteristik der jeweiligen Quelle, der Hydrogeologie des Einzugsgebietes und den anthropogenen Tätigkeiten im Quelleinzugsgebiet zusammenhängt (z. B. Auckenthaler et al., 2002). Neben der mikrobiologischen Belastung, wenn teilweise auch verzögert oder in abgeschwächter Form, spiegeln Nitrat, DOC-Erhöhungen, Atrazin und Pestizide die menschlichen Aktivitäten im Quelleinzugsgebiet wider. Mikrobiologie und chemische Inhaltsstoffe verhalten sich jedoch aufgrund ihrer Gesteins - Wasser Wechselwirkungen unterschiedlich. Neue Nachweismethoden für Mikroorganismen und die Möglichkeiten der Modellierung von Abflussdynamik und Organismentransport vom Eintrag in den Einzugsgebieten bis hin zu den Quellaustritten ermöglichen heute eine differenziertere Gefährdungsabschätzung der Rohwasserqualität von Quellen (Auckenthaler und Huggenberger, 2003). Die Anwendung GIS gestützter Multikriterien-Methoden (Vrba und Zoporozec, 1994; Dörfliger et al., 1999) erlaubt zudem eine differenzierte Vulnerabilitätskartierung in Quelleinzugsgebieten.

Ziel der vorliegenden Dissertation ist eine verbesserte Kenntnis der hydrologisch-hydrogeologischen Prozesse und eine Beurteilung der Vulnerabilität (Verletzlichkeit des Grundwassers gegenüber Verschmutzung) in den Einzugsgebieten von Quellen. Durch die im Rahmen der Arbeit durchgeführten hydrogeologischen Untersuchungen soll die Qualität des Grundwassers und des genutzten Quellwassers nachhaltig erhalten oder verbessert werden. Dabei gilt es insbesondere, den Zusammenhang Hydrologie, Einzugsgebiete und Quellschüttungsverlauf zu verstehen sowie Kriterien für die Vulnerabilität lokal anzupassen. Der Schwerpunkt der hydrologischen Untersuchungen des Projekts fand in den Quellgebieten des Röserentals (Kanton Basellandschaft) und in deren Einzugsgebieten auf dem Gempenplateau statt.

I-3. Hypothesen und angewandte Methoden

Den für diese Arbeit durchgeführten Untersuchungen liegen verschiedene Hypothesen zugrunde, die anhand geeigneter Methoden überprüft werden sollten. Die in den folgenden drei Abschnitten aufgeführten Hypothesen bilden jeweils die konzeptionelle Basis der nachfolgenden Kapitel.

(1) In Kapitel II wird die Hypothese aufgestellt, dass Grundwasserfliesssysteme wesentlich durch den strukturellen Aufbau des Untergrunds beeinflusst werden. Störzonen und der Versatz von hydrologischen Einheiten an Störungen kontrollieren die Verbindung oder

Trennung von Aquiferkörpern. Unterirdische Fliesswege können unter bestimmten Umständen von der Morphologie der stauenden Aquiferbasis bestimmt werden.

Deshalb wurde für das Untersuchungsgebiet Gempenplateau die Geometrie der geologischen Schichten im Untergrund mithilfe der Software GOCAD (Version 2.1.4) dreidimensional modelliert. Anhand der räumlichen Lage der tieferen, Wasser stauenden Schichten und verschiedener markanter Brüche konnten die Herkunftsgebiete des Wassers der einzelnen Quellen ziemlich genau eingegrenzt und verschiedene Fliess-Systeme unterschieden werden. Dies ist eine wichtige Voraussetzung für eine Angabe der Vulnerabilität im Einzugsgebiet der Quellen im Hinblick auf den qualitativen Schutz des genutzten Quellwassers.

(2) Kapitel III basiert auf der Hypothese, dass die Anteile verschiedener Grundwasserfliesssysteme am Gesamtabfluss einer Karstquelle wesentlich die Empfindlichkeit dieser Quelle gegenüber Verunreinigungen beeinflussen. Die verschiedenen Fliesssysteme sind durch unterschiedliche Aufenthaltszeiten des Wassers im Untergrund gekennzeichnet. Sowohl die Aufenthaltszeiten, als auch die Anteile der Fliesssysteme sind zeitlich variabel. Ihr Einfluss auf die Vulnerabilität des Quellwassers ist für leicht und für schwer abbaubare Verunreinigungen verschieden.

Zur Quantifizierung dieser Faktoren wurden die unterirdischen Fliessvorgänge und der Stofftransport in den verschiedenen Fliesssystemen mit Hilfe numerischer Modelle instationär nachgebildet. Als Basis der Modellierung wurde ein Quellüberwachungs-System aufgebaut. Dazu wurden ausgewählte Quellen mit Messsonden versehen, welche chemisch-physikalische Parameter (Schüttung, elektrische Leitfähigkeit, Temperatur) kontinuierlich aufzeichnen. An weiteren Quellen wurden diese Daten in regelmässigen Intervallen erhoben. Um Messdaten zu unterschiedlichen hydrologischen Situationen zu erhalten, ist ein Messprogramm auf ein vollständiges hydrologisches Jahr ausgelegt worden. Für eine effiziente Datenverwaltung wurde eine geeignete Datenbankstruktur entwickelt.

Die entwickelten Modelle wandelten das Niederschlags- und Verdunstungsgeschehen als Input-Funktion in das dynamische Schüttungsverhalten von Quellen als Output-Funktion um. Diese Transformation wird mithilfe der Software AQUASIM (Version 2.1e, Reichert, 1994) durch volumetrische Modelle erreicht, in denen verschiedene Fliess-Systeme in Form von Kompartimenten miteinander verknüpft sind. Mit Hilfe dieser Modelle konnten Grundwasser-Anreicherung und Quellschüttung simuliert und mittlere Aufenthaltszeiten in verschiedenen Fliess-Systemen quantifiziert werden. Dies ermöglichte eine zeitliche Differenzierung und Quantifizierung der Vulnerabilität unter Berücksichtigung der Charakteristika einzelner

Quellfassungen sowie eine Prognose der stattfindenden Fliessprozesse anhand des messbaren System-Zustands. Das Verfahren kann zum Schutz des Grundwassers und als Instrument für ein Bewirtschaftungs- und Nutzungsmanagement angewandt werden.

(3) Ein wichtiges Werkzeug für den planerischen Grundwasserschutz in Karstgebieten ist die Kartierung der Vulnerabilität. Statische Vulnerabilitätskarten allein werden jedoch nicht allen Anforderungen an Konzepte für einen nachhaltigen Grundwasserschutz gerecht. Deshalb wird in Kapitel IV die Hypothese aufgestellt, dass die Kenntnis der gegebenen Randbedingungen und das Verständnis der stattfindenden Prozesse eine Grundvoraussetzung für einen verbesserten Grundwasserschutz ist. Dies beinhaltet einerseits den geologisch-strukturellen Rahmen und andererseits die Dynamik des Fliessgeschehens.

Deshalb wurde für einen Teil des Untersuchungsgebiets Gempenplateau eine Vulnerabilitätskarte (Methode EPIK, Doerfliger et al., 1999) angefertigt. Die Informationen aus der Kartierung wurden mit Informationen aus der 3D geologischen und der numerischen Modellierung ergänzt. Durch die gemeinsame Anwendung der einzelnen Methoden entstand ein integratives Grundwasserschutzkonzept für Karstgebiete, das sowohl die Verteilung der Vulnerabilität in den Einzugsgebieten, als auch den strukturellen Aufbau des Untergrunds und die Dynamik des unterirdischen Fliessgeschehens berücksichtigt.

I-4. Untersuchungsgebiet

Das Untersuchungsgebiet ist rund 36 km^2 gross und umfasst das Gempenplateau sowie dessen umliegende Flanken und Täler (vgl. Abbildung 1 in Kapitel II). Es ist ein Teil des Schweizer Tafeljuras. Dieser besteht aus einer Sedimentabfolge der Trias und des Jura, welche das kristalline Grundgebirge überlagern. Die vorkommenden Gesteine weisen unterschiedliche hydraulischen Durchlässigkeiten auf. Heute bilden die geologischen Einheiten eine leicht nach Süden einfallende Platte (Gürler et al., 1987), welche durch SSW—NNE streichende Horst- und Grabenstrukturen sowie durch meist W—E streichende Transversalverschiebungen zergliedert ist. Die starke tektonische Fragmentierung zusammen mit dem Wechsel von durchlässigen und undurchlässigen Schichten führt zu sehr kleinräumigen hydrologischen Strukturen (Schmassmann, 1972).

Im Untersuchungsgebiet reicht die Stratigraphie der anstehenden Schichten von der Opalinuston-Formation (Aalen) im Liegenden bis zur Vellerat-Formation (Oxford) im Hangenden (vgl. Abbildung 2 in Kapitel II; Bitterli-Brunner und Fischer, 1988). Lithologisch

bilden die Schichten überwiegend eine Wechselfolge aus Kalksteinen, Mergel- und Tonsteinen. Die Kalkstein-Formationen bilden ein reifes Karstsystem, welches überwiegend einem seichten Karst (Bögli, 1980) entspricht: Die Karstaquifere liegen höher als ihre Vorfluter und sind ihnen zugeneigt. Die Entwässerung erfolgt rein gravitativ. Dort, wo die Topographie die Grenze zwischen Aquifer und darunter liegendem Stauer schneidet, entstehen Quellhorizonte. Ford und Williams (1989) führten für diese Art von Quellen den Begriff „free drainage springs" ein. Im Gegensatz dazu stehen „dammed springs", welche dann auftreten, wenn eine grössere Barriere im Untergrund die unterirdischen Fliesspfade zum Aufstieg zwingt. Diese Situation ist im Untersuchungsgebiet nur ausnahmsweise an Störungen gegeben.

Für das regionale Fliessgeschehen spielen zwei verschiedene Hauptaquifere eine Rolle. Der erste und stratigraphisch höher gelegene Hauptaquifer umfasst die St. Ursanne und die Vellerat Formation des Oxfords. Die massigen Kalksteine der St. Ursanne Formation sind 40—70 m mächtig und sind in einer Rifffazies ausgebildet. Die darüber liegende Vellerat-Formation besteht aus geschichteten Kalksteinen mit dünnen mergeligen Zwischenlagen. Die Aquiferbasis bildet die rund 100 m mächtige Bärschwil Formation. Diese besteht aus tonigen Mergeln, denen im oberen Teil auch karbonatreiche Bänke mit Kalkknollen eingeschaltet sind. Der zweite und stratigraphisch tiefer gelegene Hauptaquifer umfasst die 50—80 m mächtige Untere Hauptrogenstein Formation. Diese enthält oolithische Kalksteine mit nur vereinzelt mergeligen Zwischenlagen. Hier bildet die Aquiferbasis die Passwang Alloformation, eine ungefähr 80 m mächtige Wechselserie aus Kalk- Mergel- und Tonsteinen.

Auf dem Gempenplateau fallen die Schichten im Osten generell ostwärts, während sie sich im Westen zunehmend westwärts neigen. NNE—SSW streichende Horst- und Grabenstrukturen dominieren das tektonische Bild (vgl. Abbildung 1b in Kapitel II). Eine W—E streichende Transversalzone, welche durch Blattverschiebungen abgesetzt ist, gliedert das Gempenplateau in einen nördlichen und einen südlichen Teil. Im nördlichen Teil und im Osten der Transversalzone dominiert der Hauptrogenstein-Aquifer, hingegen ist im Südteil und im Westen der Transversalzone der Oxford-Aquifer vorherrschend.

65 Quellen sind aus dem Untersuchungsgebiet bekannt (Bitterli-Brunner et al. 1984). Die Einzugsgebiete der Quellen befinden sich meist auf dem Plateau selbst, während die Quellgebiete an den Flanken des Plateaus zu finden sind. Die Einzugsgebiete sind somit nicht

nur räumlich, sondern auch kulturell von den Quellen getrennt. Die dünn besiedelten Gebiete auf dem Plateau werden hauptsächlich landwirtschaftlich genutzt, die Quellen hingegen befinden sich überwiegend im Wald. Häufig sind die Quellen zur Trinkwasserversorgung gefasst, jedoch existieren auch ungefasste, naturnahe Quellen. Die Quellwassernutzer leben in den Agglomerationen in den Tälern, die das Gempenplateau umgeben. Die bewaldeten Quellgebiete werden von ihnen auch als Naherholungsgebiete geschätzt. Die Quellgebiete liegen auf dem Kantonsgebiet von Basel-Landschaft, während die landwirtschaftlich genutzten Einzugsgebiete auf dem Plateau dem Kanton Solothurn angehören. Die menschlichen Aktivitäten auf dem Plateau gefährden die umgebenden Quellen. Dies führt entsprechend auch zu Nutzungskonflikten über kantonale Grenzen hinweg.

I-5. Organisation der Dissertation

Diese Dissertation ist kumulativ uns besteht aus einer Einleitung (Kapitel I), drei unabhängigen wissenschaftlichen Artikeln, die publiziert oder zur Publikation vorbereitet und eingereicht sind (Kapitel II-IV), und einer Zusammenfassung der generellen Schlussfolgerungen (Kapitel V). Kapitel II konzentriert sich auf die 3D geologische Modellierung und darauf, wie ein daraus abgeleitetes hydrologisches Modell zur Beurteilung der Vulnerabilität in Karstgebieten beitragen kann. Es wird gezeigt, wie der vorgestellte Ansatz in der Praxis zur Lokalisierung von Einzugs- und Quellgebieten für den Quellwasserschutz genutzt werden kann. Ausserdem können damit auch Rückschlüsse auf unterirdische Wasserzirkulationsprozesse gezogen werden. In Kapitel III wird die Reaktion der Quellschüttung auf Niederschlagsereignisse simuliert. Es werden Vorschläge gemacht, wie mit kalibrierten numerischen Modellen die zeitliche Variabilität der Vulnerabilität beschrieben und quantifiziert werden kann. Kapitel IV ist darauf ausgerichtet, die im Rahmen dieser Dissertation entwickelten und in den beiden vorangegangenen Kapiteln vorgestellten Methoden in ein integratives Schutzkonzept für Quellen und Grundwasser in Karstgebieten umzusetzen.

Aufgrund dieser Organisation der Dissertation kommt es teilweise zu Wiederholungen, obwohl sich die einzelnen Kapitel auf verschiedene Aspekte der Grundwasser-Vulnerabilität in Karstgebieten konzentrieren. Dies betrifft insbesondere die Abschnitte, in denen das Untersuchungsgebiet oder vorangegangene Forschung auf Gebiet der Karst Grundwasser Vulnerabilität vorgestellt werden.

Literatur

Auckenthaler, A., Huggenberger, P., 2003. Pathogene Mikroorganismen im Grund- und Trinkwasser. Transport – Nachweismethoden – Wassermanagement. Birkhäuser, Basel.

Auckenthaler, A., Raso, G. und Huggenberger, P., 2002. Particle transport in a karst aquifer: Natural and artificial tracer experiments with bacteria, bacteriophages and microspheres. Water Science and Technology 46 (3), 131-138.

Baltes B, von Fumetti S, Küry D, Contesse E, Butscher C, Huggenberger P, Suter D, Leimgruber W und Nagel P., 2005. Basel entdeckt seine Quellen. Deutsche Gesellschaft für Limnologie (DGL). Tagungsbericht 2004 (Potsdam, 20.-24. September 2004), Berlin: Weissensee Verlag, S. 226-230.

Bitterli-Brunner P., Fischer, H. und Herzog, P., 1984. Geologische Karte Blatt Arlesheim 1067. Geologischer Atlas der Schweiz.

Bitterli-Brunner, P. und Fischer, H., 1988. Erläuterungen zum Blatt Arlesheim 1067. Geologischer Atlas der Schweiz.

Bögli, A., 1980. Karst hydrology and physical speleology. Springer, Berlin.

Doerfliger, N., Jeannin, P.-Y. und Zwahlen, F., 1999. Water vulnerability assessment in karst environments: a new method of defining protection areas using a multi-attribute approach and GIS tools (EPIK method). Environ. Geol. 39 (2),165-176.

Ford, D. C. und Williams, P. W., 1989. Karst geomorphology and hydrology. Chapman and Hall, New York.

Gürler, B., Hauber, L. und Schwander, M., 1987. Die Geologie der Umgebung von Basel mit Hinweisen über die Nutzungsmöglichkeiten der Erdwärme. Beitrag zur Geologischen Karte der Schweiz 160.

Reichert, P., 1994. AQUASIM – A tool for simulation and data analysis of aquatic systems. Water Science and Technology 30 (2), 21-30.

Schmassmann, H., 1972. Baselbieter und westlicher Aargauer Tafeljura. In: Jäckli, H. und Kempf, T., 1972. Erläuterungen zum Blatt Bözberg-Beromünster 1. Hydrogeologische Karte der Schweiz, 93-100.

Thienemann, A., 1924: Hydrobiologische Untersuchungen an Quellen. Archiv für Hydrobiologie 14, 151–190.

Vrba, J. und Zoporozec, A. (Hrsg.), 1994. Guidebook on Mapping Groundwater Vulnerability. International Contributions to Hydrogeology (IAH) 16, Hannover.

II. Implications for karst hydrology from 3D geological modeling using the aquifer base gradient approach

Abstract

We use the gradient of the aquifer base to investigate the hydrology of mature, shallow karst systems. We first present a 3D geological model of the Gempen plateau (NW Switzerland) that reveals the geometry of aquifers and aquitards and their displacement at faults, then transfer the 3D geological model to a hydrological model. The transformation is based on a conceptual karst model approximating subsurface flow in mature, shallow karst systems to open surface flow on the top of the uppermost aquitard or aquifer base. The gradient of this surface is expected to mainly influence regional groundwater flow patterns. We use the hydrological model to delineate spring catchment areas. The discharge areas and corresponding catchment areas of the model are compared with the occurrence of springs in the study area and with hydraulic links confirmed by tracer tests. We also describe the way in which the hydrological model contributes to identifying flow processes. The proposed aquifer base gradient approach enhances vulnerability assessment in mature, shallow karst regions by (1) localizing catchment areas as a precondition of source protection strategies and (2) indicating dominant flow processes associated with individual springs.

Keywords:

II-1. Introduction

This study emerged from the Basel Spring Project (Baltes et al., 2005) conducted in northern Switzerland; its goal was to develop a concept for sustainable use of springs in karst regions, and the issue of springwater quality impairment played a major role in the investigations. Human activities in the catchment areas can endanger springwater quality (e.g. Auckenthaler et al., 2002) and thus have a direct influence on the health of consumers. The main objective of the current study was to contribute to the sustainable use of springs by 1) developing an effective method to identify the spring catchment areas and 2) obtaining information about the flow processes that connect the catchment areas with the springs.

Since the mid-1980s, researchers throughout the world have developed various groundwater and springwater protection strategies. Methods of groundwater vulnerability mapping are among the most important (e.g. Aller et al., 1987; Civita and De Maio, 2000; for an overview see Vrba and Zoporozec, 1994; Magiera, 2000). Karst aquifers have complex and original characteristics, which make them very different from other aquifers (Bakalowicz, 2005). Their catchments may cover very large areas and they are extremely heterogeneous and anisotropic; thus they are particularly vulnerable to contamination (Goldscheider, 2005). Because of their distinct features, some vulnerability assessment methods have been designed specifically for karst environments (Doerfliger et al., 1999; Goldscheider et al., 2000; Daly et al., 2002; COST 620, 2003).

Vulnerability assessment methods can be divided into "source" and "resource protection" methods (Hötzl, 1996). Resource protection methods aim to protect all of the groundwater, whereas source protection methods focus on the protection of a discrete water source. Source protection methods are based on the assumption that some places within a spring's catchment area are more vulnerable to contamination than others. These methods do not address how to locate catchment areas, yet information about the actual extent of the catchment area is an important precondition for applying source protection methods.

In this study, we focus on the catchment areas and on the flow paths linking these areas to springs. Since the 1970s, many studies have dealt with the development of karst conduit systems (e.g., Ford and Ewers, 1978; White, 1999; Worthington, 2005). Recently, the numerical simulation of karst evolution has greatly improved our understanding of the processes involved (e.g., Dreybrodt, 1990; Clemens et al., 1999; Bauer et al., 2003; Birk et

al., 2003; Kaufmann, 2003; Liedl et al., 2003; Bauer et al., 2005; Birk et al., 2005). However, the conclusions drawn from these studies are difficult to transfer to the present study. In particular, the proposal to develop a draining base level at the vertical position of the discharge level (Kaufmann and Braun, 2000; Kaufmann, 2002) may not be applicable here because the aquifer base predominately slopes towards and lies above the draining valleys. Its karstification is thus limited by the underlying aquitards.

The existing models of karst evolution and hydrology center on numerous controls, such as dissolutional fracture enlargement, coupling of the conduit network and rock matrix, distribution of fracture width, geometry, permeability and spacing of fractures, and the influence of the epikarst. These models all assume a spatially predefined discharge level (with a constant head or flow rate) without an aquifer base or with an unstructured, horizontal aquitard layer as the aquifer base. The role of the aquitard underlying the aquifer and, thus, the morphology and tectonic structure of the aquifer base have rarely been investigated. However, regional hydrological investigations often stress the influence of the actual aquifer structure and include the spatial orientation and morphology of the aquifer base and its displacement at faults (e.g., Herold et al., 2000; Kovács and Jeannin, 2003; Luetscher and Perrin, 2005). In this study, we focus on the role of the aquifer base in controlling the regional flow patterns.

Regional numerical models that simulate groundwater flow based on Darcy's law (single continuum models), such as MODFLOW (Harbaugh and McDonald, 1996), include the geometry of the aquifer base. However, these kinds of models are not applicable to karst areas because of the extremely high hydraulic conductivities in the conduit network of these areas. To overcome this problem, double continuum models, where a continuum model for the diffuse system is coupled with another for the conduit system, have been developed and successfully used on a regional scale (e.g., Sauter, 1992). 3D double continuum models of karst aquifers have, however, not been published yet (Sauter et al., 2006). The main difficulty with using continuum models on a regional scale is that they require extensive field data, like those from hydraulic heads and hydraulic conductivities (e.g., from pumping tests). In our study area, not a single borehole was ever drilled down to the groundwater, which is a rather common situation in many karst regions. Other authors have simulated karst hydraulics by modeling discrete fractures (e. g., Long et al., 1982; Anderson and Dverstorp, 1987; Jeannin, 2001) or combining a discrete (channel) and continuum (matrix) approach (Kiraly, 1998;

Liedl et al., 2003), including both laminar flow in the rock matrix and turbulent flow in the conduit system. While these models provide an important tool for studying the fundamental functions of karst systems, they are difficult to apply to large, complex areas on a regional scale because of the extremely scarce data on real karst channel networks and hydraulic parameters.

To obtain information about catchment areas and subsurface flow in large complex karst regions we developed the aquifer base gradient (ABG) approach. This method is based mainly on the assumption that in unconfined, mature, shallow karst the development of conduits and the resulting conduit flow are strongly influenced by the geometry of the aquifer base. Under certain conditions, processes comparable to open surface flow may dominate at the base of such aquifers. Besides the morphology of the aquifer base, faults are important, because they displace the aquifer base and control the connection and separation of aquifer bodies.

The ABG approach includes two main steps: 1) Construction of a 3D geological model of the study area using the geomodeling software GOCAD; this step is used to illustrate and analyze the geometry of aquifers and aquitards, the morphology of their base, and displacement at faults; and 2) Development of a hydrological model based on the 3D geological model. The hydrological model includes the distribution of subsurface flow paths, which can be summarized to the underground catchment areas of individual springs.

The modeled flow paths and catchment boundaries were surveyed by comparing the discharge areas derived from the model with the actual locations of the springs. Furthermore, the proposed catchment areas were compared with hydraulic links confirmed by tracer tests. The comparison revealed the ability of the hydrological model to delineate underground spring catchments in a mature, shallow karst system. We also describe the capability of the proposed approach to identify karst flow processes. The study concludes with a discussion about the suitability of the method to contribute to vulnerability assessment.

II-2. Study Area

The Swiss tabular Jura is situated in northwest Switzerland next to the southeastern border of the Rhine Graben (Fig. 1a). The geology of the tabular Jura comprises Triassic and Jurassic sediments of varying hydraulic permeability overlaying the crystalline basement. The sediment cover builds up a slightly southward dipping plate (Gürler et al., 1987). The plate is

fractionalized by SSW-NNE trending graben structures and mostly W-E trending strike-slip faults. The intense tectonic fragmentation and the alternation of permeable and impermeable layers create very small-scale hydrological structures (Schmassmann, 1972).
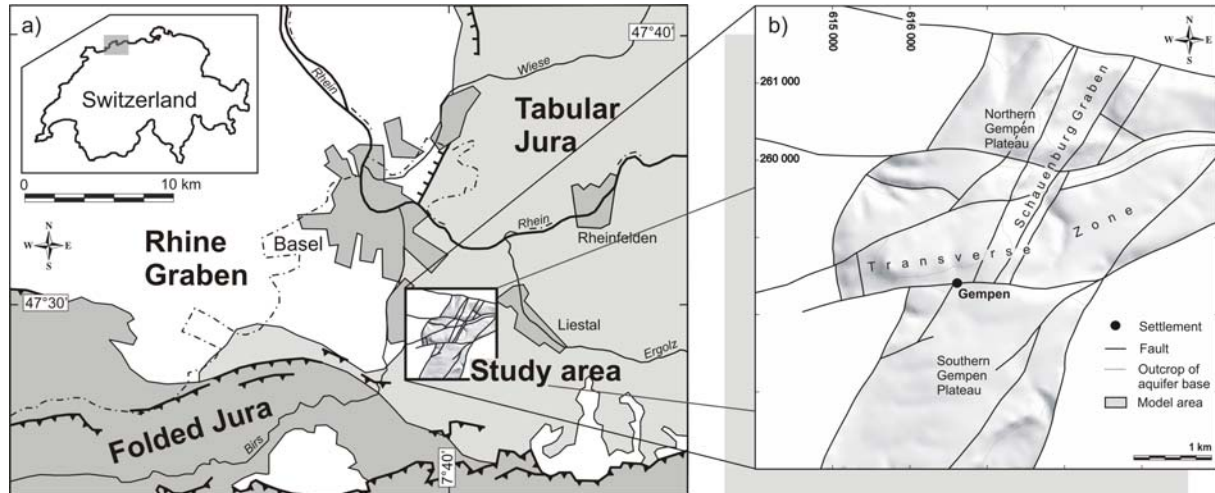
Fig. 1. Study area. (a) Location and tectonic framework. (b) Tectonic units.

We tested our method on the Gempen plateau (Fig. 1b), which forms part of the Swiss tabular Jura. It extends over 36 km^2 and consists of alternating limestone, marl, and clay sequences of Aalenian to Oxfordian age (Bitterli-Brunner and Fischer, 1988). Spring hydrographs and the exposure of the limestone rocks to the land surface since the end of the Jurassic (Gürler et al., 1987) argue for the existence of a mature karst system. The hydrogeology of the study area is characterized by karst water circulation in an unconfined setting. The karst system mainly corresponds to a shallow karst (Bögli 1980), as mostly uncapped karst rocks slope towards and lie above the adjacent valley into which the karst water drains freely by gravity. Given their hydrological control, the springs are called free drainage springs (Ford and Williams, 1989). The location of a major barrier in the path of underground drainage, which forces the water upwards, presents a special situation and sporadically leads to the occurrence of dammed springs (Ford and Williams, 1989). In the study area, such barriers are caused by faults with a subsequent impermeable layer.

Two stratigraphic units forming the main karst aquifers control the hydrology of the study area (Fig. 2). The upper main aquifer (in a stratigraphic sense) comprises (from bottom to top) the Oxfordian St. Ursanne and Vellerat Formations. The St. Ursanne Formation varies in thickness (40--70 m) and represents a reef facies with massive limestone and high primary porosity. The up-to-110 m thick Vellerat Formation is composed of bedded limestone of

varying facies with thin interbedded marl. The aquifer base is the approximately 100 m thick Oxfordian Bärschwil Formation with plastic marl in the lower part and marl with continuous bands of calcareous nodules above. The Oxfordian aquifer has never been covered by insoluble rocks and there is no evidence for an inheritance from previous karst stages. It is highly karstified as it has been exposed to the land surface since the end of the Jurassic (Gürler et al., 1987). According to the hydrogeologic evolutionary typology for karst proposed by Klimchouk and Ford (2000), the setting corresponds to an exposed, open karst.
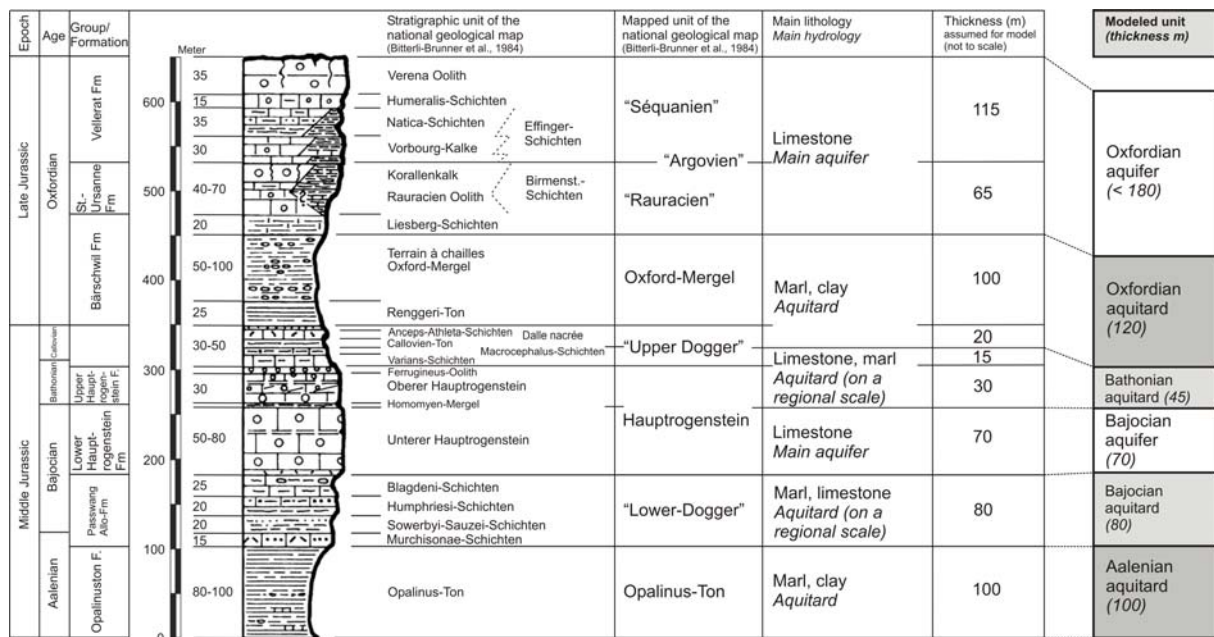
Fig. 2. Lithostratigraphy of the study area and column with modeled units.

The lower main aquifer (in a stratigraphical sense) comprises the 50--80 m thick Bajocian Lower Hauptrogenstein Formation, an oolithic limestone containing only sporadic marly interbeds. The aquifer base is formed by the approximately 80 m thick Passwang Alloformation, an alternating series of limestone, marl, and clay. In a regional context, the permeability of this underlying formation is low, but it may vary locally. The Bajocian aquifer corresponds to an exposed, open karst (Klimchouk and Ford, 2000). The karst rocks have been buried but then stripped of cover, probably before any significant development of karst circulation.

Generally, the strata dip eastwards at the eastern Gempen plateau and increasingly westwards to the west. NNE-SSW striking graben structures characterize the tectonic setting (Fig. 1b). A W-E trending transverse zone, separated by strike-slip faults, divides the northern from the southern plateau. The Bajocian aquifer controls the hydrology of the northern plateau and the

eastern transverse zone, while the Oxfordian aquifer is predominant in the southern plateau and the western transverse zone.

II-3. Modeling Approach

II-3.1. Overview

Our hydrological model presents the subsurface flow distribution, including the location of discharge areas, the corresponding catchment areas, and the groundwater flow direction. It is derived from a 3D geological model, using a conceptual karst model. In the following subsections, we introduce the 3D geological model of the study area and then the conceptual karst model. A flow scheme, based on the conceptual karst model, is subsequently presented, which illustrates the transfer of information obtained by the 3D geological model into the hydrological model.

II-3.2. The 3D geological model

The 3D geological model covers an area of 18 km^2. It is composed of six volumetric layers that represent hydrostratigraphic units. These layers are displaced by faults, which segment the model into compartments. The layers of each compartment represent individual model objects delimited by faults, hydrostratigraphic boundaries, and the topographic surface. The result is a 3D visualization of the Gempen plateau's geology, illustrating the geometry of aquifers and aquitards and their displacement at faults.

Data

The 3D geological model uses fault traces and borders of mapped units from the national geological map (Bitterli-Brunner et al., 1984). These units generally correspond to the stratigraphic units currently used for the Jurassic in northern Switzerland (Fig. 2). The resolution of the model is designed to provide a hydrological analysis on a regional scale. Local aspects, such as the Quaternary cover of the bedrock and the heterogeneities within the modeled layers (e.g., due to interbedded strata, altering facies, or distribution and orientation of fracture joints) are not resolved by the model.

Modeled aquifers and aquitards

The following six hydrostratigraphic boundaries are represented in the 3D geological model (from bottom to top): the respective base of the Opalinuston Formation; the Passwang Alloformation; the Lower Hauptrogenstein Formation; the Upper Hauptrogenstein Formation;

1) Construction of **faults** from mapped fault traces assuming an 80° dip

2) Connecting faults to **fault framework** (segmentation into compartments)

3) Displacement of mapped bedrock boundary layers to common stratigraphic level and interpolation of **root horizon** in every compartment

Morphology of root horizon plausible?

Yes   No

Introduction of an additional fault

4) Displacement of root horizon to stratigraphic level of **model horizons**, fitted to the outline of the compartment

5) Grouping of compartments lead to **faulted horizons** and to the volumetric 3D geological model

approx. 500 m

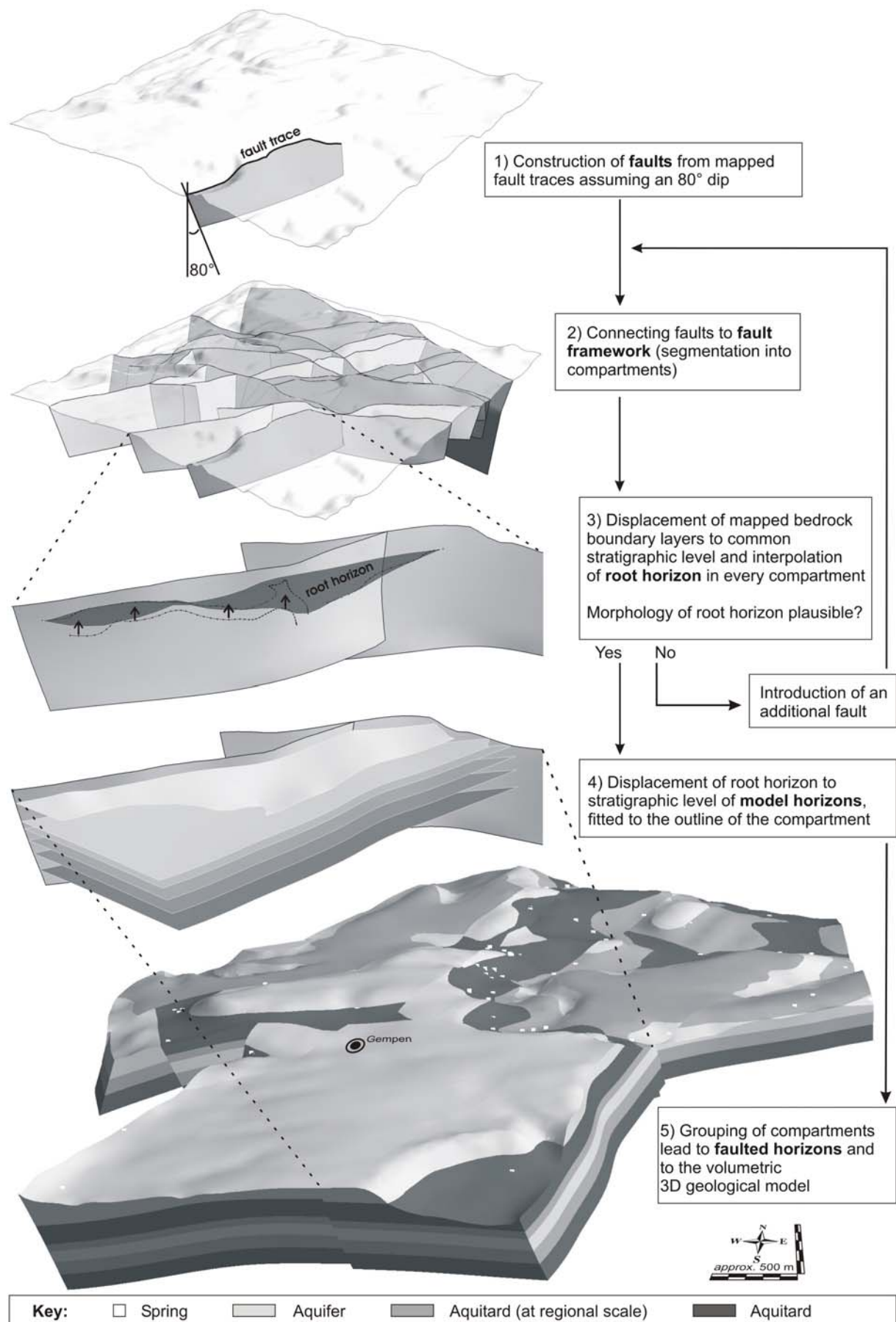| Key: | □ Spring | Aquifer | Aquitard (at regional scale) | Aquitard |

Fig. 3. Schematic representation of the 3D geological modeling process.

the Callovian clay; and the St. Ursanne Formation. The horizons divide the model into six volumetric layers termed according to their hydrological properties and dominating age (from bottom to top): the Aalenian aquitard; the Bajocian aquitard; the Bajocian aquifer; the Bathonian aquitard; the Oxfordian aquitard; and the Oxfordian aquifer (Fig. 2).

Construction of the model

The geological information used to construct the model includes a simplification of the mapped fault system: Fault zones are modeled as a single fault, detached minor faults are neglected, and minor faults that continue nearby are interpreted as being connected. The modeled faults are mainly NNE-SSW trending normal faults leading to graben and halfgraben structures. These structures are intersected by roughly E-W trending, slightly S dipping strike-slip faults. The interference of both sets of faults leads to a tectonic segmentation of the area into 21 compartments.

The Quaternary cover of the bedrock is not included in the geological model due to its supposed negligible influence on the regional hydrology. It largely consists of thin residual loams and colluvium. Combined with a steep topography, however, these sediments can accommodate interflow and may hence influence local hydrology.

3D geological modeling was conducted using the geomodeling software GOCAD 2.1.4. The data provided by the geological map were first digitized and then projected onto the topographic surface of a digital elevation model. The subsequent modeling process comprised five main steps (Fig. 3):

(1) The faults of the model were constructed from their traces, assuming an 80° dipping angle. This simplification generalizes the findings of Spottke et al. (2005) concerning dipping angles of faults in the tabular Jura at the southeastern border of the Upper Rhine Graben. These authors proposed a steeply inclined geometry for fault structures in the upper strata.

(2) The faults were connected to a closed fault framework. This step resulted in a tectonic segmentation of the model area into compartments.

(3) A root horizon was introduced for every compartment. For that purpose, all bedrock data for the compartment were displaced vertically to the best-documented stratigraphic level within the compartment. The amount of displacement Δz is given

by $\Delta z = m \cdot \cos(\alpha)$, where m is the thickness of the displaced strata and α the dipping angle of the horizons. The thickness was assumed to be constant for the entire model. It was derived from the information provided by the comments on the national geologic map (Bitterli-Brunner and Fischer, 1988) and from constructed cross-sections. The dip was derived for every compartment separately from dip strike symbols on the geologic map as well as from the cross-sections. Based on this data set, the root horizon was interpolated using the DSI interpolation algorithm (Discrete Smooth Interpolator; Mallet, 2002) of the GOCAD software. After interpolation, the morphology and geological plausibility of the horizon were examined. Unreasonable morphologies were rejected and a new modeling loop with an additional dividing fault was performed to obtain an adapted root horizon. If the morphology of the surface seemed reasonable, the segmentation procedure was stopped and the resulting root horizon accepted.

(4) The root horizon served as the basis for the construction of the model horizons in every compartment. It was displaced vertically to the stratigraphic level of the horizons to be modeled (c.f., step 3). The surrounding faults and topographic surface were then set as constraints for the lateral extent of the horizons. By re-running the DSI interpolation algorithm of the GOCAD-software, the displaced horizons were fit into the proper compartment.

(5) Volumes, defined by horizons, faults, and the topographic surface, were introduced as discrete objects using the GOCAD routine Model3d. Final assembly of these volumetric objects and their properties made up the 3D geological model.

II-3.3. Conceptual karst model

The conceptual model proposed in this study is based on the ideas of Bauer et al. (2005) on karst development in unconfined settings: "During the total evolution, surface runoff decreases from a large proportion of the available total runoff to zero or small values, the fraction of water flowing through the conduit system increases from negligible amounts to nearly all available infiltration water while the amount percolating through the fissured system does not increase significantly. The karst water table falls from near the land surface to base level…"

The position of the base level is controlled by the vertical position of the aquifers discharge (Kaufmann and Braun, 2000; Kaufmann 2002). In the case of free drainage springs, the base
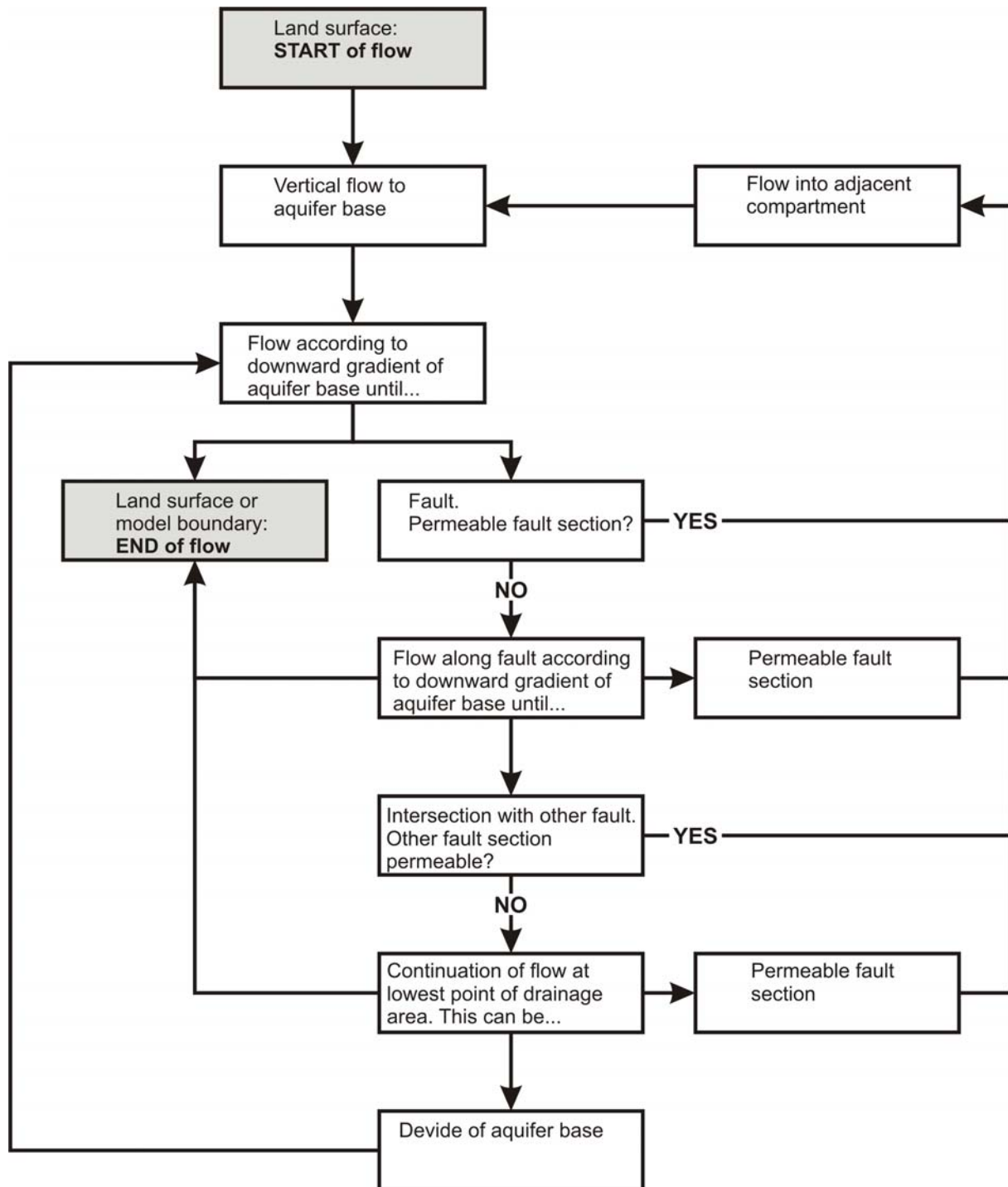
Fig. 4. Flow scheme of subsurface flow used to transfer the 3D geological model into the hydrological model (water particle tracking).

level cannot drop to a horizontal discharge level but must develop above at the aquifer base. The hydraulic gradient is then strongly influenced by the ABG and the direction of groundwater flow is controlled by the topography and structure of the aquifer base.

Based on these ideas, our conceptual model comprises the following characteristics: Surface runoff can be neglected; The groundwater flow direction corresponds to the downward

gradient of the base level; The base level is determined by the aquifer base or, in the case of dammed springs, by the vertical position of the draining outflow. Two further simplifications have been included: Recharge to the groundwater table (base level) is assumed to be vertical, and faults are assumed to be permeable to water flow where two aquifer layers come up against each other; otherwise they are assumed to be impermeable. The assumptions underlying the conceptual model are specific to mature, unconfined, shallow karst systems.

II-3.4. Flow scheme and hydrological model

Based on the conceptual karst model, we determined subsurface flow paths manually by water particle tracking according to a simple flow scheme (Fig. 4): Starting from the land surface, water infiltrates vertically until it reaches the base of an aquifer. It subsequently flows downward along that surface depending on its gradient (i.e., perpendicular to the contour lines). If the flow path meets a fault, the water either crosses the fault and flows into the adjacent compartment of the model or it flows along the fault, depending on the permeability of the fault. A fault section is permeable if the adjacent layer behind the fault section is an aquifer. If it is an aquitard, the fault section is impermeable. Flow running into an impermeable fault junction continues at the lowest permeable point on the outline of the studied drainage area. Flow ends at a model boundary or at the land surface. The latter leads to a model discharge corresponding to a spring. Neighboring model discharges at the land surface are summarized to a spring horizon. The area contributing flow to a common model discharge represents the catchment area of the respective spring or spring horizon.

By applying the flow scheme to the entire model area it is possible to derive all model discharges, their respective catchment areas and the general groundwater flow direction. The information obtained is summarized in the hydrological model.

II-4. Results and Interpretation

The results of the 3D geological modeling are illustrated in Figures 3 and 5. Fig. 6a illustrates the hydrological model of the study area. To verify the hydrological model, we compared the model discharges to the occurrence of springs in the study area and the catchment areas to hydraulic links confirmed by tracer tests (Cantonal Archive Basel, unpublished reports) (Fig. 6b). For the reason of clearness, we divide the study area into four sub-areas (c.f., Fig. 6b). Below we present and interpret the results of each of these areas. We focus on different flow

processes in each area, and illustrate the influence of interflow (area 1 and 3), direction of rock cleavage (area 2), and fault systems (area 4) on the model results.
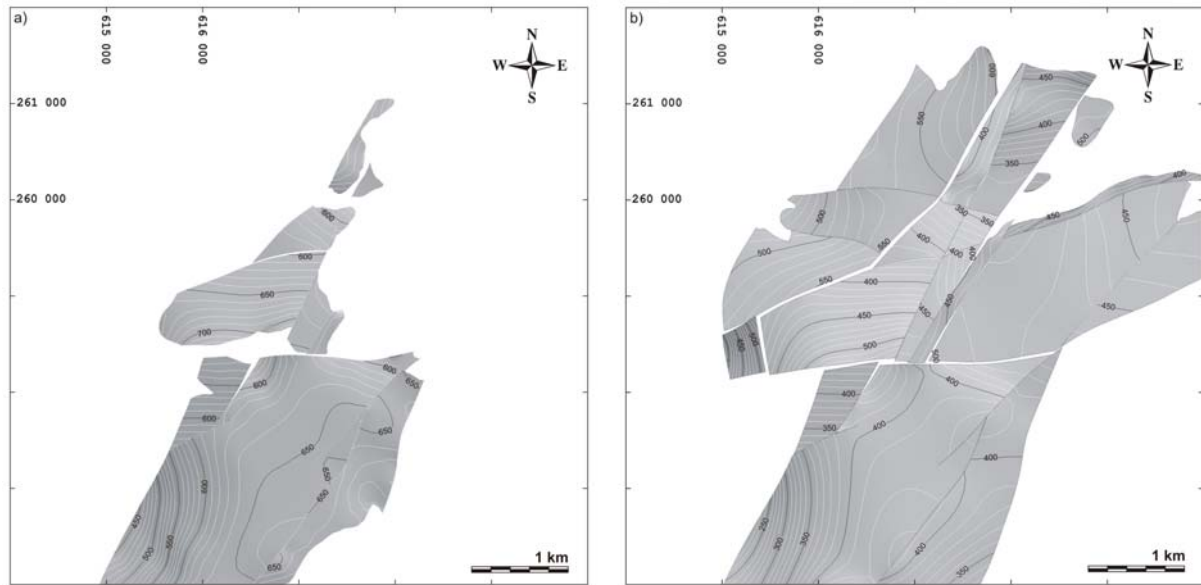

Fig. 5. Contoured illustration of the morphology of the aquifer base (vertical distance of contour lines: 10 m). (a) Oxfordian aquifer. (b) Bajocian aquifer.

II-4.1. Area 1

In area 1 (Fig. 7), five model discharges and their respective catchment areas have been identified. A comparison of the model discharges with the occurrence of springs reveals that the spring locations are in good agreement with the position of the model discharges. Local deviations are caused by the Quaternary cover, which is not included in the model: The springs in the study area discharge from colluvium, which covers the outcrop of the aquifer base and the slope below. The discharges predicted by the model, however, are located exactly at the outcrop of the aquifer base, as there is no Quaternary cover in the model.

A comparison of the hypothesized catchment areas with the results of tracer experiments reveals that most of the confirmed hydraulic links (Nos. 1–6, 10–13) verify the model. Hydraulic links Nos. 7—9 cannot be explained by the model and are interpreted as interflow: The injection sites are located within the overground catchment in a valley above the spring, and spring temperature variations of 5°C indicate the presence of a significant interflow component in spring discharge. Hydraulic link No. 14 can neither be explained by the subsurface flow predicted by the model nor by interflow.
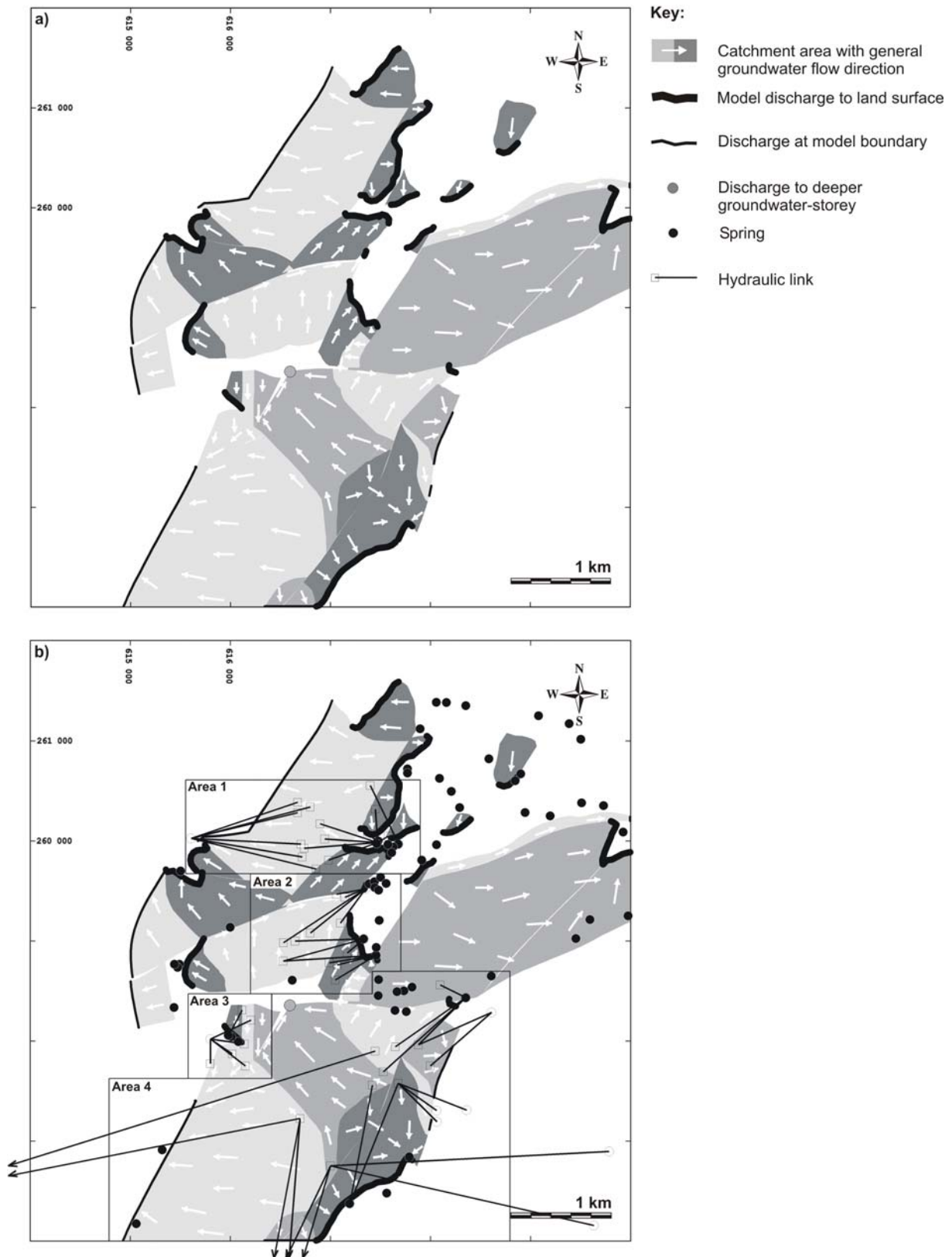
Fig. 6. Illustration of the hydrological model. (a) Model discharges, subsurface catchment areas and general direction of groundwater flow derived from the model. (b) The results of the model compared to the occurrence of springs and to hydraulic links confirmed by tracer tests. The model area is divided into sub-areas that are illustrated in detail in Figures 7–10.
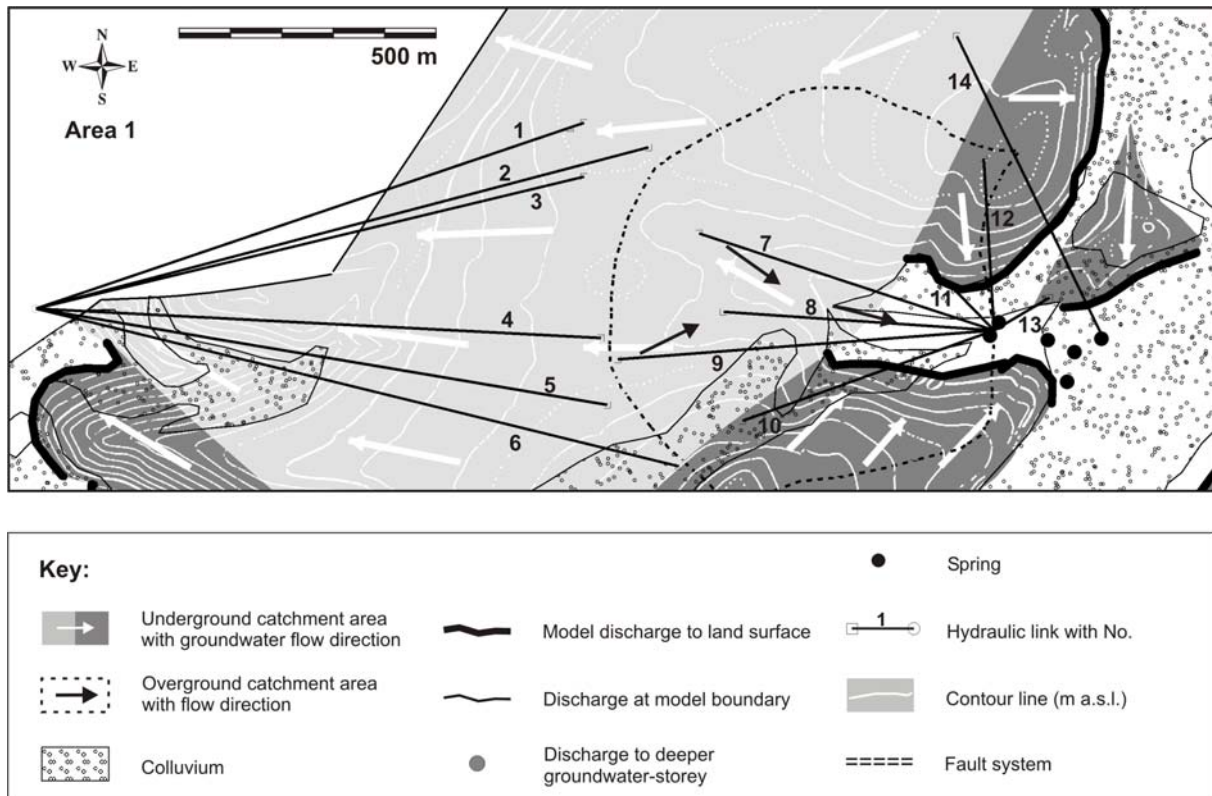
Fig. 7. Model results of area 1. The springs occur in colluvium below model discharges. Most of the links are associated with groundwater flow predicted by the model. Hydraulic link Nos. 7–9 are associated with interflow.

II-4.2. Area 2

In area 2 (Fig. 8), most springs are situated within colluvium below a model discharge. The uphill areas of the few springs not related to a model discharge are all sloping at > 20° angles, again suggesting interflow dominance. According to the tracer tests, 9 out of 12 hydraulic links connect the predicted catchment area with a spring related to the corresponding model discharge. However, according to the modeled groundwater flow direction, the tracers of link Nos. 10–12 are expected to appear in a spring further NW. Both springs are, however, related to the same model discharge. For link Nos. 6–8, the same deviation from the predicted groundwater flow direction is observed. Here, the input sites are not within the predicted catchment area of the studied springs. However, the direction of these hydraulic links corresponds to one of the main directions of fracture joints measured in the catchment area. Different authors have already described the influence of fracture joints on karst water circulation (e.g., Apel, 1971). Thus, the link Nos. 6–8 and 10–12 are probably strongly influenced by rock cleavage.
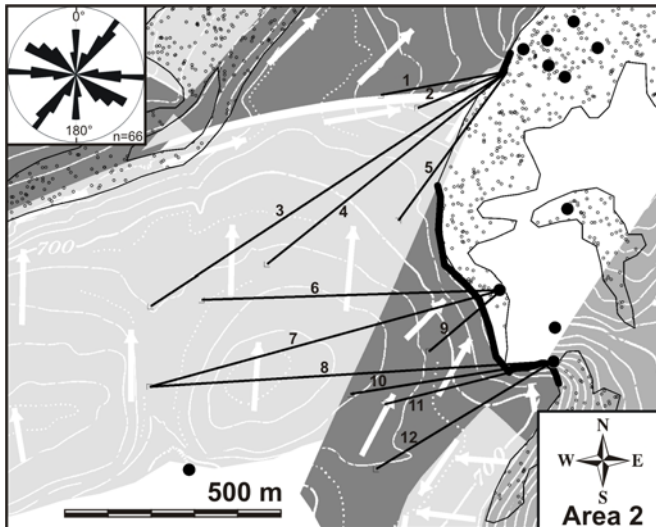
Fig. 8. Model results of area 2 (key: c.f., Fig. 7). The springs occur mainly in colluvium below a model discharge. Most links are associated with groundwater flow predicted by the model. Hydraulic link Nos. 6–8 and 10–12 are associated with one of the main directions of fracture joints.

II-4.3. Area 3

The occurrence of springs within area 3 (Fig. 9) agrees with the position of the model discharges. Hydraulic link Nos. 1 and 2 correspond to the model predictions. The other tracer tests can be explained by interflow: The tracers appeared in a spring situated at the bottom of a caldera-like topography with tracer input sites within the overground catchment.
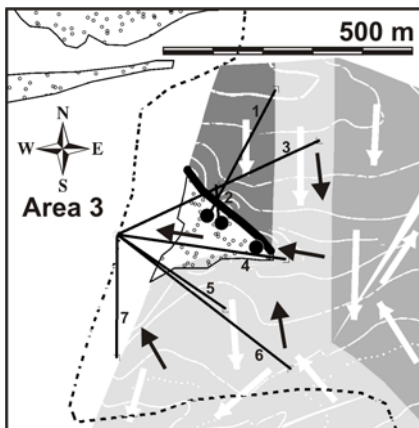
Fig. 9. Model results of area 3 (key: c.f., Fig. 7). The springs occur at the model discharge. Link Nos. 1 and 2 are related to groundwater flow predicted by the model. Link Nos. 3–7 are associated with interflow.
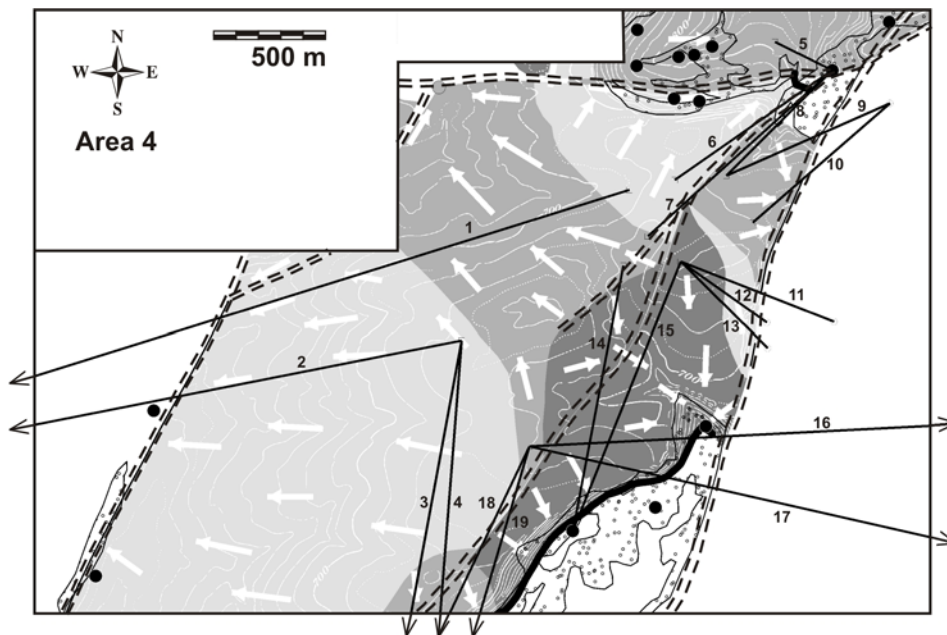
Fig. 10. Model results of area 4 (key: c.f., Fig. 7). Some springs occur in colluvium below model discharges. Nearly all other springs occur in colluvium below a > 20° slope and are associated with interflow. In addition to groundwater flow predicted by the model, other processes are important (c.f., text).

II-4.4. Area 4

Except for one spring in the SW of area 4 (Fig. 10), the spring locations can be related to a model discharge or they can be attributed to interflow as they are situated below a > 20° slope. The hydraulic link situation is more complex. Tracer tests conducted in the eastern part of the study area generally show drainage to the east, whereas tracer tests conducted in the western part reveal drainage to the west. The hydrological model agrees with this trend.

The injection sites of 19 hydraulic links confirmed by former tracer tests are located in area 4. Strictly speaking, only two links (Nos. 2 and 6) agree with the model. Link No. 15 also connects the catchment area with a spring related to the associated model discharge; however, according to the modeled groundwater flow direction, the tracer should have appeared further north.

Link No. 8 can be attributed to interflow, as the injection site is situated in a valley above the spring where the tracer was found. Despite the low topographic gradient at the input site, interflow could also be ascribed to link No. 5.

Key:

Model discharge

● Karstic spring associated with model discharge

● Spring associated with interflow

○ Spring not associated with model discharge or interflow, or spring outside model area

■— Hydraulic link associated with subsurface flow proposed by the conceptual model

■— Hydraulic link associated with other processes than those proposed by the conceptual model (interflow, rock cleavage, faults)

□- - - Hydraulic link associated with process not recognized by the existing data

Model area

Colluvium

---- Fault

······ Outcrop of aquifer base

Fig. 11. Overview of model results. The occurrence of springs is mainly associated with a model discharge. The hydrological model can explain about half of the tracer tests.

As previously mentioned, the model predictions are based on the assumption that groundwater flows along a fault only if an aquitard layer behind the fault acts as a barrier to water flow. However, fault systems are zones of rock weakness and can provide paths for preferential flow. Thus, even if the layer behind the fault is an aquifer, preferential flow

parallel to fault structures can be an important process that is insufficiently accounted for by the model assumptions. The direction of hydraulic link Nos. 6–8, 14, 15, 18, and 19 corresponds to the direction of a major fault system. The tracers of the link Nos. 1–4, 8, 9, and 11–19 have been injected in dolines believed to be associated with fault systems.

Hydraulic link Nos. 1, 2, 16, and 17 connect the Oxfordian aquifer with the deeper Bajocian aquifer. The model predicts such a connection for a catchment area in the NW of area 4, where both aquifers are situated next to each other due to a fault displacement. The injection sites of link Nos. 1 and 2 are very close to this catchment area. For these links, the model also correctly predicts drainage to the west. For link Nos. 16 and 17, however, a changeover to the deeper aquifer must occur solely along the fault zone situated at the tracer injection sites because the 3D geological model reveals no direct contact between the aquifers.

Most of the tracers were injected close to a catchment area boundary of the model. If we do not want to overstrain the model and want to accept minor deviations from the delineated boundaries, hydraulic link Nos. 1, 7, 8, 11–14, 16, and 17 are in agreement with the model. Because their injection sites are very close to a catchment area boundary, deviation from the model prediction is assumed to be very small. Hence, an explanation of these hydraulic links by processes other than those underlying the model assumptions is not mandatory.

Interpretation of hydraulic link Nos. 3 and 4 remains difficult. A N-S trending fault is suggested, as the injection site is a doline ascribed to a fault system by those who conducted the tracer test. However, such a fault is not mapped.

A main difficulty in interpreting the hydraulic links in area 4 is that only six are completely within the model area. Thirteen of the tracers were detected outside the model area, eight of them very far outside. Processes occurring outside the model area cannot be considered by the model but may influence the model results.

II-4.5. Summary

Of the 65 springs located in the model area, 57% can be attributed to a model discharge (Fig. 11, Table 1). 32% are explained by interflow, as they are discharging from Quaternary colluvium below an uphill area sloping at $> 20°$. Only 11% of the springs cannot be explained by subsurface flow predicted by the model or by interflow.

Of the 52 tracer tests conducted in the model area (i.e., the injection sites are within the model area), the hydrological model directly predicts 35% of the hydraulic links (Fig. 11, Table 2), and 56% can be explained further (interflow, cleavage, preferential flow along faults) or the model predictions exhibit very small deviations. Only 10% of the hydraulic links cannot be explained by the existing data.

Table 1: Comparison of model results with the occurrence of springs. Most of the springs agree with the model predictions. One third of the springs is associated with interflow, which is a process not included in the model.

Springs	Percentage (number)
Associated with model discharge	57% (37)
Associated with interflow	32% (21)
Other	11% (7)
Total	100% (65)

Table 2: Comparison of model results with hydraulic links confirmed by tracer tests. More than one third of the tracer tests agree with the model predictions, more than half are associated with processes not included in the model. Better model predictions are obtained if only links with both input and output site within the model area are included. *Italic values*: *results obtained if only catchment areas and model discharges are taken into account and not the groundwater flow direction. The model predicts more than half of the hydraulic links.*

	Percentage (number) of hydraulic links	
	All	With both input and output site within the model area
Predicted by model	34.6% (18) *42.3% (22)*	39.3% (11) *53.6% (15)*
Associated with interflow	21.2% (11) *21.2% (11)*	21.4% (6) *21.4% (6)*
Associated with rock cleavage	11.5% (6) *5.8% (3)*	21.4% (6) *10.7% (3)*
Associated with fault	15.4% (8) *13.5% (7)*	14.3% (4) *10.7% (3)*
Input close to boundary of catchment area	7.7% (4) *7.7% (4)*	0.0% (0) *0.0% (0)*
{ subtotal }	55.8% (29) *48.1% (25)*	57.1% (16) *42.8% (12)*
Open interpretation	9.6% (5)	3.6% (1)
Total	100% (52)	100% (28)

So far, evaluation of model performance does not discriminate between hydraulic links with output sites located outside the model and those with output sites inside the model area. If only the latter tracer tests are considered, 39% of the hydraulic links agree with the subsurface flow predicted by the model and only one (4%) cannot be explained. Because the main focus of the study is the springs within the model area, it is justified to neglect tracer tests in which the tracer showed up in springs outside the model area.

If we relax prediction accuracy further and assume the hydrological model to be validated if a model discharge is linked to its associated catchment area by a tracer test (even though the groundwater flow direction derived from the model suggests the appearance of the tracer somewhere else at the same model discharge), 54% of the tracer tests validate the model. Prediction therefore focuses on a general output area of tracer tests rather than on the exact output locations.

II-5. Discussion

II-5.1. The aquifer base gradient (ABG) approach

When applied to real aquifers, numerical flow simulation approaches require extensive data sets (like hydraulic heads and hydraulic conductivities) for both model setup and calibration. Such data are extremely rare in karst areas and are costly to obtain. Moreover, numerical models accounting for the special situation in karst areas nearly always have to combine a continuum with a discrete channel approach. This is difficult to implement due to the unknown geometry of the conduit network. In contrast, the ABG approach requires only data from geological maps, which often are readily available and are of high quality. In this study, based on the data from the national geological map, the ABG approach reproduced 57% of the spring occurrences in the study area and up to 54% of the hydraulic links confirmed by tracer tests.

The ABG approach is a first step to including geological and tectonic structures in the investigation of karst hydrology on a regional scale. Unlike most previous karst modeling approaches, this method ascribes the main influence on the modeled hydrology to the gradient and the structure of the aquifer base. When applying the ABG approach to the study area, deviations from model predictions indicate that flow processes not yet included in the hydrological model contribute to the discharge of individual springs. The approach has great potential if further geological and structural data are integrated.

Application of the ABG approach to the study area suggests interflow, fracture geometry, and preferential flow along faults to be important factors that influence the hydrology of karst areas, as most deviations from model predictions can be explained by these processes. The inclusion of these factors into an improved hydrological model, with each process leading to different model results, would allow model calibration by comparing the different results to field data. The data needed to calibrate the improved hydrological model include the location of springs and hydraulic links confirmed by tracer tests. These data needs are moderate compared to those of numerical simulation models.

II-5.2. Vulnerability assessment

Because the heterogeneous structure of karst environments is difficult to characterize, groundwater protection in such areas presents a challenge for hydrogeologists. At the same time, karst aquifers are especially vulnerable to human impacts due to high transport velocities and low storage capacities in the conduit flow system. Vulnerability mapping is a well-accepted tool in many countries to provide basic hydrogeologic information for the protection of wells and spring captures used as a drinking water supply. Information about the extent and position of catchment areas is an important constraint of vulnerability mapping designed to protect a drinking water well (source protection). The ABG approach is a straightforward and cost-effective method to delineate catchment areas. Compared to tracer tests, this method does not evaluate selected points but the entire catchment area. The ABG approach allows hypothesizing about subsurface flow paths while tracer tests specify a straight-lined link of the input and output location. Although breakthrough curves resulting from tracer tests can provide valuable information about aquifer properties, tracer tests in karst areas often bear resemblance to a game of chance if they are not founded on a hydrological model.

Evaluation of the dominating flow processes associated with individual springs by the hydrological model allows researches to draw conclusions about the vulnerability distribution of a spring area. Springs connected to the catchment area by preferential flow along fault systems or by interflow, for instance, are expected to be more vulnerable to contamination than springs deriving their water from deeply penetrating flow paths not subjected to preferential flow. However, vulnerability grading as provided by mapping methods is not possible.

The ABG approach cannot replace existing vulnerability assessment methods; rather, it constitutes one element within an integrative groundwater protection strategy. It adds information to existing methods, like the extent of catchment areas, evidence of flow processes contributing to the discharge of individual springs, and the overall structural framework. Other methods provide, for instance, a grading of the vulnerability in the catchment areas or flow velocities. The hydrological model can be a useful planning tool, especially during an early phase of the hydrological investigation of large and complex karst areas. An integrative concept of vulnerability assessment may, for instance, include the following steps: (1) Catchment areas are delineated based on the applied ABG approach; (2) The proposed catchment areas are verified by well-founded tracer tests, providing additional information on flow velocities; (3) Deviations from model predictions indicate processes that cannot be assessed by the hydrological model. As far as relevant springs are concerned, field investigations are subsequently conducted. These may include the evaluation of fracture joints, spring hydrographs or temperature measurements; and (4) Vulnerability maps are established based on the determined catchment areas, results of tracer tests, and other field investigations.

II-5.3. Future work

Linking 3D geological models to numerical models is a future challenge. Numerical modeling of flow and transport from spring hydrographs and tracer breakthrough curves provide quantitative and time-related information. These data could subsequently be combined with spatial data obtained by a 3D geological model. Quantification of the aquifer geometry can in return serve as input data for such a numerical model (Butscher and Huggenberger, 2005).

Because the conceptual karst model that underlies our hydrological model is only valid for mature, shallow, and unconfined karst systems, the ABG approach is restricted to such environments. Other karst regions besides the Swiss tabular Jura to which the aforementioned constraints can also be applied occur throughout the world (e.g., the Swabian Alb in Germany, the limestone formations of the Paris Basin in France, and the Interior Low Plateau region of central Kentucky and southern Indiana in the United States) (e.g., Herak and Stringfield, 1972). Because corresponding hydrological models of different karst settings (e.g., folded limestone formations or deep karst) would require a different conceptual karst model, they are not dealt with in this paper but are certainly worth studying.

II-6. Summary and Conclusions

3D geological modeling is a useful tool for establishing the geological and structural framework of a hydrological model. The ABG approach does not require extensive data sets and provides a conceptual background to design well-founded field experiments. The ABG approach presented in this study was used to delineate spring catchment areas and to identify flow processes in mature, shallow karst regions. It was based on a hydrological model for which the ABG was assumed to mainly control the regional hydrology. In this study, the model predicted the occurrence of more than half of the springs in the study area and up to 54% of the hydraulic links confirmed by tracer tests. Thus, the ABG approach can contribute to vulnerability assessment and can be used as an efficient planning tool within an integrative source protection concept, especially for large and complex karst areas.

Acknowledgments

References

Aller, L., Bennett, T., Lehr, J. H., Petty, R. J., 1987. DRASTIC: A Standardized System for Evaluating Ground Water Pollution Potential Using Hydrogeological Settings. U.S. Environmental Protection Agency, Oklahoma.

Anderson, J., Dverstorp, B., 1987. Conditional Simulations of fluid flow in three-dimensional networks of discrete fractures. Water Resour. Res. 23 (10), 1876-1886.

Apel, R., 1971. Hydrologische Untersuchungen im Malmkarst der Südlichen und Mittleren Frankenalb. Geologica Bavarica 64, 268-355.

Auckenthaler, A., Raso, G., Huggenberger, P., 2002. Particle transport in a karst aquifer: Natural and artificial tracer experiments with bacteria, bacteriophages and microspheres. Wat. Sci. Technol. 46 (3), 131-138.

Bakalowicz, M., 2005. Karst Groundwater: a challenge for new resources. Hydrogeol. J. 13 (1), 148-160, doi 10.1007/s10040-004-0402-9.

Baltes, B., von Fumetti, S., Küry, D., Contesse, E., Butscher, C., Huggenberger, P., Suter, D., Leimgruber, W., Nagel, P., 2005. Basel entdeckt seine Quellen. Deutsche Gesellschaft für Limnologie (DGL). Proceedings 2004, Potsdam, September 20-24, 226-230.

Bauer, S., Liedl, R., Sauter, M., 2003. Modeling of karst aquifer genesis: influence of exchange flow. Water Resour. Res. 39 (10), 1285, doi 10.1029/2003WR002218.

Bauer, S., Liedl, R., Sauter, M., 2005. Modeling the influence of epikarst evolution on karst aquifer genesis: A time-variant recharge boundary condition for joint karst-epikarst development. Water Resour. Res. 41, W09416, doi 10.1029/2004WR003321.

Birk, S., Liedl, R., Sauter, M., Teutsch, G., 2003. Hydraulic boundary conditions as a controlling factor in karst genesis: A numerical modeling study on artesian conduit development in gypsum. Water Resour. Res. 39 (1), 1004, doi 10.1029/2002WR001308.

Birk, S., Liedl, R., Sauter, M., Teutsch, G., 2005. Simulation of the development of gypsum maze caves. Environ. Geol. 48 (3), 296-306, doi 10.1007/s00254-005-1276-4.

Bitterli-Brunner P., Fischer, H., Herzog, P., 1984. Geologische Karte Blatt Arlesheim 1067. Geologischer Atlas der Schweiz.

Bitterli-Brunner, P., Fischer, H., 1988. Erläuterungen zum Blatt Arlesheim 1067. Geologischer Atlas der Schweiz.

Bögli, A., 1980. Karst hydrology and physical speleology. Springer, Berlin.

Butscher, C., Huggenberger, P., 2005. Vulnerability assessment by combined 3D geological and mathematical modeling. Geophysical Research Abstracts 7, 3600.

Civita, M., De Maio, M., 2000. Valutazione e cartografia automatica della vulnerabilità degli acquiferi all'inquinamento con il systema parametrico SINTACS R5 (Evaluation and automatic cartography of aquifer vulnerability using the parametric system SINTACS R5). Pitagora Editrice, Bologna.

Clemens, T., Hückinghaus, D., Liedl, R., Sauter, M., 1999. Simulation of the development of karst aquifers: role of the Epikarst. Int. J. Earth Sci. 88, 157-162.

COST 620, 2003. Vulnerability and risk mapping for the protection of carbonate (karst) aquifers, Final report (COST action 620). European Comission, Directorat-General XII Science, Research and Development, Brüssel.

Daly, D., Dassargues, A., Drew, D., Dunne, S., Goldscheider, N., Neale, S., Popescu, I. C., Zwahlen, F., 2002. Main concepts of the „European approach" to karst-groundwater-vulnerability assessment and mapping. Hydrogeol. J. 10, 340-345.

Doerfliger, N., Jeannin, P.-Y., Zwahlen, F., 1999. Water vulnerability assessment in karst environments: a new method of defining protection areas using a multi-attribute approach and GIS tools (EPIK method). Environ. Geol. 39 (2), 165-176.

Dreybrodt, W., 1990. The role of dissolution kinetics in the development of karst aquifers in limestone: a model simulation of karst evolution. J. Geol. 98 (5), 639-655.

Ford, D. C., Ewers, R. O., 1978. The development of cave systems in the dimensions of length and depth. Can. J. Earth Sci. 15 (11), 1783-1798.

Ford, D. C., Williams, P. W., 1989. Karst geomorphology and hydrology. Chapman and Hall, New York.

Goldscheider, N., 2005. Karst groundwater vulnerability mapping: application of a new method in the Swabian Alb, Germany. Hydrogeol. J. 13, 555-564, doi 10.1007/s10040-003-0291-3.

Goldscheider, N., Klute, M., Sturm, S., Hötzl, H., 2000. The PI method − a GIS-based approach to mapping groundwater vulnerability with special consideration of karst aquifers. Zeitschrift für angewandte Geologie 46 (3), 157-166.

Gürler, B., Hauber, L., Schwander, M., 1987. Die Geologie der Umgebung von Basel mit Hinweisen über die Nutzungsmöglichkeiten der Erdwärme. Beitrag zur Geologischen Karte der Schweiz 160.

Harbaugh, A. W., McDonald, M. G., 1996. Programmers documentation for MODFLOW-96 − An update to the US Geological Survey modular finite-difference groundwater model. U. S. Geol. Surv. Open File Rep., 96-486.

Herak, M., Stringfield, V. T., 1972. Karst - Important Karst Regions of the Norhtern Hemisphere. Elsevier, Amsterdam.

Herold, T., Jordan, P., Zwahlen, F., 2000. Influence of tectonic structures on karst flow patterns. Eclogae Geol. Helv. 93, 349-362.

Hötzl, H., 1996. Grundwasserschutz in Karstgebieten. Grundwasser 1 (1), 5-11.

Jeannin, P.-Y., 2001. Modeling flow in phreatic and epiphreatic karst conduits in the Hölloch Cave (Muotathal, Switzerland). Water Resour. Res. 37 (2), 191-200.

Kaufmann, G., Braun, J., 2000. Karst aquifer evolution in fractured, porous rocks. Water Resour. Res. 36, 1381-1391.

Kaufmann, G., 2002. Karst aquifer evolution in a changing water table environment. Water Resour. Res. 38 (6), doi 10.1029/2001WR000256.

Kaufmann, G., 2003. Modelling unsaturated flow in an evolving karst aquifer. J. Hydrol. 276, 53-70.

Kiraly, L., 1998. Modeling karst aquifers by the combined discrete channel and continuum approach. Bulletin d'Hydrogéologie 16, 77-98.

Klimchouk, A. and Ford, D., 2000. Types of Karst and Evolution of Hydrogeologic Setting. In: Klimchouk, A. B., Ford, D. C., Palmer, A. N., Dreybrodt, W., (Eds.), Speleogenesis: Evolution of karst aquifers, 45-53, Nat. Speleologic Soc., Huntsville, Ala.

Kovács, A., Jeannin, P.-Y., 2003. Hydrogeological overview of the Bure plateau, Ajoie, Switzerland. Eclogae Geol. Helv. 96, 367-379.

Liedl, R., Sauter, M., Hückinghaus, D., Clemens, T., Teutsch, G., 2003. Simulation of the development of karst aquifers using a coupled continuum pipe flow model. Water Resour. Res. 39 (3), 1057, doi 10.1029/2001WR001206.

Long, J. C. S., Remer, J. S., Wilson, C. R., Witherspoon, P. A., 1982. Porous media equivalents for networks of discontinuous fractures. Water Resour. Res. 18 (3), 645-658.

Luetscher, M., Perrin, J., 2005. The Aubonne karst aquifer (Swiss Jura). Eclogae Geol. Helv. 98, 237-248.

Magiera, P., 2000. Methoden zur Abschätzung der Verschmutzungsempfindlichkeit des Grundwassers. Grundwasser 3 (2000), 103-114.

Mallet, J. L., 2002. Geomodeling. Oxford University Press, Oxford.

Sauter, M., 1992. Quantification and forecasting of regional groundwater flow and transport in a karst aquifer (Gallusquelle, Malm, SW Germany). Tübinger Geowissenschaftliche Arbeiten C13, Tübingen.

Sauter, M., Kovács, A., Geyer, T., Teutsch, G., 2006. Modellieruing der Hydraulik von Grundwasserleitern − Eine Übersicht. Grundwasser 3 (2006), 143-156, doi 10.1007/s00767-006-0140-0.

Schmassmann, H., 1972. Baselbieter und westlicher Aargauer Tafeljura. In: Jäckli, H., Kempf, T., 1972, Erläuterungen zum Blatt Bözberg-Beromünster 1. Hydrogeologische Karte der Schweiz, 93-100.

Spottke, I., Zechner, E., Huggenberger, P., 2005. The southeastern border of the Upper Rhine Graben: a 3D geological model and its importance for tectonics and groundwater flow. Int. J. Earth Sci. 94, 580-593.

Vrba, J., Zoporozec, A., (Eds.), 1994. Guidebook on Mapping Groundwater Vulnerability. International Contributions to Hydrogeology (IAH) 16, Hannover.

White, W. B., 1999. Conceptual models for karst aquifers. In: Palmer, A. N., Palmer, M. V., Sasowsky, I. D., (Eds.), Karst modeling. Karst Waters Inst. Spec. Publ. 5, 11-16, Karst Waters Inst., Charles town, W. Va.

Worthington, S. R. H., 2005. Hydraulic and geological factors influencing conduit flow depth. Cave and Karst Science 31 (3), 123-134.

III. Intrinsic vulnerability assessment in karst areas: a numerical modeling approach

Abstract

The main objective of this study was to quantify the intrinsic vulnerability of karst springs by numerical modeling. A global approach is used, modeling the discharge of a karst spring. This approach includes the hydrological dynamics of karst systems and is applicable to complex karst settings, where structural and hydraulic characteristics cannot be spatially resolved with sufficient accuracy. A basis model and four extended versions were set up to determine the individual characteristics of the present karst system and to include different flow processes that could affect the vulnerability of the system. All these model setups consider, besides recharge (soil and epikarst system), the conduit and the diffuse flow system as the main characteristics of the karst aquifer. The extended setups additionally account for surface runoff, an intermediate flow system, exchange flow between the conduit and the diffuse system and seasonal variation in the water storage capacity of the recharge system. Potential use of the calibrated models to quantify the intrinsic vulnerability of karst springs is discussed on the basis of (1) the temporally changing contributions of the conduit and diffuse flow systems to spring discharge, and (2) modeled breakthrough curves resulting from a standardized contaminant input into the karst system. The modeling approach complements vulnerability mapping methods by addressing temporal and quantitative aspects of vulnerability.

III-1. Introduction

This study originated in the context of an interdisciplinary spring project [*Baltes et al.*, 2005], which was implemented in a karst area of northern Switzerland. Concern about the endangerment of the water quality of springs played a major role throughout the investigations. During the past decade, scientific research has developed diverse strategies for the protection of groundwater and spring water, with methods for groundwater vulnerability mapping being the most important [e.g., *Aller et al.*, 1987; *Civita and De Maio*, 2000; for an overview see *Vrba and Zoporozec*, 1994; *Magiera*, 2000]. Karst aquifers have complex and distinct characteristics, which make them very different from other aquifers [*Bakalowicz*, 2005]. They are extremely heterogeneous and anisotropic and therefore particularly vulnerable to contamination [*Goldscheider*, 2005]. In view of these special characteristics, some of the methods used for vulnerability assessment are specifically designed for karst environments [*Doerfliger et al.*, 1999; *Daly et al.*, 2002; *COST 620*, 2003].

However, important points remain unresolved. First, mapping approaches disregard the dynamics of vulnerability: They assume that some places within the catchment area are more vulnerable to contamination than others, but they fail to consider the temporal variation in vulnerability that may arise in a given place in response to hydrological variation. Secondly, the various indices used to generate vulnerability maps are largely conceptual (and thus subjective) [*Connell and Van den Daele*, 2003]. There is a need for an examination of vulnerability concepts from a quantitative point of view, and for the establishment of clearly identified reference criteria for quantification, comparison and validation purposes [*Brouyère*, 2003]. Thirdly, the existing techniques relate vulnerability to the catchment area, which is the preferable approach in many cases. In the present case, however, it is more practical to relate vulnerability to the spring, because the above-mentioned spring project entailed a comparison of different springs with respect to their sensitivity to contamination. Comparison of spring captures in terms of vulnerability may also be relevant for drinking water suppliers and regional planners.

In the literature it is often stated that the limitations of vulnerability maps, such as those cited above, could be overcome by mathematical modeling. *Goldscheider* [2002] remarked that, despite the large number of mathematical flow and transport models, models have rarely been used for vulnerability mapping. *Gogu and Dassargues* [2000] pointed out that new challenges for hydrogeologists will consist in the integration of results from process-based numerical

models into vulnerability mapping techniques. Numerical flow and transport models have been successfully used to assess specific vulnerability to a certain contaminant, mostly nitrate or pesticides [e.g., *Fogg et al.*, 1999]. However, there have been few attempts to quantify intrinsic vulnerability by numerical modeling, i.e., taking into account the hydrogeological characteristics of an area independently of the nature of the contaminants. In *COST 620* [2003], the use of calibrated numerical simulations is suggested for the validation of vulnerability maps. *Jeannin et al.* [2001] developed the analytical computer program VULK to validate vulnerability maps on the basis of tracer tests (advection-dispersion model). This approach, however, is restricted to a few selected points within the catchment area. Distributed numerical models that include the whole catchment area in a karst environment [e.g. *Quinn and Tomasko*, 2000] require extensive field data, both for model setup (e.g., geometry of karst channel network) and model calibration (e.g., hydraulic head and hydraulic conductivities). Such data are extremely rare in karst areas. For this reason, distributed models have mostly been interpretive, with a focus on demonstrating a method rather than providing a refined, calibrated solution [e.g. *Quinn et al.*, 2006], or have been used for studying the fundamental functions of karst systems [e.g., *Kiraly*, 1998; *Liedl et al.*, 2003], rather than simulating the groundwater flow of a specific study area.

In view of these limitations to the assessment of the vulnerability of karst systems, the main objective of this study was to develop a technique to determine the intrinsic vulnerability of individual karst springs. The method should provide quantitative information on vulnerability and include the hydrological dynamics of karst systems. Moreover, it should be applicable to complex karst settings that cannot be spatially resolved. Hydrograph separation methods based on mass balance [e.g., *Atkinson*, 1977; *Dreiss*, 1989] meet all these requirements, but have limited predictive power for conditions different from those of the observation period.

Therefore, we have chosen a global approach to modeling the discharge of a karst spring [*Sauter et al.*, 2006]. The data include time series of precipitation, evapotranspiration, and spring discharge, with the lattermost representing the integration of all active hydraulic processes. As a first step, we set up a basis model and four extended versions to account for the individual characteristics of the present karst system, with each setup having different flow processes that could affect the vulnerability of the system. In a second step, we suggest ways to quantify the intrinsic vulnerability of karst springs and its variation in time. These are based (1) on the relative contributions of flow systems to spring discharge, which are

temporally variable, and (2) on the modeled breakthrough curves resulting from a standardized input of contaminant into the system. This modeling approach complements static information on the vulnerability distribution in the catchment areas, e.g., obtained from vulnerability mapping, by quantitative information on the temporal vulnerability distribution at the springs.

III-2. Study Area

The spring (Untere Rappenfluhquelle) selected for this study is 10 km southeast of the city of Basel in northwest Switzerland (Figure 1). It is one of six spring captures together draining a catchment of approximately 1 km^2. The catchment is situated on a karst plateau (Gempen Plateau) of the Swiss Tabular Jura, a low mountain range composed of predominantly flat-lying Triassic and Jurassic sediments. The aquifer comprises massive Oxfordian limestone of varying thickness (40-70 m) with high primary porosity, representing a patch-reef facies of a shallow carbonate platform. The aquifer base is made up of Oxfordian plastic marls approximately 100 m thick. The aquifer is fractured and highly karstified, having been exposed to the land surface since the end of the Jurassic [*Gürler et al.*, 1987]. The hydrogeology of the study area is characterized by karst water circulation in an unconfined setting. According to the hydrogeologic evolutionary typology for karst proposed by *Klimchouk and Ford* [2000], the setting corresponds to an exposed, open karst.
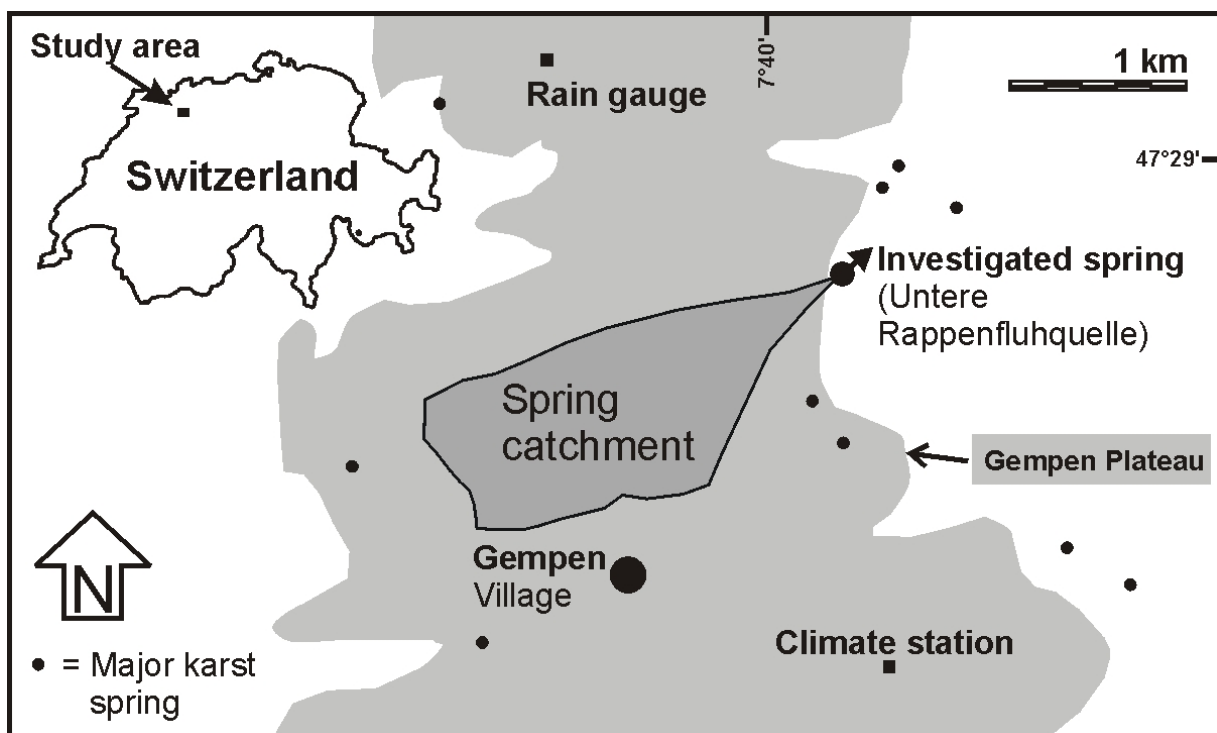

Figure 1. Study area.

III-3. Modeling Technique

III-3.1. Method

Model simulation and parameter estimation used the software AQUASIM (version 2.1e), which is designed for the identification and simulation of aquatic systems [*Reichert*, 1994a]. For details concerning the numerical algorithms used by AQUASIM refer to *Reichert* [1994b].

We used the mixed reactor compartments of the software with a variable volume to represent different flow systems. The current volume of each compartment is calculated by AQUASIM as the solution of the differential equation

$$\frac{dV_R}{dt} = Q_{R,in} - Q_{R,out} \tag{1}$$

where V_R is the reactor volume, t is time, $Q_{R,in}$ is the volumetric inflow and $Q_{R,out}$ is the volumetric outflow of the reactor. The outflow must be specified by the program user. The inflow must also be specified by the program user when it originates from outside the system; else it is given by the calculated flow from connected compartments (see below). The temporal change in the concentration of substances dissolved in the water is given as

$$\frac{dC}{dt} = \frac{I_{in}}{V_R} - \frac{Q_{R,out}}{V_R} \cdot C + r_c \tag{2}$$

where C is the substance concentration, I_{in} is the loading of that substance into the reactor (mass per unit time), and r_c is the transformation rate of that substance. This rate is given as

$$r_c = -k_{deg\,r} \cdot C \tag{3}$$

where k_{degr} is the degradation rate coefficient.

The compartments can be connected by links. The water inflow and the mass flow of substances into the link are given by the outflow from the compartment to which the inflow of the link is connected. A link can have bifurcations to other compartments or out of the system.

The flows of water and substance through the bifurcations must be specified by the program user, who must ensure that these flows do not exceed the inflow into the link. The water and substance outflows of the link are then calculated by AQUASIM according to the equations

$$Q_{L,out} = Q_{L,in} - \sum Q_{L,bif} \tag{4}$$

and

$$I_{L,out} = I_{L,in} - \sum I_{L,bif} \tag{5}$$

where $Q_{L,in}$ and $Q_{L,out}$ are the water inflow from and outflow to the connected reactor, $I_{L,in}$ and $I_{L,out}$ are the respective substance loadings, and $Q_{L,bif}$ and $I_{L,bif}$ are, respectively, the flow and loading through a bifurcation.

Model parameters are estimated minimizing the sum of the squares of the weighted deviations between measurements and calculated model results

$$\chi^2(p) = \sum_{i=1}^{n} \left(\frac{y_{meas,i} - y_i(p)}{\sigma_{meas,i}} \right)^2 \tag{6}$$

where $y_{meas,i}$ is the ith measurement, $y_i(p)$ is the value calculated by the model at the time of the ith measurement, p is the set of model parameters to be estimated, $\sigma_{meas,i}$ is the standard deviation of ith measurement and n is the number of measured data points. The standard deviation $\sigma_{meas,i}$ is calculated as

$$\sigma_{meas,i} = \sqrt{\sigma_{abs}^2 + \left(\sigma_{rel} \cdot y_{meas,i} \right)^2} \tag{7}$$

where σ_{abs} and σ_{rel} are the absolute and relative standard deviation, respectively, specified by the program user (σ_{abs} is the contribution to $\sigma_{meas,i}$ that is independent from the measured value, and σ_{rel} is a factor determining the contribution to $\sigma_{meas,i}$ that is proportional to the measured value).

III-3.2. Input Data and Boundary Conditions

Discharge from the spring under investigation was recorded continuously with a V-notch (triangular) weir combined with a pressure probe to measure the water level [*Ackers et al.*, 1978]. Precipitation and other meteorological data were recorded every 10 minutes at an automatic climate station (operated by the Institute of Meteorology, Climate and Remote Sensing, University of Basel) approximately 1.6 km south of the spring (Figure 1). Calculation of the potential evapotranspiration was based on the Penman equation [*Penman*, 1956] and used air temperature, shortwave downward radiation, wind velocity and relative humidity [*DVWK*, 1996] according to the formula of *Wendling et al.* [1991]. As the rain gauge of the meteorological station was not heated, daily precipitation for months with snowfall was taken from a rain gauge (operated by MeteoSwiss) approx. 1.4 km northwest of the spring. For these months, a rainfall equivalent that considered solid precipitation and runoff generated by snowmelt was calculated by use of the snow routine of the HBV model of *Bergström* [1992]. This routine is based on the temperature index method (for a recent overview of this approach see *Hock* [2003], and the physical basis is discussed by *Ohmura* [2001]), and was provided by the computer program HBV-light version 2.0 [*Seibert*, 2002]. The model parameters of the snow routine were estimated according to the findings of *Braun* [1985] in a comparable catchment in northern Switzerland.

In the present study, we simulated a period of 461 days from 28 May 2004 until 31 August 2005 for all model setups (investigation period). In order to minimize the influence of initial reactor volumes on the model results, the simulation was started 240 days before the investigation period on 1 October 2003 ("warming-up" period). For this period meteorological data, but no discharge data, were available.

At first, parameter estimation was performed by fitting the calculated spring discharge to the daily average of the measured spring hydrograph. The resulting best fit, however, poorly reproduced the discharge peaks. This was due to the fact that times with base flow conditions are overrepresented in the spring hydrograph. Therefore, local extreme values of the spring hydrograph were chosen as fit targets. As a result, the best fits reproduce the rise to local maxima and the following recession to local minima much better than the previous efforts.

We used a value of 0.74 m^3/d for the absolute standard deviation, corresponding to the accuracy of the pressure-probe used for the discharge measurement, and a value of 0.015 for

the relative standard deviation, as this is the average standard deviation of the gauging measurements conducted to calibrate the relationship between the measured water level at the V-notch weir and the discharge.

All constant model parameters of the different setups were estimated by the described parameter estimation routine except the initial reactor volume $V_{ini,C}$ of the compartment representing the conduit flow system. Residence times in this compartment are very short compared with the warming-up period preceding the actual simulation, suggesting that $V_{ini,C}$ has very little influence on the model results.

III-3.3. Model Setups

Every karst system has its own unique characteristics. To find out the important processes of the present karst system, simulations of spring discharge were based on a basis model and four extended model setups, each considering an additional characteristic of the system. This approach also allows investigation of the influence of the different flow processes on vulnerability. The basis model considers, besides recharge (soil and epikarst system), the conduit and the diffuse flow system as the main characteristics of karst aquifers. The extended setups additionally account for surface runoff, an intermediate flow system, exchange flow between the conduit and the diffuse system, and seasonal variation in the water storage capacity of the recharge system.

Basis model RCD

Karst aquifers exhibit a dual flow system [*Kiraly*, 1998]: water flows in pipe-like conduits and open cave stream channels as well as through fractures and pores [*White*, 1988]. This dual "conduit and diffuse" concept is widely accepted and confirmed [*Schuster and White*, 1971; *Atkinson*, 1977; *Ford and Williams*, 1989]. Recharge to the conduit and diffuse system is controlled by the above-lying soil and, as a special characteristic of karst, the epikarst system [*Williams*, 1983]. The epikarst determines the distribution of recharge to a karst aquifer in both space and time [*Bauer et al.*, 2005].

The basis model RCD is designed to account for the main characteristics of karst systems and therefore comprises the compartments R, C and D, representing the groundwater Recharge system (soil and epikarst system), the Conduit flow system and the Diffuse flow system.
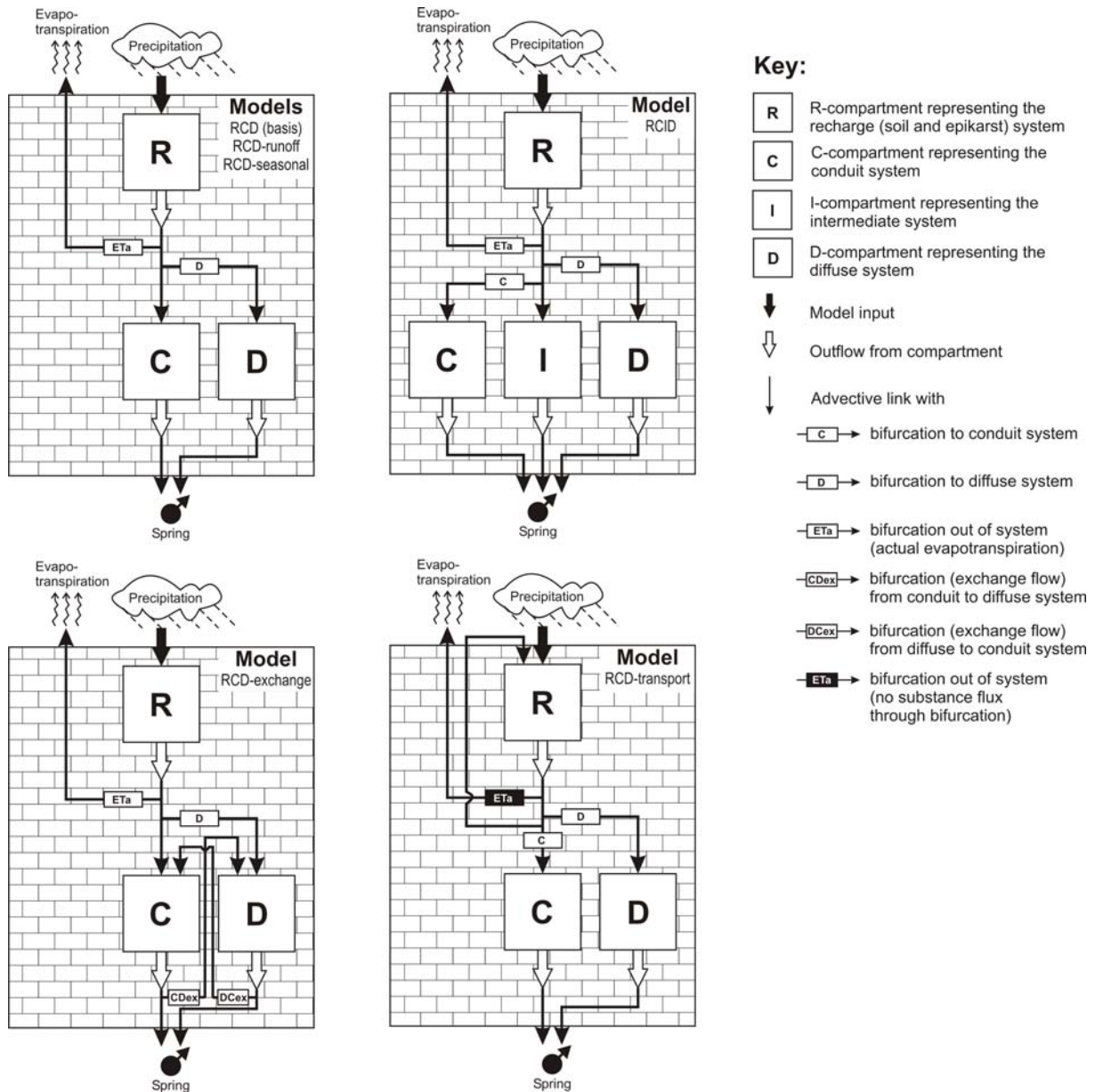
Figure 2. Illustration of model setups.

Measured precipitation defines the input of the recharge system and is available for actual evapotranspiration. The latter is represented by the calculated potential evapotranspiration, which is increasingly reduced when the available water of the recharge system drops below a "water stress" threshold value, V_{ws}. Groundwater recharge to the karst systems occurs when the water content of the recharge system exceeds the retention capacity ("field capacity" [*Sumner*, 2000]) defined as the threshold volume, V_{fc}. One part of the groundwater recharge, which is determined by the constant model parameter X_D, enters the diffuse system; the rest enters the conduit system. The diffuse system and the conduit system both contribute to spring discharge according to their water content, with shorter residence times (greater outflow coefficient) in the conduit system. The model formulation is given in detail by

illustration of the model setup (Figure 2) and further system definitions (inflow to model, outflow of compartments, bifurcating flows; Tables 1 and 2). The simulated spring discharge of the basis model RCD (Figure 3) is based on estimated model parameters indicated in Table 3, leading to a best fit of calculated to measured spring discharge quantified by $\chi^2 = 15{,}394$.

Table 1. Notation of model variables.

Variable	Description, [unit], (type)
A	Extent of catchment area, [m2], (constant model parameter)
amp	Amplitude of Vfc,max reduction function, [-], (constant model parameter)
C	Concentration of standard contaminant, [mg/m3], (system variable)
C_C	Capacity of compartment C (conduit system), [m3/Pa], (constant model parameter)
C_D	Capacity of compartment D (diffuse system), [m3/Pa], (constant model parameter)
ETp	Potential evapotranspiration, [m/d], (value spreadsheet)
I_{in}	Input loading to model, [mg/d], (value spreadsheet)
k_{degr}	Degradation rate coefficient, [1/d], (constant)
P	Phase shift of ρseas, [d], (constant model parameter)
P_C	Potential of compartment C (conduit system), [Pa], (expression)
P_D	Potential of compartment D (diffuse system), [Pa], (expression)
$Prec$	Precipitation, [m/d], (value spreadsheet)
$Prec_{eff}$	Effective precipitation (precipitation – actual evapotranspiration), [m/d], (value spreadsheet)
Q	Flow, [m3/d], (system variable)
$Q_{bif,C}$	Bifurcating flow to compartment C (fraction of groundwater recharge to conduit system), [m3/d], (expression)
$Q_{bif,CDex}$	Bifurcating exchange flow from compartment C (conduit system) to compartment D (diffuse system), [m3/d], (expression)
$Q_{bif,D}$	Bifurcating flow to compartment D (fraction of groundwater recharge to diffuse system), [m3/d], (expression)
$Q_{bif,DCex}$	Bifurcating exchange flow from compartment D (diffuse system) to compartment C (conduit system), [m3/d], (expression)
$Q_{bif,ETa}$	Bifurcating flow (actual evapotranspiration) out of model system, [m3/d], (expression)
Q_{in}	Input flow to model, [m3/d], (expression)
Q_{meas}	Measured spring discharge, [m3/d], (value spreadsheet, fit target)
$Q_{out,C}$	Outflow of compartment C (conduit system), [m3/d], (expression)
$Q_{out,D}$	Outflow of compartment D (diffuse system), [m3/d], (expression)
$Q_{out,I}$	Outflow of compartment I (intermediate system), [m3/d], (expression)
$Q_{out,R}$	Outflow of compartment R (recharge system), [m3/d], (expression)
$Q_{recharge}$	Groundwater recharge, [m3/d], (expression)
$Q_{spring,C}$	Outflow of compartment C (conduit system) to spring, [m3/d], (expression)
$Q_{spring,D}$	Outflow of compartment D (diffuse system) to spring, [m3/d], (expression)
t	Time, [d], (system variable)
V	Volume of regarded compartment, [m3], (system variable)
V_C	Actual volume of compartment C (conduit system), [m3], (system variable)
V_D	Actual volume of compartment D (diffuse system), [m3], (system variable)
V_{fc}	Threshold volume for groundwater recharge ("field capacity"), [m3], (constant model parameter)
$V_{fc,max}$	Maximum threshold volume for groundwater recharge ("maximum field capacity"), [m3], (constant model parameter)
$V_{fc,var}$	Variable threshold volume for groundwater recharge (variable "field capacity"), [m3], (expression)
V_I	Actual volume of compartment I (intermediate system), [m3], (system variable)
VI	Vulnerability Index, [-], (expression)
$V_{ini,D}$	Initial volume of compartment D (diffuse system), [m3], (constant model parameter)
$V_{ini,R}$	Initial volume of compartment R (recharge system), [m3], (constant model parameter)
$V_{ini,C}$	Initial volume of compartment C (conduit system), [m3], (constant)
$V_{ini,I}$	Initial volume of compartment I (intermediate system), [m3], (constant model parameter)
V_R	Actual volume of compartment R (recharge system), [m3], (system variable)
V_{sat}	Threshold volume for input to system ("saturation of recharge system"), [m3], (constant model parameter)
V_{ws}	Threshold volume for limiting ETp to actual Evapotranspiration ("water stress"), [m3], (constant model parameter)
X_C	Coefficient determining fraction of groundwater recharge to conduit system ($0 \leq XC \leq 1$), [-], (constant model parameter)
X_D	Coefficient determining fraction of groundwater recharge to diffuse system ($0 \leq XD \leq 1$), [-], (constant model parameter)
α_C	Outflow coefficient of compartment C (conduit system), [1/d], (constant model parameter)
α_D	Outflow coefficient of compartment D (diffuse system), [1/d], (constant model parameter)
α_I	Outflow coefficient of compartment I (intermediate system), [1/d], (constant model parameter)
α_R	Outflow coefficient of compartment R (recharge system), [1/d], (constant model parameter)
ε	Exchange coefficient of compartments C (conduit system) and D (diffuse system), [1/d], (constant model parameter)
ρ_{seas}	Vfc,max reduction function, [-], (expression)

Table 2. System definitions of the different model setups (for description of model variables see Table 1).

	Expression (**bold:** expression different from basis model RCD)					
Variable	Basis model RCD	Model RCD-runoff	Model RCID	Model RCD-exchange	Model RCD-seasonal	Model RCD-transport
P_C				V_C / C_C		
P_D				V_D / C_D		
$Q_{bif,C}$			$X_C \cdot (1 - X_D) \cdot Q_{recharge}$			$(1 - X_D) \cdot Q_{recharge}$
$Q_{bif,CDex}$				**if $P_C > P_D$ then $(P_C - P_D) \cdot \varepsilon$ else 0**		
$Q_{bif,D}$	$X_D \cdot Q_{recharge}$	$X_D \cdot Q_{recharge}$	$X_D \cdot Q_{recharge}$	$X_D \cdot Q_{recharge}$	$X_D \cdot Q_{recharge}$	$X_D \cdot Q_{recharge}$
$Q_{bif,DCex}$				**if $P_D > P_C$ then $(P_D - P_C) \cdot \varepsilon$ else 0**		
$Q_{bif,ETa}$	if $V_R < V_{ws}$ then $(V_R / V_{ws}) \cdot ETp \cdot A$ else $ETp \cdot A$	if $V_R < V_{ws}$ then $(V_R / V_{ws}) \cdot ETp \cdot A$ else $ETp \cdot A$	if $V_R < V_{ws}$ then $(V_R / V_{ws}) \cdot ETp \cdot A$ else $ETp \cdot A$	if $V_R < V_{ws}$ then $(V_R / V_{ws}) \cdot ETp \cdot A$ else $ETp \cdot A$	if $V_R < V_{ws}$ then $(V_R / V_{ws}) \cdot ETp \cdot A$ else $ETp \cdot A$	if $V_R < V_{ws}$ then $(V_R / V_{ws}) \cdot ETp \cdot A$ else $ETp \cdot A$
Q_{in}	$Prec \cdot A$	**if $V_R < (V_{fc}+V_{sat})$ then $Prec \cdot A$ else $[(V_{fc}+V_{sat})/V_R]$**	$Prec \cdot A$	$Prec \cdot A$	$Prec \cdot A$	$Prec \cdot A$
$Q_{out,C}$	$\alpha_C \cdot V_C$	$\alpha_C \cdot V_C$	$\alpha_C \cdot V_C$	$\boldsymbol{Q_{spring,C} + Q_{bif,CDex}}$	$\alpha_C \cdot V_C$	$\alpha_C \cdot V_C$
$Q_{out,D}$	$\alpha_D \cdot V_D$	$\alpha_D \cdot V_D$	$\alpha_D \cdot V_D$	$\boldsymbol{Q_{spring,D} + Q_{bif,DCex}}$	$\alpha_D \cdot V_D$	$\alpha_D \cdot V_D$
$Q_{out,I}$			$\alpha_I \cdot V_I$			
$Q_{out,R}$	$Q_{bif,ETa} + Q_{recharge}$	$Q_{bif,ETa} + Q_{recharge}$	$Q_{bif,ETa} + Q_{recharge}$	$Q_{bif,ETa} + Q_{recharge}$	$Q_{bif,ETa} + Q_{recharge}$	$Q_{bif,ETa} + Q_{recharge}$
$Q_{recharge}$	if $V_R < V_{fc}$ then 0 else $\alpha_R \cdot (V_R - V_{fc})$	if $V_R < V_{fc}$ then 0 else $\alpha_R \cdot (V_R - V_{fc})$	if $V_R < V_{fc}$ then 0 else $\alpha_R \cdot (V_R - V_{fc})$	if $V_R < V_{fc}$ then 0 else $\alpha_R \cdot (V_R - V_{fc})$	**if $V_R < V_{fc,var}$ then 0 else $(V_R - V_{fc,var}) \cdot \alpha_R$**	if $V_R < V_{fc}$ then 0 else $\alpha_R \cdot (V_R - V_{fc})$
$Q_{spring,C}$				$\alpha_C \cdot V_C$		
$Q_{spring,D}$				$\alpha_D \cdot V_D$		
$V_{fc,var}$					$V_{fc,max} \cdot \rho_{seas}$	
VI	$Q_{out,C} / Q_{out,D}$	$Q_{out,C} / Q_{out,D}$	$\boldsymbol{(Q_{out,C} + Q_{out,I}) / Q_{out,D}}$	$\boldsymbol{Q_{spring,C} / Q_{spring,D}}$	$Q_{out,C} / Q_{out,D}$	
ρ_{seas}					**$(1 - amp) + amp \cdot \sin(2 \cdot \pi/365 \cdot t + p/365 \cdot 2 \cdot \pi)$**	

Table 3. Estimated model parameters and χ^2.

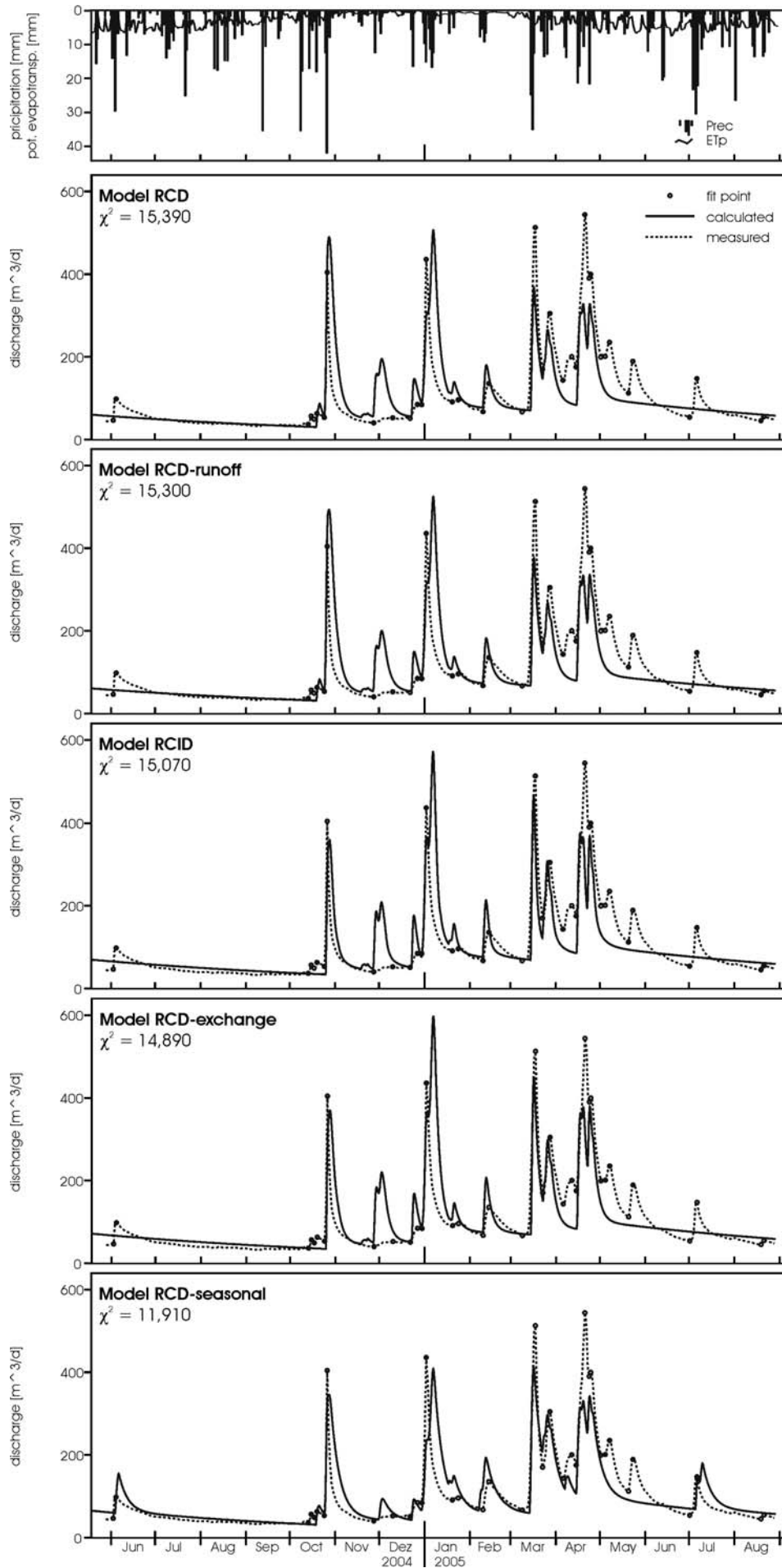| Variable	Estimated value				
	Basis Model RCD and RCD-transport ($\chi^2 = 15{,}390$)	Model RCD-runoff ($\chi^2 = 15{,}300$)	Model RCID ($\chi^2 = 15{,}070$)	Model RCD-exchange ($\chi^2 = 14{,}890$)	Model RCD-seasonal ($\chi^2 = 11{,}910$)
A	161,620 m^2	166,450 m^2	178,740 m^2	176,980 m^2	126,200 m^2
amp					0.29
C_C				490 m^3/Pa^{-1}	
C_D				15,960 m^3/Pa^{-1}	
p					6.36 d
V_{fc}	18,440 m^3	19,040 m^3	35,310 m^3	27,590 m^3	
$V_{fc,max}$					19,990 m^3
$V_{ini,D}$	6,590 m^3	1,840 m^3	11,270 m^3	5,470 m^3	3,160 m^3
$V_{ini,R}$	2,280 m^3	6,520 m^3	14,710 m^3	16,850 m^3	17,830 m^3
V_{sat}		1,530 m^3			
V_{ws}	1,290 m^3	1,500 m^3	15,770 m^3	6,180 m^3	5,330 m^3
X_C			0.56		
X_D	0.66	0.67	0.67	0.46	0.60
α_C	0.27 d^{-1}	0.26 d^{-1}	0.67 d^{-1}	0.19 d^{-1}	0.17 d^{-1}
α_D	0.0047 d^{-1}	0.0044 d^{-1}	0.0043 d^{-1}	0.0026 d^{-1}	0.0053 d^{-1}
α_I			0.19 d^{-1}		
α_R	1.24 d^{-1}	1.33 d^{-1}	0.90 d^{-1}	1.34 d^{-1}	1.85 d^{-1}
ε				52.02 d^{-1}	

Figure 3. Calculated spring discharge based on different model setups and compared to measured spring discharge. Precipitation and potential evapotranspiration are indicated above.

Model RCD-runoff

Especially after heavy rainfall events or during annual snow melt, saturated soils can prevent seepage of water to the karst system. Surface runoff water may bypass the karst system and thus not contribute to spring discharge. The model RCD-runoff is therefore designed to include surface runoff among the processes considered. Saturation is simulated by the threshold value V_{sat}. In contrast to the basis model RCD, precipitation enters the recharge system only when this system is not saturated (i.e., $V_R < V_{sat}$); else the precipitation excess is removed from the system (Figure 2, Table 2). Any further model definitions correspond to the basis model RCD. With the calibrated model RCD-runoff (best fit: $\chi^2 = 15,300$; Table 3), the simulated spring discharge (Figure 3) is almost the same as for the basis model RCD, because the estimated saturation level of the recharge system is hardly ever reached in this simulation (Figure 4). Given that the thickness of the soil coverage is generally low in the catchment area, the result, implicating unrestricted infiltration, is plausible.
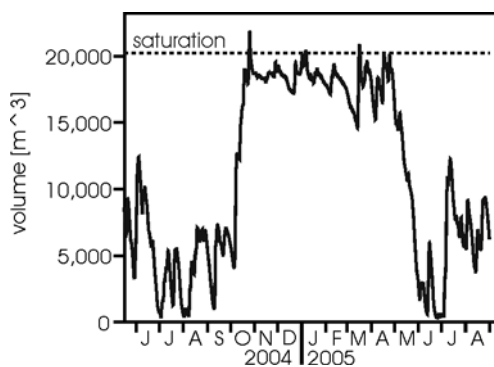

Figure 4. Simulated volume of the recharge compartment for the model RCD-runoff. The threshold value leading to surface runoff (saturation) is hardly ever reached.

Model RCID

Baedke and Krothe [2001] distinguish three distinct portions of the karst continuum issuing from karst aquifers by analyzing discharge hydrographs. Also, *Worthington et al.* [2000] use a triple porosity concept for the description of karst aquifers. The model RCID therefore includes a third, Intermediate, flow system (compartment I) in addition to the conduit and diffuse flow systems already introduced with the basis model RCD (Figure 2, Table 2). The intermediate flow system is characterized by a residence time (or outflow coefficient) with a value between those of the conduit and the diffuse system. The simulated spring discharge (Figure 3) is roughly the same as the one for the basis model RCD (best fit: $\chi^2 = 15,065$; Table 3).

Model RCD-exchange

Exchange flow between the conduit and diffuse systems may have a strong influence on karst processes. *Bauer et al.* [2003], for instance, demonstrated a strong influence of exchange flow on the evolution of the conduit network. The model RCD-exchange is therefore designed to simulate an exchange between the conduit and the diffuse system. This is achieved by defining a potential for each system that is proportional to the respective compartment volume (Figure 2, Table 2). The proportional coefficient is the reciprocal of the capacity of the compartments. The system with the greater potential drains into the other system (additionally to its drainage to the spring) depending on the potential difference and the exchange coefficient. The simulated spring discharge (Figure 3) does not differ very much from the discharge simulated by the basis model RCD (best fit: $\chi^2 = 14,893$; Table 3).

Model RCD-seasonal

When the calculated spring discharge of the basis model RCD is compared with the measured spring discharge, it can be seen that there are too few modeled recharge events during the summer and too many during the winter months. The model RCD-seasonal was therefore developed with a seasonal variation in the water storage capacity of the recharge system ("field capacity"). This is realized by a variable threshold value $V_{fc,var}$ for the recharge system, which is the parameter responsible for "triggering" groundwater recharge (Figure 2, Table 2). $V_{fc,max}$ is reduced sinusoidal with a one-year period (365 days) and a maximum reduction of 58 % (i.e., $V_{fc,var} = 0.42 \cdot V_{fc,max}$) at around summer solstice. The phase shift of approximately 6 days (i.e., the maximum of the reduction is 6 days after solstice) was deduced from trial-and-error simulations minimizing χ^2. The amplitude of the reduction function is estimated by the parameter estimation routine of the software. The model RCD-seasonal significantly improves the quality of the spring discharge simulation (Figure 3). In contrast to the basis model RCD, measured discharge peaks during summer are reproduced, and the calculated peak heights of the model RCD-seasonal during winter fit better to measured values than those of the basis model RCD (best fit: $\chi^2 = 11,913$; Table 3).

Model RCD-transport

The model RCD-transport is designed to simulate the transport of substances in addition to water flow. Unlike the basis model RCD, in this model the outflow of the compartment R is

connected with its own inflow via an advective link, and all other connections are realized by bifurcations of this link (Figure 2, Table 2). This "trick" is necessary because substances leaving the compartment R together with evapotranspiration ($Q_{bif,ETa}$) have to be recirculated until the water leaving the compartment R contributes to groundwater recharge ($Q_{recharge} > 0$). No substances leave the system together with evapotranspiration, because AQUASIM allows the prevention of mass flow of substances through bifurcations and we used this option for the bifurcation of the evapotranspiration. Hydraulically, the model RCD-transport corresponds to the basis model RCD (cf. Table 3). The simulations with the model RCD-transport are employed for vulnerability assessment and presented in Section 4.

III-4. Vulnerability Assessment

III-4.1. Vulnerability Index *VI*

Karst aquifers are especially sensitive to contamination because the rapid travel times and the low storage capacity in the conduit system reduce the effectiveness of natural attenuation processes such as adsorption, degradation and filtration. The sensitivity of a karst spring to contamination is reduced by dilution of the water from the conduit system with water from the diffuse system, in which the above-mentioned processes are much more effective. The relative proportions of spring water discharging from the conduit and diffuse systems as a function of time is an intrinsic property of a karst system. Therefore, we introduce the vulnerability index *VI*, defined as the ratio of the contributions of these systems to spring discharge (e.g., in the case of the model RCD: $VI = Q_{out,C} / Q_{out,D}$; in the case of other model setups refer to Table 2). We use *VI* as a quantitative indicator of the intrinsic vulnerability of a karst spring. High values of *VI* (i.e., a high proportion of water from the conduit system) indicate that the spring is highly sensitive to contamination at this time. This is plausible for contaminants that are effectively attenuated by adsorption, degradation or filtration (e.g., short-lived or large contaminants such as fecal bacteria) or for contaminants that present few problems when highly diluted (which may be the case for accidental spills).

The vulnerability index *VI* can be used to analyze the dynamics of vulnerability. In addition, different springs can be compared with respect to their sensitivity to short-lived contaminants. *VI* can serve as a vulnerability measure that helps to decide, for instance, which springs of a certain area are preferable for drinking water supply.

The *VI*-graphs of the different model setups (Figure 5) all show the same characteristics. Concerning the peak position, *VI* is strongly related to spring discharge. High contaminant concentration during strong responses of spring discharge to recharge events is a well known feature of karst springs and is well represented by the *VI*-graphs. However, the peak height of *VI* is not proportional to spring discharge. Spring responses after long periods without recharge lead to a higher *VI* than during times with frequent recharge events. This is due to the lower water storage in the diffuse system and thus lower dilution of event water with pre-event water after long times without recharge.

III-4.2. Vulnerability Concentration C_V

The vulnerability index introduced above can serve to characterize the dynamics of vulnerability with respect to short-lived contaminants. However, it is not a direct representation of the potential effect of a contaminant. To have an objective measure of the endangerment of spring water quality, we introduce the vulnerability concentration C_V. This is the simulated concentration of a "standard contaminant" (SC) in spring water resulting from a standardized input of SC into the karst system. The larger the catchment area, the more water can be stored in the karst system. Therefore, the input of SC is implemented in proportion to the calibrated size of the catchment area. In the following, we suggest two ways to use breakthrough curves (bt curves) of the vulnerability concentration C_V for assessment of intrinsic vulnerability. For demonstration purposes, the simulations use only the model RCD-transport, which is based on the basis model RCD. Processes introduced with the extended versions are not considered.

Continuous contaminant input, observed water input:

So that the vulnerability assessment is independent of the hydrological situation at the time of input, the input of SC is implemented continuously. This is also a realistic scenario (as a simplification) for frequent contaminant inputs (e.g., from the atmosphere, but also from agricultural or industrial activity). A non-degradable contaminant ($k_{degr} = 0$), representing an ideal tracer, can be used for assessment of intrinsic vulnerability, taking into account only the hydrological characteristics of the system independently of the quality of the contaminant. On the other hand, a degradation rate of zero already is a quality of a contaminant. Therefore, simulations using a range of degradation rates of SC allow an assessment of vulnerability that is influenced less by the properties of the contaminant.
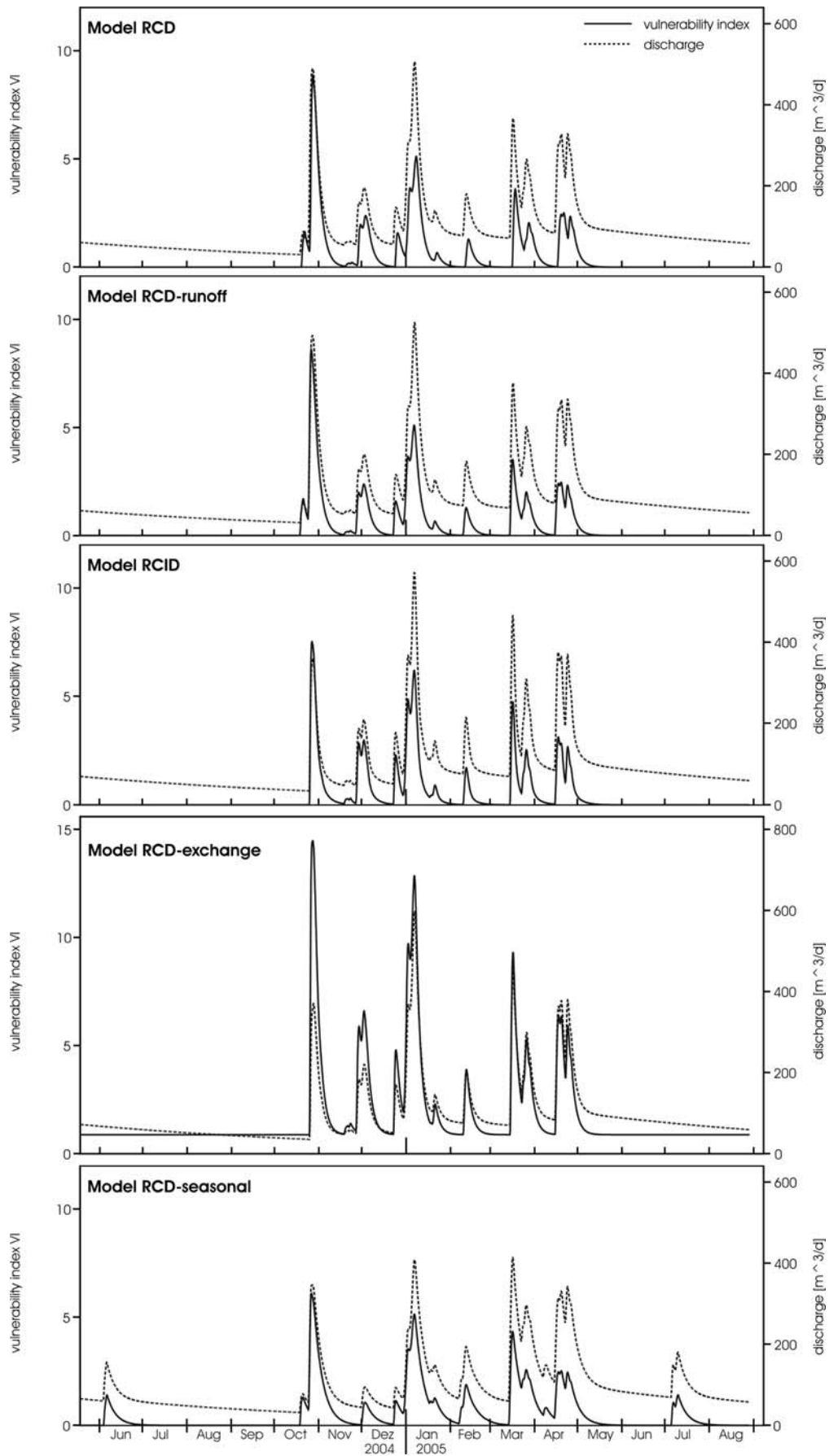
Figure 5. Calculated vulnerability index, *VI*, of each model setup, representing a temporal vulnerability distribution, and simulated spring discharge.
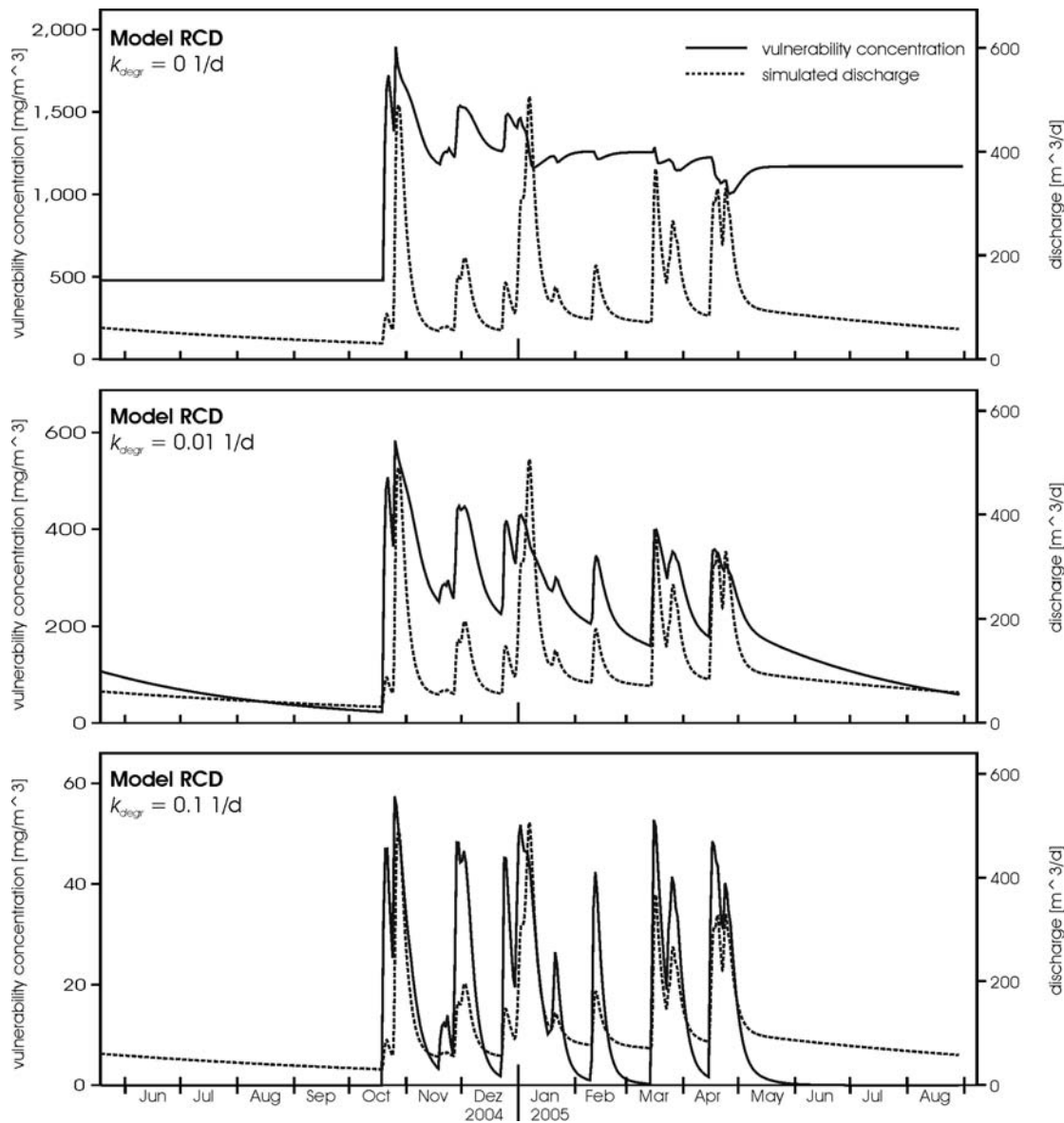
Figure 6. Calculated vulnerability concentration, C_v, in spring water as the result of a continuous input of a standard contaminant, SC. To account for different types of contaminants when assessing the intrinsic vulnerability of spring water, different degradation rates of SC are used. Note the different scaling of the C_V axis.

Figure 6 shows bt curves resulting from a continuous input of SC with an input rate of 1 mg/d per m^2 of the catchment area. Without degradation (Figure 6 upper), recharge events may cause a concentration peak, or the concentration may decrease as a result of dilution effects, depending on the hydrological situation. In our example, maximum vulnerability concentrations of almost 2,000 mg/m^3 are obtained. Introduction of a degradation of SC (Figure 6 middle and lower) leads to bt curves that are related to the spring hydrograph with regard to the timing of peaks. The peak heights, however, do not correlate. The temporal correlation of discharge peaks with concentration peaks is most obvious when degradation of

66

contaminant is rapid (as is the case with bacteria), a characteristic often documented at karst springs [e.g., *Auckenthaler et al.*, 2002]. Simulation with degradation of SC leads to lower vulnerability concentrations than does simulation without degradation; in our example, with $k_{degr} = 0.1$ 1/d, approximately 60 mg/m^3 can be observed in spring water.

Dirac contaminant input, standard water input (SWI)

To find a measure of vulnerability that is independent of the hydrological conditions during the observation period, we introduce a standard water input (SWI). This is characterized by a constant effective precipitation, Prec$_{eff}$, corresponding to the long-term mean groundwater recharge (long-term mean precipitation less the long-term actual evapotranspiration). By including the long-term mean groundwater recharge, the influence of climate on vulnerability is considered independently of actual (weather-dependent) hydrological conditions. In the catchment area of the investigated spring, the long-term yearly mean precipitation is 1,200 mm and the long-term yearly mean actual evapotranspiration is 550 mm [*Weingartner et al.*, 1999], leading to an annual *Prec$_{eff}$* of 650 mm and a water input rate of 1.78 mm/d. As evapotranspiration is already included in *Prec$_{eff}$*, potential evapotranspiration is set to zero in the model setup.

In *COST 620* [2003], *Brouyére* advocates the assessment of vulnerability from a quantitative point of view. He argues that the main questions to be addressed are (1) when, (2) at what level and (3) for how long a contamination will occur at a spring or well. He suggests that a threshold value, C_{thresh}, be defined as an arbitrary percentage of the maximum concentration, C_{max}, observed at the target. From this, a transfer time ($t_{first} - t_0$) is obtained from the time of the contaminant input and the first time that the concentration at the target exceeds C_{thresh}, and the duration ($t_{end} - t_{first}$) of a contamination is given by the difference between t_{first} and the time, when the contaminant concentration falls below C_{thresh}. The contamination level is represented by the ratio C^* between C_{max} at the target and C_0 at the origin. According to *Brouyére* [2003], the transfer time, the duration and the contamination level represent an objective quantification of vulnerability that can be used for the validation of vulnerability maps. The bt curves required for the derivation of those parameters can be either provided by tracer tests or calculated by models. The author suggests the use of (analytical) advection-dispersion-models, e.g., calculated with the computer program VULK [*Jeannin et al.*, 2001].

On the basis of these ideas, we derived the relevant parameters $C_{V,max}$, $(t_{first} - t_0)$ and $(t_{end} - t_{first})$ globally from the bt curve calculated with the calibrated numerical models of this work, resulting from a Dirac input of 1 mg standard contaminant SC per m^2 of the catchment area at $t_0 = 1{,}825$ d (five years after start of simulation), using the standard water input introduced above and a degradation rate of SC at $k_{degr} = 0$ (Figure 7). In this case, it is not necessary to relate $C_{V,max}$ to the input concentration C_0, because the input is already standardized. Further, we suggest the use of an absolute threshold value $C_{V,thresh} = 1$ mg/m^3 instead of a relative percentage, so that t_{first} and the duration will be independent of $C_{V,max}$; this will allow the comparison of different springs with respect to these parameters. In our example, we obtain a maximum vulnerability concentration of 2.8 mg/m^3 two weeks after the contaminant input. A contamination above the threshold value occurs one and a half days after the input and lasts for approximately 200 days.
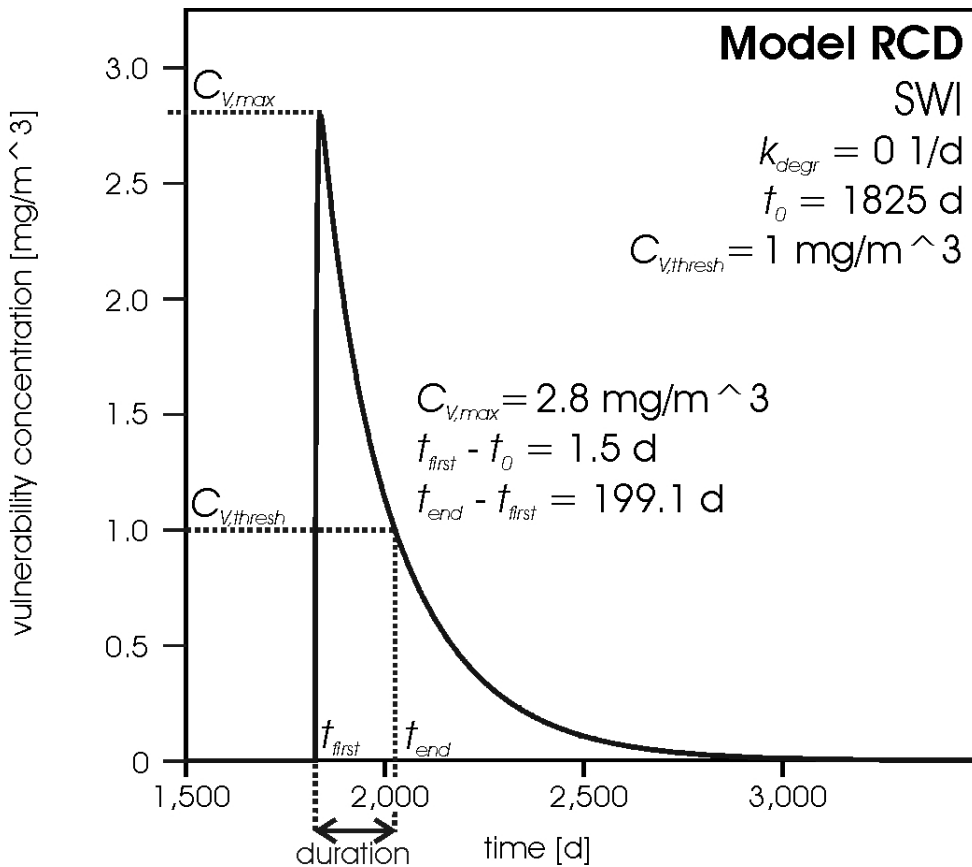

Figure 7. Calculated vulnerability concentration, C_V, in spring water as the result of a Dirac input of a standard contaminant, SC, and a constant standard water input, SWI. The parameters $(t_{first} - t_0)$, $C_{V,max}$ and $(t_{end} - t_{first})$ can be used to quantify vulnerability.

III-5. Discussion

III-5.1. Modeling Technique

We tested the plausibility of the volumes obtained from our models by comparing them with general ideas about the study area. The modeled water volume (model RCD) of the diffuse flow system varies between 6,550 and 22,150 m^3. Assuming a porosity of the rock matrix of 2 %, this corresponds to a groundwater thickness varying between 2 and 7 m. This is reasonable for a shallow karst such as our study area. The modeled maximum water volume (model RCD) of the conduit flow system is 1,720 m^3. Assuming an average diameter of 1 m for the conduits of a mature karst, this corresponds to a length of 2 km for the conduit system. Also this is reasonable for a catchment area of approximately 1 km^2, given that the conduits are organized in a branched system.

In this study, karst flow systems are represented by mixed reactor models. Water inflow into a model compartment directly leads to an increase of water discharge out of the compartment. This characteristic is very similar to karst systems, in which recharge to the groundwater table directly leads to increased spring discharge as a result of an increased pressure head within the flow system. Flow through the unsaturated zone, however, is not considered by the models. In mature karst systems, the existence of a well developed epikarst and conduit system in the unsaturated zone leads to rapid recharge to the water table. In the case of our study, the discharge responds to precipitation within only a few hours (Figure 8). This time span is of minor importance on the time scale at which the present approach is applied (months to years; cf. Figures 3—7).

Transport simulation by mixed reactor models is more difficult. Substances are transported through conduits, fissures and pores by advection and dispersion, and they need time to travel a given distance. This leads to a time lag between the substance signal (concentration) and the hydraulic signal (discharge) at the spring [*Ashton*, 1966]. Transport simulations by mixed reactor models do not take this characteristic into account. However, transport velocities in mature karst systems are very high, and the expected time lag in small catchments is in the order of hours [e.g., *Birk et al.*, 2004]. In the case of our study, the time lag between the discharge and electrical conductivity signal is only a few hours (Figure 8). Again, this time span is of minor importance for this approach.

This transport model is therefore a good approximation particularly for small catchments, in which residence times are generally short. In large catchments, however, the effect of advective-dispersive transport on the residence time distribution of contaminants might become important for the approach. *Haitjema* [1995] showed for diffuse-source pollution (e.g., from the application of agricultural chemicals or liquid manure to cropland) that the cumulative residence time distribution of ideal catchments is exponential. This is exactly the case for the linear storage used in our volumetric model. By contrast, the residence time distribution of point-source pollution (e.g., from leaking storage tanks or industrial sites) will depend on many local factors. Therefore, the approach is well suited to assess diffuse-source pollution also in large catchments, whereas the assessment of point-source pollution in large catchments remains critical.
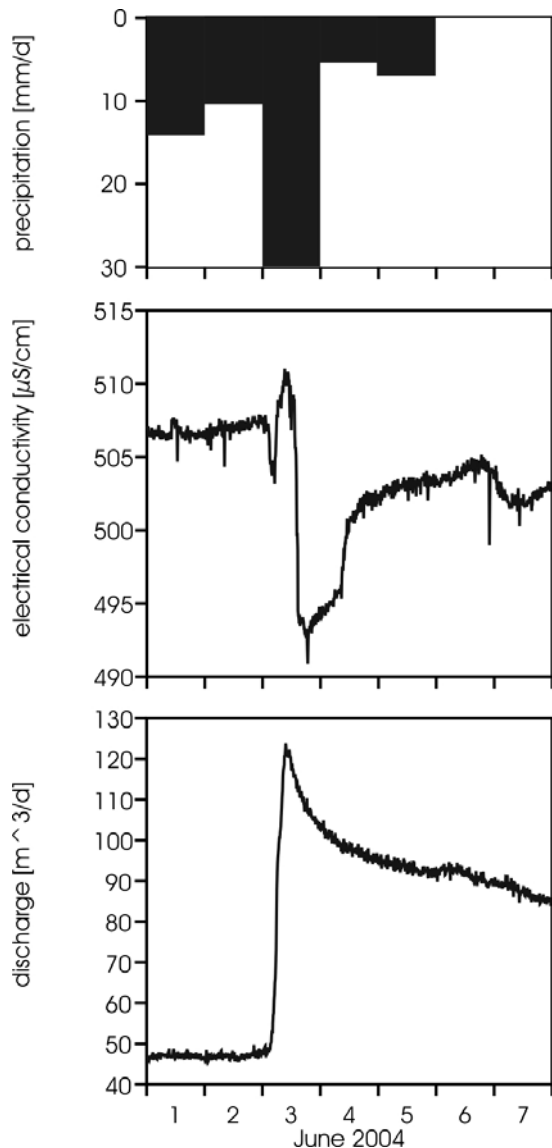
Figure 8. Response of the spring (Untere Rappenfluhquelle) to a heavy rainfall event (3 June 2004): Both the hydraulic signal (discharge, below) and the substance signal (electrical conductivity, middle) react within a few hours to the rainfall event (above) – a very short time span compared with the time scale of months to years at which the present approach is applied (cf. Figs 3—7).

70

Each karst system has its individual characteristics [*COST 620*, 2003]. The basis model RCD is a very simple model setup already able to reproduce most responses of the investigated karst system to rainfall events. The features included in the extended model setups are examples of possibly important processes that can improve the modeling results. In our case, seasonal variation of the field capacity seems to be an effective process. The observed lower field capacity during summer can be explained by the development of macropores when the soil is drying out [e.g., *Sumner*, 2000]. Other field sites may require the inclusion of different processes in the model setup, such as surface runoff, an intermediate flow system or exchange flow between the conduit and the diffuse system. The present results show that the global modeling technique used here is a flexible tool to characterize the individual hydraulics of karst springs. The flexibility of the approach allows not only an adaptation of the model to the individual characteristics of a given karst system, but also a separate study of each process involved.

A great advantage of this global approach over distributed modeling techniques [*Sauter et al.*, 2006] is the low data requirement. All necessary data are provided by a climate station in the catchment area and a discharge recording at the spring. Hydraulic head data are not necessary, nor is knowledge of the geometry of the karst conduits. In large and complex karst areas, such data are costly or impossible to obtain. Thus, in many cases global models may offer the most effective (and sometimes the only) way to represent the karst system.

Existing global methods include hydrograph separation techniques based on mass balance [e.g., *Atkinson*, 1977; *Dreiss*, 1989]. Very similar to the vulnerability index *VI* used in our study, these methods provide an estimate of the fast flow proportion in spring water. A disadvantage of the mass balance approach is its limited use for predictions, e. g. in situations different from those that have been observed. Moreover, in contrast to the numerical modeling approach, it requires physicochemical data. While such data can generally be measured at the spring, assumptions have to been made for the recharge water. We conducted a hydrograph separation analysis based on the electrical conductivity (EC) data presented in figure 8. At first, the calculation was conducted assuming 25 $\mu S/cm^2$ for the EC of the recharge water. This value was measured in rain water collected with rain gauges in the catchment area. The calculated maximum fast flow component in spring water based on this assumption corresponded to a *VI* of 0.03, whereas our model predicted a maximum *VI* of 1.4 for this event (c.f., figure 5). In a second step, the *VI* obtained from the mass balance approach

was calibrated to the *VI* calculated with our model by adjusting the assumed EC of the recharge water. The best fit was obtained for a value of 483 μS/cm^2.

Sensitivity analysis indicated that the proportion of fast flow calculated from the mass balance approach is very sensitive to the assumed EC of recharge water if the EC of the recharge water and spring water are close. Thus, the mass balance approach is well suited if the EC (or, generally speaking, concentration) of recharge water is very different from the EC of spring water, or if it can be measured accurately. This is the case, for example, when a ditch infiltrates into the subsurface rapidly at a sink [e.g., *Birk et al.*, 2004]. In our and many other cases, however, a large proportion of the recharge water is stored in the soil and epikarst system before it is drained by a karst conduit [*Perrin et al.*, 2003]. There is enough time to allow for significant dissolution, which is difficult to quantify. If so, the application of a mass balance approach is difficult, and the results of the numerical modeling are more reliable. Accounting for storage in the soil and epikarst, the EC obtained from the above-described calibration is reasonable.

III-5.2. Vulnerability Assessment

We introduce the vulnerability index *VI*, based on the relative proportions of spring discharge originating from the conduit system and from the diffuse system. This index allows the temporal variations of vulnerability to be assessed. Moreover, it can serve as an absolute measure, quantifying vulnerability and thus facilitating the comparison of springs in terms of their sensitivity to contamination. Application of the vulnerability index, however, is restricted to contaminants that are effectively attenuated in the diffuse system, such as fecal bacteria.

For this reason, we further introduce the vulnerability concentration, C_v. It represents the modeled concentration of a standard contaminant, SC, in spring water. Like *VI*, C_v includes temporal as well as quantitative aspects of vulnerability. The advantage of modeling C_v over modeling *VI* arises from the fact that C_v is a direct representation of the potential effect of a contaminant impact. An intrinsic (i.e., contaminant-independent) vulnerability assessment can be obtained by either of two ways. First, a conservative standard contaminant (no degradation) can be used for the simulations; in this case, C_v will be affected only by the hydraulics of the system. Secondly, the effects on the vulnerability of the system of different types of contaminants (conservative, slightly reactive or strongly reactive), realized by

different degradation rates of SC, can be considered coevally. We favor the second approach, because a conservative behavior already constitutes a characteristic of the contaminant (and hence the first approach is not completely independent of the characteristics of the contaminant).

The first application of C_V in this study is the simulated concentration of SC in spring water resulting from a continuous SC input, and this reveals the temporal vulnerability distribution of spring water under observed hydrological conditions.

The term vulnerability is generally used in the sense of *Vrba and Zaporozec* [1994], who defined vulnerability as an intrinsic property of a groundwater system that depends on the sensitivity of that system to human and/or natural impact. *Brouyère* [2003], however, points out that vulnerability can mean different things: in some cases a brief but heavy contamination might be worse than a protracted moderate contamination, but in other cases vice versa. He therefore claims that vulnerability assessment should answer the three practical questions already introduced above: (1) How long does it take until a contamination reaches the target, (2) at what concentration level will the target be contaminated, and (3) for how long will the contamination last? As the second application of C_V in this study, the standardized Dirac input of SC gives a modeled breakthrough curve that can answer these questions by quantifying the first arrival ($t_{first} - t_0$), maximum level ($C_{V,max}$) and duration ($t_{end} - t_{first}$) of the simulated pollution ($C_v > C_{V,thresh}$) at the spring. Using the standard water input, SWI, the results are independent of observed hydrological conditions.

The proposed vulnerability assessment using global numerical models could be of great interest for drinking water management. First, when spring water quality is insufficient in spite of a protection zone delineated by vulnerability mapping, the benefit of the invested mapping efforts is low. The present modeling technique, in contrast, does contribute to a better understanding of the actual groundwater system. Secondly, the inclusion of the dimension of time into this approach adds a degree of freedom to water protection strategies. Temporally limited land use restrictions in the catchment areas of drinking water sources and water withdrawal management are possible future applications of temporal approaches. And thirdly, the present approach allows the comparison of different springs with respect to their sensitivity to contamination from a quantitative point of view, providing an objective basis for a regional planning of drinking water supply. However, the approach gives no information on

the spatial vulnerability distribution in the spring catchments. Therefore, the present modeling approach is a valuable complement to vulnerability mapping techniques, but the protection of a drinking water source requires a combination of both methods.

Acknowledgements

References

Ackers, P., W. R. White, J. A. Perkins, and A. J. M. Harrison (1978), *Weirs and Flumes for Flow Measurement*, Wiley, Chichester.

Aller, L., T. Bennett, J. H. Lehr, and R. J. Petty (1987), DRASTIC: A Standardized System for Evaluating Ground Water Pollution Potential Using Hydrogeological Settings, U. S. Environmental Protection Agency, Oklahoma.

Ashton, K. (1966), The analysis of flow data from karst drainage systems, *Transactions of the Cave Research Group of Great Britain*, 7, 161—203.

Atkinson, T. C. (1977), Diffuse flow and conduit flow in limestone terrain in the Mendip Hills, Somerset (Great Britain), *J. Hydrol.*, 35, 93—110.

Auckenthaler, A., G. Raso, and P. Huggenberger (2002), Particle transport in a karst aquifer: Natural and artificial tracer experiments with bacteria, bacteriophages and microspheres, *Water Science Technol.*, 46(3), 131—138.

Baedke, S. J. and N. C. Krothe (2001), Derivation of effective hydraulic parameters of a karst aquifer from discharge hydrograph analysis, *Water Resour. Res.*, 37(1), 13—19.

Bakalowicz, M. (2005), Karst Groundwater: a challenge for new resources, *Hydrogeol. J.*, 13(1), 148—160, doi:10.1007/s10040-004-0402-9.

Baltes B, S. von Fumetti, D. Küry, E. Contesse, C. Butscher, P. Huggenberger, D. Suter, W. Leimgruber, and P. Nagel (2005), Basel entdeckt seine Quellen (Basel discovers ist springs), Deutsche Gesellschaft für Limnologie (DGL), *Proceedings 2004, Potsdam, 20-24 September*, 226—230, Weissensee Verlag, Berlin.

Bauer, S., R. Liedl, and M. Sauter (2003), Modeling of karst aquifer genesis: influence of exchange flow, *Water Resour. Res.*, 39(10), 1285, doi:10.1029/2003WR002218.

Bauer, S., R. Liedl, and M. Sauter (2005), Modeling the influence of epikarst evolution on karst aquifer genesis: A time-variant recharge boundary condition for joint karst-epikarst development, *Water Resour. Res.*, 41, W09416, doi:10.1029/2004WR003321.

Bergström, S. (1992), The HBV model - its structure and applications, *SMHI RH*, 4, Norrköping.

Birk, S., R. Liedl, and M. Sauter (2004), Identification of localized recharge and conduit flow by combined analysis of hydraulic and physico-chemical spring responses (Urenbrunnen, SW-Germany), *J. Hydrol.*, 286, 179—193, doi:10.1016/j.jhydrol.2003.09.007.

Braun, L. (1985), Simulation of snowmelt-runoff in lowland and lower Alpine regions of Switzerland, *Zürcher Geographische Schriften*, 21.

Brouyère, S. (2003), A quantitative point of view of the concept of vulnerability, in *Vulnerability and risk mapping for the protection of carbonate (karst) aquifers*, edited by F. Zwahlen, COST action 620, Final report, European Comission, Brüssel.

Civita, M., and M. De Maio (2000), Valutazione e cartografia automatica della vulnerabilità degli acquiferi all'inquinamento con il systema parametrico SINTACS R5 (Evaluation and automatic cartography of aquifer vulnerability using the parametric system SINTACS R5), Pitagora Editrice, Bologna.

Connell, L. D., and G. van den Daele (2003), A quantitative approach to aquifer vulnerability mapping, *J. Hydrol.*, 276, 71—88.

COST 620 (2003), *Vulnerability and risk mapping for the protection of carbonate (karst) aquifers*, edited by F. Zwahlen, COST action 620, Final report, European Comission, Brüssel.

Daly, D., A. Dassargues, D. Drew, S. Dunne, N. Goldscheider, S. Neale, I. C. Popescu, and F. Zwahlen (2002), Main concepts of the „European approach" to karst-groundwater-vulnerability assessment and mapping, *Hydrogeol. J.*, 10, 340—345.

Doerfliger, N., P.-Y. Jeannin, and F. Zwahlen (1999), Water vulnerability assessment in karst environments: a new method of defining protection areas using a multi-attribute approach and GIS tools (EPIK method), *Environ. Geol.*, 39(2), 165—176.

Dreiss, S. J. (1989), Regional scale transport in a karst aquifer, 1, Component separation of spring flow hydrographs, *Water Resour. Research*, 25(1), 117—125.

DVWK (1996), Ermittlung der Verdunstung von Land- und Wasserflächen (Estimating the evaporation of land and water surfaces), *Merkblätter zur Wasserwirtschaft*, 238, Deutscher Verband für Wasserwirtschaft und Kulturbau e.V.

Fogg, G., E. LaBolle, and G. Weissmann (1999), Groundwater vulnerability assessment: hydrogeologic perspective and example from Salinas Valley, California, in *Assessment of non-point source pollution in the vadose zone*, edited by D. Corwin, K. Loague, and T. Ellsworth, American Geophysical Union, *Geophysical Monograph*, 108, 45—61.

Ford, D. C., and P. W. Williams (1989), *Karst geomorphology and hydrology*, Chapman and Hall, New York.

Gogu, R. C., and A. Dassargues (2000), Current trends and future challenges in groundwater vulnerability assessment using overlay and index methods, *Environ. Geol.*, 39(6), 549—559.

Goldscheider, N. (2002), Hydrogeology and vulnerability of karst systems – examples from the Northern Alps and the Swabian Alb, Ph. D. thesis, University of Karlsruhe.

Goldscheider, N. (2005), Karst groundwater vulnerability mapping: application of a new method in the Swabian Alb, Germany, *Hydrogeol. J.*, 13, 555—564, doi:10.1007/s10040-003-0291-3.

Gürler, B., L. Hauber, and M. Schwander (1987), Die Geologie der Umgebung von Basel mit Hinweisen über die Nutzungsmöglichkeiten der Erdwärme (The geology in the vicinity of Basel with reference to the usage of geothermal energy) , *Beitrag zur Geologischen Karte der Schweiz*, 160.

Haitjema, H. M. (1995), On the residence time distribution in idealized groundwatersheds, *J. Hydrol.*, 172, 127—146.

Hock, R. (2003), Temperature-index melt modelling in mountain areas, *J. Hydrol.*, 282(1—4), 104—115.

Jeannin, P.-Y., F. Cornaton, F. Zwahlen, and P. Perrochet (2001), VULK: a tool for intrinsic vulnerability assessment and validation, 7th Conference on Limestone Hydrology and Fissured Media, Besançon 20–22 Sep. 2001, *Sci. Tech. Envir.*, Mém. H . S., 13, 185—190.

Kiraly, L. (1998), Modeling karst aquifers by the combined discrete channel and continuum approach, *Bull. Hydrogeol.*, 16, 77—98.

Klimchouk, A., and D. Ford, (2000), Types of Karst and Evolution of Hydrogeologic Setting, in *Speleogenesis: Evolution of karst aquifers, edited by* A. B. Klimchouk, D. C. Ford, A. N. Palmer, and W. Dreybrodt, 45-53, Nat. Speleologic Soc., Huntsville, Ala.

Liedl, R., M. Sauter, D. Hückinghaus, T. Clemens, and G. Teutsch (2003), Simulation of the development of karst aquifers using a coupled continuum pipe flow model, *Water Resour. Res.*, 39(3), 1057, doi:10.1029/2001WR001206.

Magiera, P. (2000), Methoden zur Abschätzung der Verschmutzungsempfindlichkeit des Grundwassers (Methods of groundwater vulnerability assessment), *Grundwasser*, 3, 103—114.

Ohmura, A. (2001), Physical basis for the temperature-based melt-index method, *J. Applied Meteorology*, 40, 753—761.

Penman, H. L. (1956), Estimating Evaporation, *Trans. Amer. Geophys. Union*, 37(1), 43—50.

Perrin, J., P.-Y. Jeannin, and F. Zwahlen (2003), Epikarst storage in a karst aquifer: a conceptual model based on isotopic data, Milandre test site, Switzerland, *J. Hydrol.*, 279, 106—124, doi:10.1016/S0022-1694(03)00171-9.

Quinn, J., and D. Tomasko (2000), A Numerical Approach to Simulating Mixed Flow in Karst Aquifers, in *Groundwater Flow and Contaminant Transport in Carbonate Aquifers*, edited by I. Sasowsky, and C. Wicks, 147—156, Balkema, Rotterdam.

Quinn, J. J., D. Tomasko, and J. A. Kuiper (2006), Modeling Complex Flow in a Karst Aquifer, *Sedimentary Geology*, 184, 343—351, plus electronic supplement.

Reichert, P. (1994a), AQUASIM – A tool for simulation and data analysis of aquatic systems, *Wat. Sci. Tech.*, 30(2), 21—30.

Reichert, P. (1994b), Concepts underlying a computer program for the identification and simulation of aquatic systems, *Schriftenreihe der EAWAG*, 7, Swiss Federal Institute for Environmental Science and Technology (EAWAG), Dübendorf.

Sauter, M., A. Kovács, T. Geyer, and G. Teutsch (2006), Modellierung der Hydraulik von Grundwasserleitern – Eine Übersicht (Modelling karst groundwater hydraulics – an overview), *Grundwasser* 3/2006, 143—156, doi:10.1007/s00767-006-0140-0.

Schuster, E. T., and W. B. White (1971), Seasonal fluctuations in the chemestry of limestone springs: A possible means for characterizing carbonate aquifers, *J. Hydrol.*, 14(2), 93—128.

Seibert, J. (2002), HBV light – User's manual, Uppsala University, Department of Earth Sciences, Hydrology.

Sumner, M. E. (Ed.) (2000), *Handbook of soil science*, CRC Press, Boca Raton.

Vrba, J., and A. Zoporozec (Ed.) (1994), Guidebook on Mapping Groundwater Vulnerability, *International Contributions to Hydrogeology (IAH)*, 16, Hannover.

Weingartner, R., M. Spreafico, and C. Leibundgut (1999), *Hydrological atlas of Switzerland*, Bundesamt für Wasser und Geologie, Bern.

Wendling, U., H.-G. Schellin, and M. Thomä (1991), Bereitstellung von täglichen Informationen zum Wasserhaushalt des Bodens für die Zwecke der agrar-meteorologischen Beratung (Provision of daily information on soil water balance for the purpose of meteorological consulting), *Zeitschrift für Meteorologie*, 41, 468—475.

White, W. B. (1988), *Geomorphology and hydrology of karst terrains*, Oxford University Press, Oxford.

Williams, P. W. (1983), The role of the subcutaneous zone in karst hydrology, *J. Hydrol.*, 61, 45–67.

Worthington, S. R. H., D. C. Ford, and P. A. Beddows (2000), Porosity and permeability enhancement in unconfined carbonate aquifers as a result of solution, in *Speleogenesis: Evolution of karst aquifers*, edited by A. B. Klimchouk, D. C. Ford, A. N. Palmer, and W. Dreybrodt, 463—472, Natl. Speleologic Soc., Huntsville, Ala.

IV. Integrative vulnerability assessment in karst areas: a combined mapping and modeling approach

Abstract

The objective of this work is to facilitate a sustainable regional planning of water resources in karst areas by providing a conceptual framework for an integrative vulnerability assessment. A combined mapping and modeling approach is proposed, taking into account both spatial and temporal aspects of karst groundwater vulnerability. The conceptual framework comprises the delineation of recharge and discharge areas, vulnerability mapping, numerical flow and transport modeling and the integration of information into a combined vulnerability map and time series. The approach is illustrated at a field site in northwest Switzerland (Gempen plateau). The results show that the combination of vulnerability mapping and numerical modeling allows the vulnerability distribution, both in the recharge and discharge areas, to be identified, and at the same time, the time dependence of karst groundwater vulnerability to be assessed. The combined vulnerability map and time series provides a quantitative basis for regional drinking water management as well as for ecological and geotechnical considerations.

Key words

Groundwater hydrology; vulnerability; karst; numerical modeling; 3D geological modeling

IV-1. Introduction

Water is one of the most valuable natural resources of all, crucial to human and most other kinds of life. Karst groundwater is among the most important water resources. Karst waters supply about 25 % of the global population (Ford and Williams, 1989). In Europe, a significant portion of the drinking water supply is abstracted from karst aquifers and in many regions it is the only available source of fresh water (COST 620, 2003). Besides its value as drinking water supply, another aspect becomes more and more important for researchers.

Karst water is an indispensable resource for very specific ecosystems. Natural springs at the interface between groundwater and surface water, for example, are important freshwater habitats that provide refuge for many species (e.g., Von Fumetti et al., 2006). The ecology of pristine springs is assumed to depend much on spring water quality. Glazier (1991), for example, investigated the influence of various chemical factors on specific spring fauna. However, information on the overall relationship between spring organisms and their environment is scarce, because spring ecology has only recently become the focus of research (e.g. Botosaneanu, 1998), and only little consideration has been given to the role of hydrogeologic processes in the overall spring environment (Van der Kamp 1995). So far, most ecologists have largely neglected the relationship between springs and their catchments. However, the interconnection between discharge and the corresponding recharge areas, for example, is known to have a significant influence on the species found in natural karst springs (Gibert et al., 1994). In addition, spring discharge is considered to exercise an important influence on spring ecology (Gibert et al., 2000; von Fumetti et al., 2006). Apart from its ecological role for natural spring habitats, karst groundwater also has an important ecological function as feeder of brooks, rivers and streams. Increasing impact on groundwater systems due to intensified land use by a growing population, industry and agriculture increases the pressure on water resources – both as a drinking water supply and as a basic prerequisite for ecological systems. At the same time, public authorities, and also more and more citizens, accept only irreproachable drinking water, and they are equally concerned about an intact environment.

In view of this situation, diverse strategies have been developed for the protection of groundwater and spring water, with methods for groundwater vulnerability mapping as the most important (National Research Council, 1993). Karst aquifers have complex and distinct characteristics, which make them very different from other aquifers (Bakalowicz, 2005). They are extremely heterogeneous and anisotropic and therefore particularly vulnerable to contamination (Goldscheider, 2005). In view of these special characteristics, some of the methods used for vulnerability assessment are specifically designed for karst environments (Doerfliger et al., 1999; Daly et al., 2002; COST 620, 2003). In practice, however, there are still major problems with the protection of karst springs.

Important points remain unresolved. First, mapping approaches disregard the dynamics of vulnerability. Many studies clearly show that spring water quality is a function of time (e.g.,

Ryan and Meiman, 1996; Auckenthaler et al., 2002). This fact is completely neglected by the existing mapping techniques. Secondly, the various indices used to generate vulnerability maps are largely conceptual, and thus subjective (Connell and Van den Daele, 2003). There is a need to examine the vulnerability concepts from a quantitative point of view, and for clearly identified reference criteria for quantification, comparison and validation purposes, to be established (Brouyère, 2003). Thirdly, though vulnerability maps take important characteristics of karst terrains into account, they are not adequate to explain the actual processes taking place. And last, the existing mapping techniques assign groundwater vulnerability solely to the recharge areas. However, the assignment of groundwater vulnerability to the springs as well would provide a major aid to drinking water suppliers, regional planners and ecologists, when evaluating the possible future use of individual springs.

In the literature it is often stated that the limitations of vulnerability maps, such as those cited above, could be overcome by mathematical modeling. Goldscheider (2002) remarked that, despite the large number of mathematical flow and transport models, these have rarely been used for vulnerability mapping. Gogu and Dassargues (2000) pointed out that new challenges for hydrogeologists will be posed by the integration of results from process-based numerical models into vulnerability mapping techniques. In COST 620 (2003), the use of calibrated numerical simulations is suggested for the validation of vulnerability maps.

This study aims to provide a sustainable regional planning concept for the use and protection of karst water resources. The main objective of this study is to offer quantitative answers to practical questions about the "Where?" and "When?" of karst groundwater vulnerability. To this end, mapping methods were combined with modeling methods. This approach allows both spatial and temporal aspects of karst groundwater vulnerability to be addressed. Numerical flow and transport modeling was conducted, which contributed to vulnerability assessment based on modeled proportions of spring discharge from different flow systems and contaminant loads in spring water as the result of different recharge and flow conditions. The numerical modeling was complemented by 3D geological modeling to provide the structural framework for the hydrology of the study area and for the conducted vulnerability mapping.

This paper is set up as follows: First, a general approach for integrative vulnerability assessment is proposed, followed by a description the methods used in this study, which are

specific to an open, shallow karst. The methods are then applied to a field site and illustration is given of how the results can be integrated into a combined vulnerability map and time series. The paper concludes with the discussion of our findings.
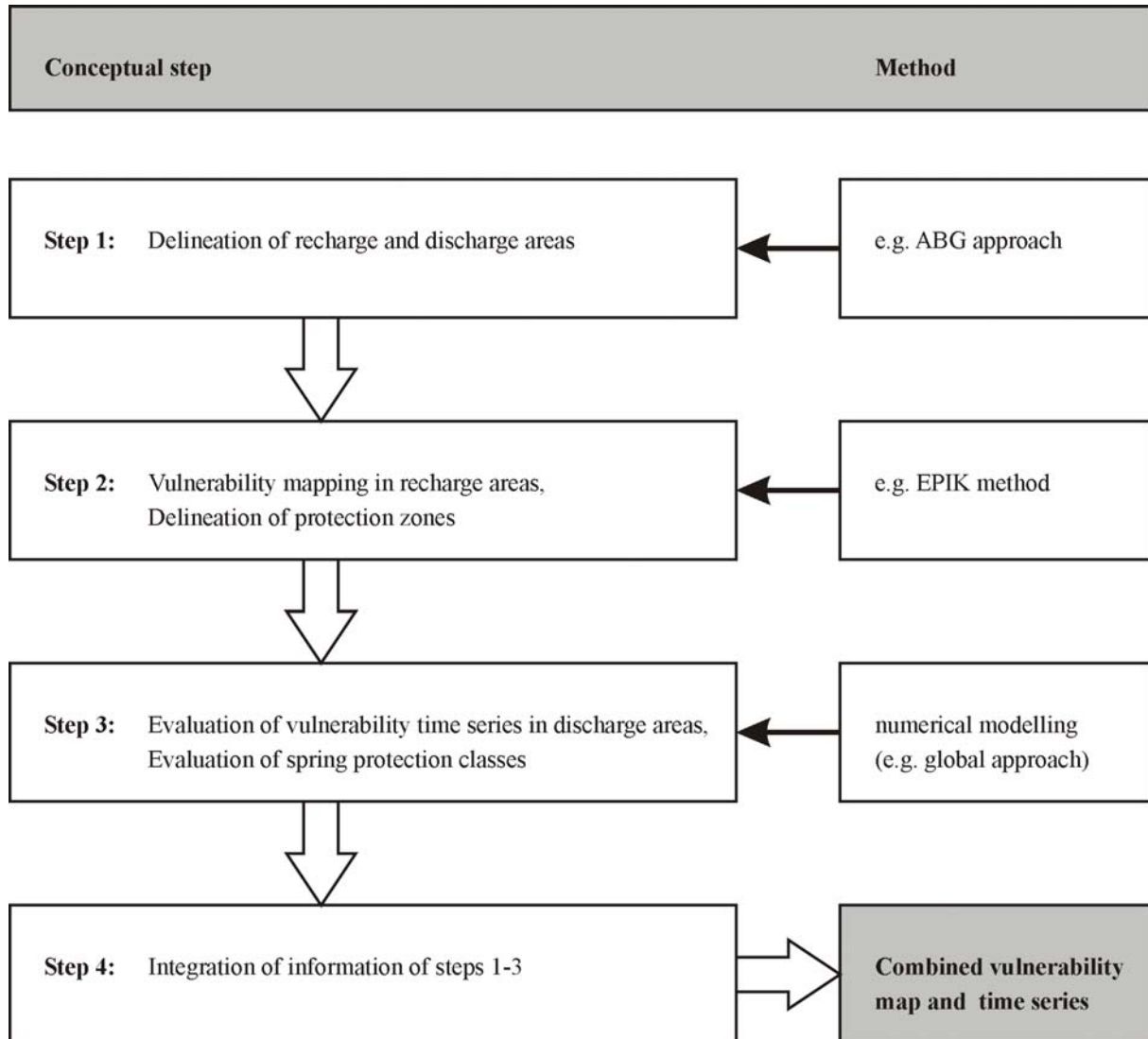
Figure 1: Conceptual four-step approach proposed for integrative vulnerability assessment in karst areas. The approach concludes with a combined vulnerability map and time series providing quantitative spatial and temporal information.

IV-2. Methods

IV-2.1. General approach

A four-step approach resulting in a combined vulnerability map and time series is suggested to provide all spatial and temporal information needed for an integrative vulnerability assessment (Figure 1):

1) In a first step, a hydrological model of the study area is established. The hydrological model reveals a conceptual background that allows recharge and discharge areas to be evaluated. In our study, we use the aquifer base gradient (ABG) approach (Butscher and Huggenberger, 2007a), which is based on 3D geological modeling of the study area.

2) The second step comprises vulnerability mapping in the delineated recharge areas of springs and water catchworks that are of regional importance. The EPIK method (Dörfliger et al. 1999) is used, as it is recommended for vulnerability assessment in Switzerland by the Swiss Agency for the Environment, Forests and Landscape (SAEFL).

3) In a third step, quantitative and temporal information on vulnerability is deduced from vulnerability time series using numerical models (Butscher and Huggenberger, 2007b). This step is conducted only for regionally important springs.

4) The last step is the composition of all information on the recharge and discharge areas in the form of a combined vulnerability map (spatial information) and time series (temporal information) (Table 1).

The sections below describe the individual methods we used to generate the combined vulnerability map and time series. These methods are adjusted to our study area, which is characterized by a mature, unconfined, shallow karst.

Table 1: The sum of the information gathered in conceptual steps 1—3 corresponds to conceptual step 4 and results in a combined vulnerability map and time series, which contains quantitative spatial and temporal information on both recharge and discharge areas.

Conceptual step	Spatial information on		Temporal information on	
	Recharge area	Discharge area	Recharge area	Discharge area
step 1 (ABG approach)	x	x		
step 2 (EPIK method)	x			
step 3 (numerical modeling)		x	x	x
step 4 **= total** (combined vulnerability map and time series)	x	x	x	x

IV-2.2. Delineation of recharge and discharge areas using the ABG approach

The ABG approach (Butscher and Huggenberger, 2007a) is based mainly on the assumption that in the case of a mature, unconfined, shallow karst the development of conduits and the resulting flow are strongly influenced by the gradient of the aquifer base. Processes comparable to open surface flow may dominate at the base of such aquifers. Besides the geometry of the aquifer base, faults are important because they displace the aquifer base and control the connection and separation of aquifer bodies.

The ABG approach consists of two main steps (Figure 2): 1) Construction of a 3D geological model of the study area, to establish the geometry of the aquifer base and its displacement at faults; and 2) Development of a hydrological model, based on the 3D geological model, including recharge and discharge areas and subsurface flow paths.
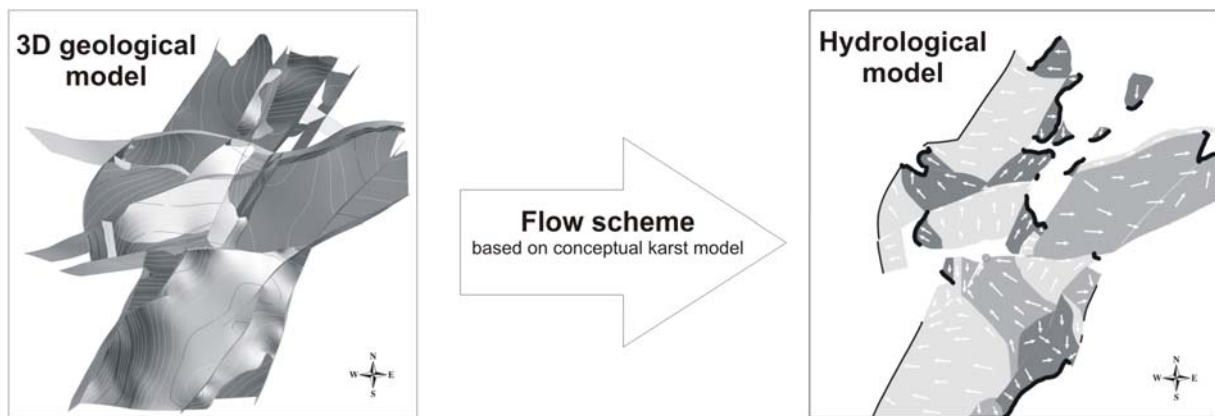

Figure 2: Schematic illustration of the ABG approach. The resulting hydrological model includes recharge and discharge areas, and the groundwater flow direction.

The conceptual model underlying the ABG approach is based on the ideas of Bauer et al. (2005) on karst development in unconfined settings, proposing that during karst evolution the karst water table falls from near the land surface to base level. The position of the base level is generally controlled by the vertical position of the aquifer discharge (Kaufmann and Braun, 2000; Kaufmann 2002). In the case of a shallow karst, however, the base level cannot drop to a horizontal discharge level, but must develop above at the aquifer base. The hydraulic gradient is strongly influenced then by the ABG, and the direction of groundwater flow is controlled by the topography and structure of the aquifer base.

Based on these ideas, the conceptual model underlying the ABG approach includes following features: Surface runoff can be neglected. The groundwater flow direction corresponds to the

downward gradient of the base level. The base level is determined by the aquifer base or, in the case of dammed springs (Ford and Williams, 1989), by the vertical position of the draining outflow. Two further simplifications have been included: recharge to the groundwater table (base level) is assumed to be vertical, and faults are assumed to be permeable to water flow where two aquifer layers come up against each other; otherwise they are assumed to be impermeable.

When this conceptual karst model is applied to a 3D geological model of the study area, subsurface flow paths can be determined manually by water particle tracking according to the proposed flow principles. The end of a flow path at the land surface of the 3D geological model represents a model discharge, and neighboring discharges are grouped to discharge areas. The area that is contributing flow to a common discharge area represents the corresponding recharge area. The hydrological model is developed by performing the particle tracking in the entire model area and thus deriving all model discharges, their corresponding recharge areas and the general groundwater flow direction.

IV-2.3. Vulnerability mapping using the EPIK method

The EPIK method (Doerfliger et al., 1999) is a multi-parameter approach to intrinsic vulnerability mapping in karst areas. It was developed for the delineation of source protection zones in Switzerland. A protection index F is calculated on the basis of four attributes which form the acronym: Epikarst, Protective cover, Infiltration and Karst network development.

The epikarst (E) is a highly karstified zone situated under the soil cover. It can extend from decimeters to tens of meters. Its main functions are water storage and flow concentration. Three classes of epikarst development can be distinguished by the EPIK method, based on geomorphological karst features. There are four categories of protective cover (P), defined by the thickness of the soil and other non-karstic formations overlying the karst aquifer. The infiltration conditions (I) take into account the recharge into the karst aquifer. Four types of infiltration conditions are considered by the EPIK method. Areas with diffuse infiltration, for instance, are considered to be less vulnerable than areas that drain by concentrated recharge via a swallow hole. Karst network development (K) is divided into three categories ranging from fissured non-karstic limestone to well-developed karst network.

Values are attributed to each of the attribute classes, which are weighted and summed up. The resulting protection index F (with a high F value indicating high protection or low vulnerability) is subdivided into four vulnerability classes, with three of them constituting the protection zones S1 (very high vulnerability) to S3 (moderate vulnerability), and one comprising the rest of the recharge area (low vulnerability).

IV-2.4. Evaluation of spring vulnerability from numerical models

This method is based on the modeled discharge of karst springs using a global (lumped parameter; Singh, 1995) approach (Butscher and Huggenberger, 2007b). Simulations are performed using the software AQUASIM 2.1e (Reichert, 1994), which is designed for the identification and simulation of aquatic systems. In this program, the configuration of a model system is represented by volumetric compartments, which are connected by links. We used a model setup comprising three "mixed reactor" compartments with a variable volume to represent the groundwater recharge system (soil and epikarst system), the conduit flow system and the diffuse flow system, accounting for the main characteristics of karst systems. The model formulation is given in detail by the illustration of the model setup and the further system definitions (inflow to model, outflow of compartments, bifurcating flows; c.f. appendix).

The calibrated models are used to define spring protection classes and to generate vulnerability time series, quantifying the intrinsic vulnerability of individual karst springs and its variation in time. The quantification is based on (1) the vulnerability index VI, representing varying relative contributions of the conduit and diffuse flow system to spring discharge, and (2) the modeled vulnerability concentration C_V in spring water resulting from a standardized contaminant input into the system.

Karst aquifers are especially sensitive to contamination because of fast travel times and low storage capacity in the conduit system, making natural attenuation processes like adsorption, degradation and filtration little effective. The sensitivity of a karst spring to contamination is reduced by dilution of the water from the conduit system with water from the diffuse system, where the above mentioned processes are much more effective. The relative proportion of spring water discharging from the conduit and diffuse system as a function of time is an intrinsic property of a karst system. Therefore, we introduced the vulnerability index VI, defined as the ratio of the contributions of these systems to spring discharge ($VI = Q_{out,C}$ /

$Q_{out,D}$). VI can be used as a quantitative indicator of the intrinsic vulnerability of a karst spring. High values of VI (i.e., high relative proportion of water from the conduit system) indicate that the spring is highly sensitive to contamination at this time. This is plausible for transient contaminants being effectively attenuated by adsorption, degradation or filtration (e.g., fecal bacteria) or for contaminants that are little problematic when highly diluted (which may be the case for accidental spills).

VI can also be used in combination with a constant standard water input SWI into the model. SWI is characterized by a constant effective precipitation $Prec_{eff}$, corresponding to the long-term mean groundwater recharge. SWI ensures that the simulation is independent from the hydrologic conditions of the observation period. As SWI is constant, the simulated spring discharge as well as the contribution from the conduit and the diffuse system, and thus VI, is constant.

However, VI is not a direct representation of a potential contaminant impact and its application is restricted to assessing the impact of transient contaminants that are effectively attenuated in the diffuse system, such as fecal bacteria. For this reason the vulnerability concentration C_V is introduced. It is the simulated concentration of a "standard contaminant" SC in spring water. A non-degradable contaminant is used in this study, representing the impact of a persistent contaminant that is not effectively attenuated by adsorption, degradation or filtration in the diffuse system (e.g., nitrate, pesticides). In the following, two different applications are described, which indicate how to use breakthrough curves and time series of the vulnerability concentration C_V for intrinsic vulnerability assessment.

The first application of C_V is the simulated breakthrough curve of SC in spring water resulting from a Dirac SC input, and the standard water input SWI as introduced above. The simulated breakthrough curve allows vulnerability to be assessed from a quantitative point of view by addressing three practical questions: (1) when, (2) at what level, and (3) for how long, will contamination occur at a spring or well (Brouyére, 2003). This information is provided by (1) the first time after the contaminant input ($t_{first} - t_0$) when C_V exceeds a certain threshold value $C_{V,thresh}$, (2) the maximum concentration of the contaminant ($C_{V,max}$), and (3) the time span ($t_{end} - t_{first}$) when $C_V > C_{V,thresh}$ in spring water.

The second application of C_V is the simulated concentration of SC in spring water resulting from a continuous SC input under observed hydrological conditions. The concentration level of C_V can be used as a quantitative indicator of the temporal vulnerability distribution at the spring under observed hydrological conditions.

IV-2.5. Integration of information generating a combined vulnerability map and time series

The methods described above constitute the first three steps of the proposed approach, to give quantitative answers to questions that are both spatial (Where and how large are the recharge and discharge areas? How is the spatial distribution of vulnerability in the recharge and in the discharge areas?), and temporal in nature (How is the temporal vulnerability distribution?), both of which pertain to vulnerability assessment in karst areas. The fourth step is the composition of this information (c.f., Table 1). A vulnerability map indicates (1) the recharge and discharge areas revealed from the hydrological model (e.g., using the ABG approach); (2) the spatial vulnerability distribution in the recharge areas, transformed to protection areas S1—S3, revealed by vulnerability mapping (e.g., using the EPIK method); and (3) the spatial vulnerability distribution in the discharge areas, indicated by spring protection classes P1—P3 analogous to protection areas. The spring protection classes are obtained from the numerical simulations using the standard water input SWI. We distinguish two different types of spring protection classes, P_t and P_p. P_t is based on a classification of the (constant) vulnerability index VI indicating the protection demand of a spring with a view to transient contaminants (e.g., fecal bacteria). P_p is based on a classification of the CV breakthrough curves, indicating the protection demand of a spring with a view to persistent contaminants (e.g., nitrate, pesticides). Depending on the problem, either P_t or P_p can be used in the vulnerability map. The spatial information of the vulnerability map is then complemented by the temporal information indicated by the vulnerability time series of springs under observed hydrological conditions, based on the modeled (time variant) vulnerability index VI and the vulnerability concentration C_V. The result is the combined vulnerability map and time series proposed in this study.

IV-2.6. Test site

We developed and tested the individual methods and the overall concept on a karst plateau (Gempen plateau, Figure 3) of the Swiss Tabular Jura, a low mountain range in northwest Switzerland. It is composed of predominantly flat-lying Triassic and Jurassic sediments, and

the tectonic setting is mainly characterized by horst and graben structures. The aquifers comprise Oxfordian massive limestone (patch-reef facies) and Bajocian bedded, oolithic limestone, both representing sediments of a shallow carbonate platform. The hydrogeology of the study area is controlled by an unconfined, mature karst system. It corresponds mainly to a shallow karst (Bögli 1980), as the karst rocks slope towards and lie above the adjacent valleys into which the karst water drains freely by gravity.
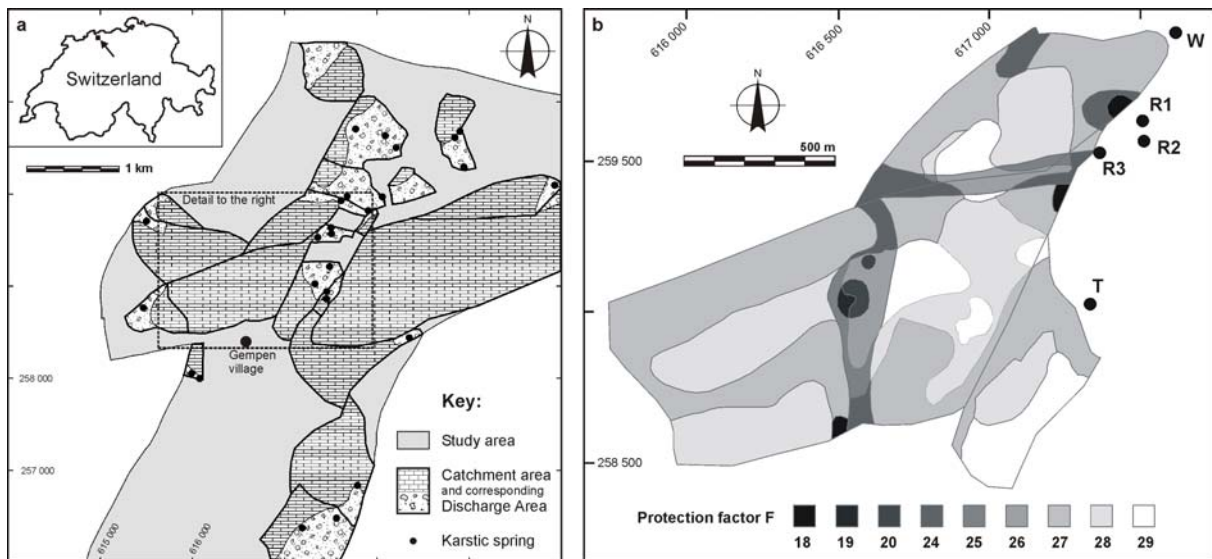

Figure 3: (a) Recharge and corresponding discharge areas of the study area delineated using the ABG approach. Recharge areas with discharge outside the study area are not indicated. (b) Protection factor F derived from vulnerability mapping applying the EPIK method to the recharge areas of the karst springs W, R1 to R3, and T.

IV-3. Results

IV-3.1. Delineation of recharge and discharge areas

The delineation of recharge and discharge areas was conducted on a regional scale covering most parts of the Gempen plateau (Figure 3a). Sixteen discharge areas and their respective recharge areas could be identified in the study area using the ABG approach. The recharge areas of the aquifers are situated on the plateau itself, while discharge generally occurs on the slopes at the plateau margins. The recharge areas are not only spatially, but also 'culturally' separated from the spring areas. The sparsely populated recharge areas on the plateau are used mainly for agriculture, whereas the springs are located in a forested environment. For the most part, the spring water is captured and used for the supply of drinking water, but pristine springs do still exist. The consumers of spring water live in large settlements in the valleys flanking the plateau. They belong to different administrative units than those living and cultivating land on the plateau. The forested discharge areas at the plateau margins are also

used for recreation purposes by the people living in the large settlements. Human activities on the plateau can endanger the springs located around the plateau. This leads to land use conflicts beyond the borders of the administrative units.

IV-3.2. Vulnerability mapping

For vulnerability mapping, we focused on the recharge areas of five springs in the central part of the plateau, which are important to the local drinking water supply: the Wolfenried (W), the Rappenfluh (R), and the Tugmatt (T) recharge areas. Applying the EPIK method to these recharge areas, a distribution of the protection factor F is obtained, with F ranging from 18—29 (Figure 3b). As a typical characteristic of vulnerability maps in karst areas, F is not distributed homogeneously. There is no systematic relation between the protective ability in the recharge areas and the distance to the discharges.
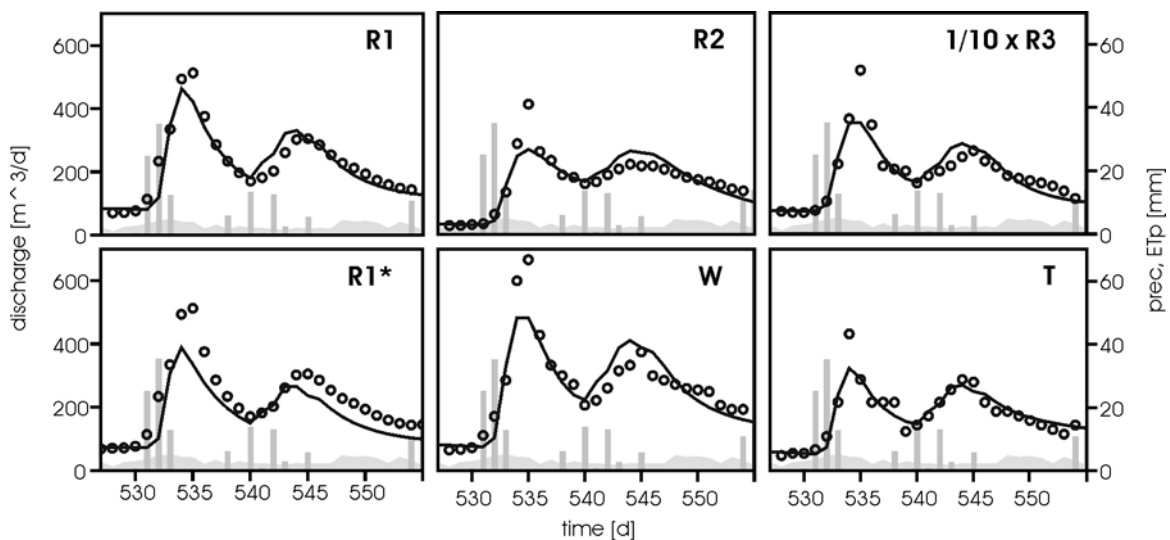

Figure 4: Measured (circles) and calculated (line) spring discharge of springs W, R1, R2, R3, and T (simulation period: 26 days, R1* extract of 461 days simulation period). Precipitation (columns) and potential evapotranspiration (area) are indicated in grey.

IV-3.3. Modeling spring vulnerability

We simulated the hydrographs of the springs Wolfenriedquielle (W), Rappenfluhquellen (R1, R2, R3) and Tugmattquelle (T), which drain the areas where the vulnerability mapping was conducted. The simulation period was 26 days from 12 March to 7 April 2005 (Figure 4 and Table 2). The calibrated models were used to calculate breakthrough curves of the vulnerability concentration C_V in spring water, resulting from a Dirac input of 1 mg standard contaminant SC per m^2 of the catchment area and a standardized water input rate SWI of 1.78 mm/d, which corresponds to the long-term mean effective precipitation (long-term mean

precipitation minus long-term mean actual evapotranspiration in the catchment areas of the investigated springs; Weingartner et al., 1999) (Figure 5). From these breakthrough curves, the potential contamination level $C_{V,max}$, the first arrival of a potential contamination at the spring t_{first}—t_0 and the duration of the contamination t_{end}—t_{first} were determined. We defined a threshold value $C_{V,thresh} = 1$ mg/m^3 for the determination of t_{first} and t_{end}. Protection classes P_p1—P_p3 were attributed to the springs indicating the protection demand of the springs with respect to persistent contaminants (P_p1 corresponding to a high protection demand). In this study, we classified the protection demand based on $C_{V,max}$: we attributed the protection class P_p1 to a spring if $C_{V,max} > 2$ mg/m^3; P_p2 if $1,5$ mg/m$^3 < C_{V,max} < 2$ mg/m^3; and P_p3 if $C_{V,max} < 1.5$ mg/m^3. Using these definitions, spring T corresponds to the spring protection class P_p1, springs R1 and W correspond to the protection class P_p2, and springs R2 and R3 correspond to the protection class P_p3 (Table 3). Other definitions of the protection classes would also be possible, either with different threshold values separating the protection classes, or taking into account the first arrival or the duration of the contamination.

Table 2: Selected estimated model parameters of the investigated springs (R1* refers to extended data set, Butscher and Huggenberger, 2007b). Notation of model parameters: c.f. annex.

	R1	R1*	R2	R3	W	T
A	190737 m^2	161619 m^2	150487 m^2	1889138 m^2	205303 m^2	146177 m^2
X_D	0.68	0.66	0.44	0.67	0.64	0.82
$1/\alpha_C$	3 d	4 d	7 d	3 d	3 d	2 d
$1/\alpha_D$	110 d	213 d	258 d	259 d	47 d	31 d

The calibrated models with the standard water input were also used to calculate VI. Analogous to P_p, protection classes P_t1—P_t3 were attributed to the springs indicating the protection demand of the springs with respect to transient contaminants. In this study, the protection class P_t1 was attributed to a spring if VI > 1.0; P_t2 if 0.3 < VI < 1.0; and P_t3 if VI < 0.3. Using these definitions, spring R2 corresponds to the spring protection class P_t1, springs R1, R3 and W correspond to the protection class P_t2, and spring T corresponds to the protection class P_t3 (Table 3). Also for P_t, other definitions, with different threshold values separating the protection classes, would be possible.
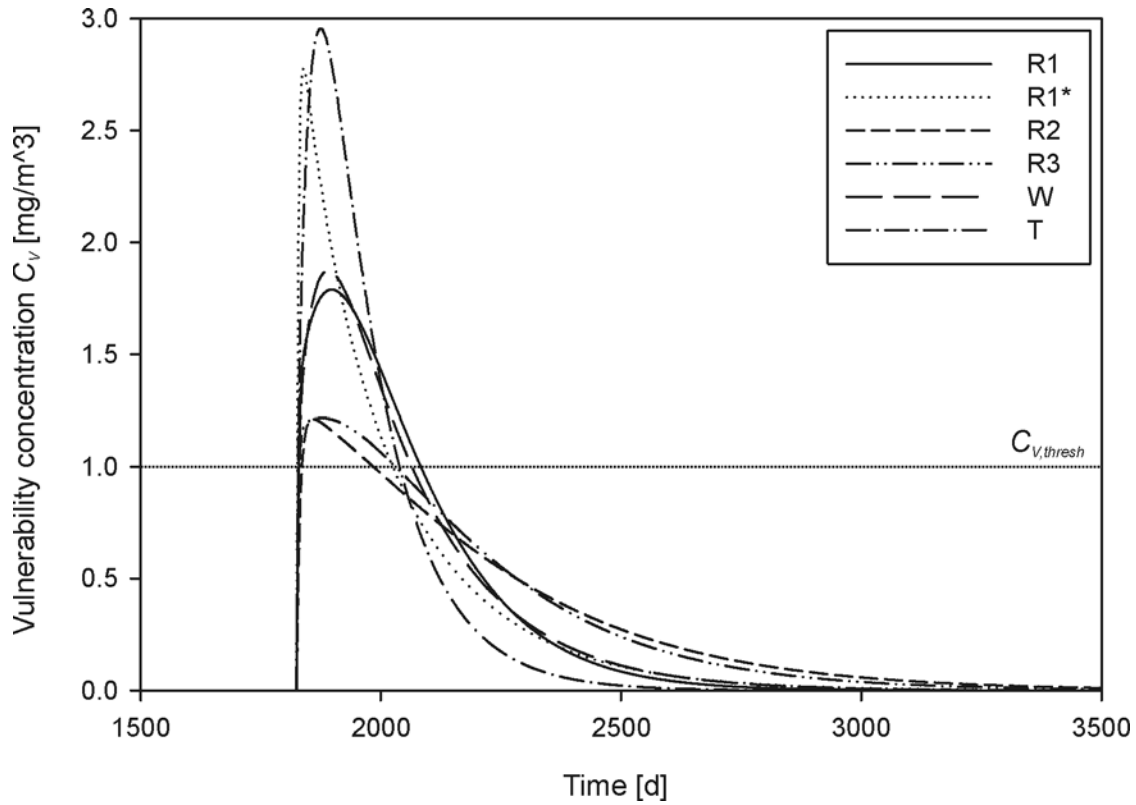
Figure 5: Simulated breakthrough curves of springs W, R1, R2, R3, and T. The maximum concentration level, as well as the first time and the last time that the concentration is above threshold $C_{V,thresh}$, reveal quantitative information on spring water vulnerability which can be used for classification purposes.

Table 3: Spring protection classes of investigated springs based on vulnerability index VI and on breakthrough curves of vulnerability concentration C_V using calibrated numerical models with standard water input SWI.

	R1	R1*	R2	R3	W	T
$C_{V,max}$	1.79 mg/m^3	2.78 mg/m^3	1.21 mg/m^3	1.22 mg/m^3	1.87 mg/m^3	2.95 mg/m^3
t_{first}—t_0	4.1 d	1.5 d	11.6 d	6.1 d	5.2 d	3.3 d
t_{end}—t_{first}	254.6 d	199.1 d	148.1 d	200.1 d	235.2 d	211.6 d
VI	0.47	0.52	1.29	0.46	0.57	0.22
Spring protection class (transient contaminants)	P_t2	P_t2	P_t1	P_t2	P_t2	P_t3
Spring protection class (persistent contaminants)	P_p2	P_p1	P_p3	P_p3	P_p2	P_p1

For the spring R1 an additional extended data set was used (data: Butscher and Huggenberger, 2007b), covering a period of 461 days from 28 May 2004 to 31 August 2005. Time series of the vulnerability index VI and vulnerability concentration C_V were calculated based on the extended data set (c.f. Figure 6, below). The resulting VI time series has the following characteristics: Concerning the peak position, VI is strongly related to the spring discharge. A significant increase in fecal bacteria concentrations during strong responses of spring discharge to recharge events is a well-known feature of karst springs and is well represented by the VI-graphs. The vulnerability index VI can therefore be used to analyze the time dependence of vulnerability. However, the peak height of VI is not proportional to the spring discharge. Spring responses after long periods without recharge lead to a higher VI than those at times with frequent recharge events. This is due to the lower water storage in the diffuse system and thus lower dilution of event water with pre-event water after long periods without recharge. In addition to assessing the dynamics of vulnerability of individual springs, different springs can be compared with respect to their sensitivity to transient contaminants that are effectively attenuated in the diffuse, but not in the conduit flow system (e.g. fecal bacteria). VI can serve as a vulnerability measure helping to distinguish, for instance, which springs in a certain area are better suited as a drinking water supply.

Analogous to the above-introduced C_V breakthrough curves, the C_V time series is calculated with an input rate of 1 mg/d per m^2 recharge area. In this case, recorded precipitation and evapotranspiration are used as water input. As a result, recharge events may cause a concentration peak, or the concentration may decrease due to dilution effects, depending on the actual hydrological situation. The C_V time series reflects the time dependence of vulnerability with respect to persistent contaminants and is, just as well as VI, suited for the purpose of quantitative comparison. In our example, maximum vulnerability concentrations of almost 2000 mg/m^3 are obtained.

IV-3.4. Combined vulnerability map and time series

The integration of information revealed by the delineation of recharge and discharge areas, the vulnerability mapping and the numerical vulnerability modeling results in a combined vulnerability map and time series (Figure 6). The delineated recharge areas are divided into the protection zones S1 (indicating high vulnerability) to S3 (indicating low vulnerability) and the springs in the discharge areas are classified by the spring protection classes P_t1 (indicating

high vulnerability with respect to transient contaminants) to P_t3 (indicating low vulnerability). In this study, we favored P_t, because transient contaminants such as fecal bacteria present the worst problem in the study area. Alternatively, e.g., if nitrate or other persistent contamination poses a major problem, P_p can be indicated on the map. In addition to this spatial information, the results of the numerical vulnerability modeling reveal temporal information, which is indicated on the vulnerability map by the time series of the vulnerability index VI and the vulnerability concentration C_V.
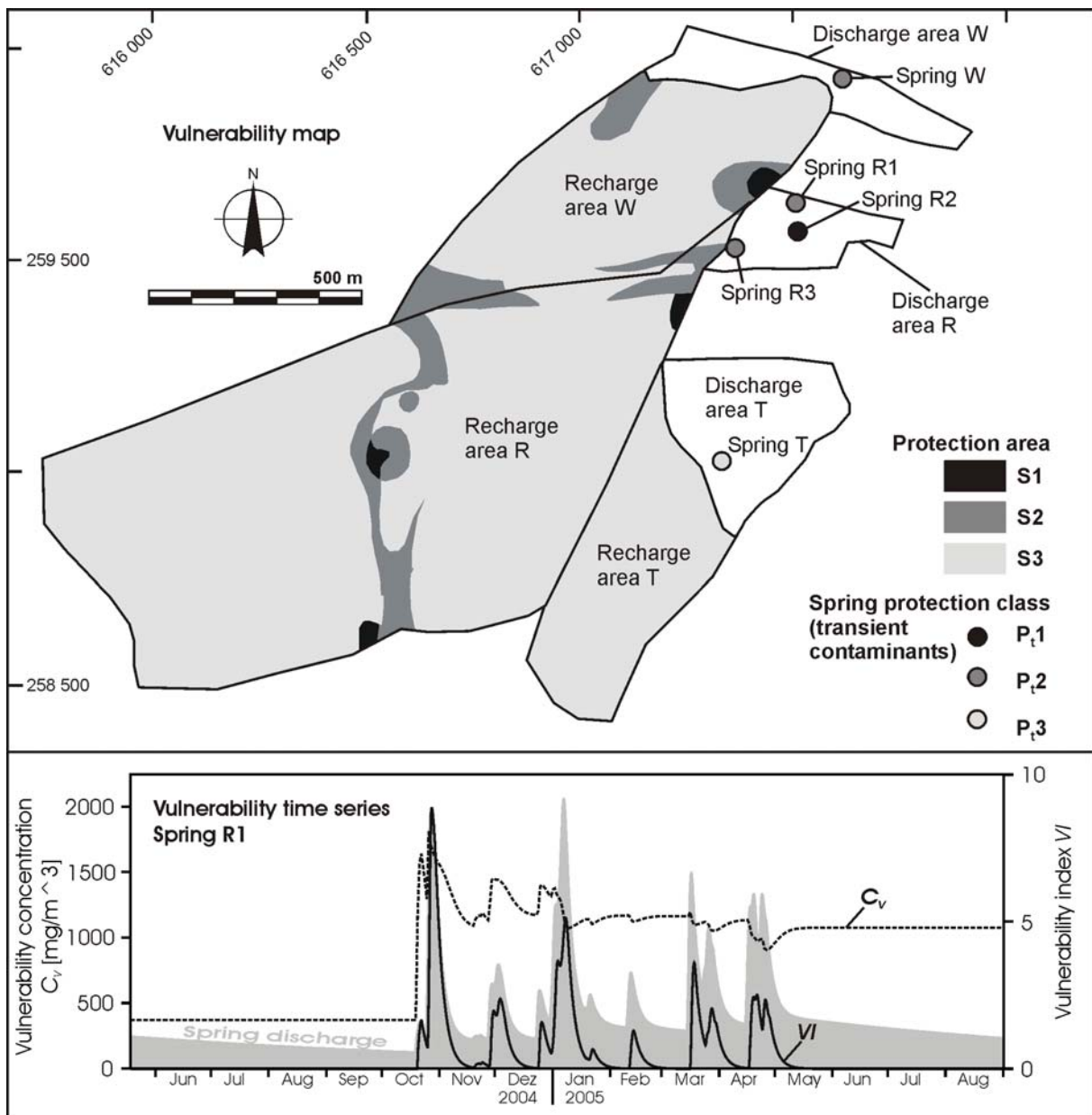

Figure 6: Combined vulnerability map and time series of vulnerability index *VI* and vulnerability concentration C_V, indicating the spatial and temporal vulnerability distribution in the recharge and discharge areas of karst springs.

IV-4. Discussion

A combined mapping and modeling approach for quantitative spatial and temporal vulnerability assessment in karst areas has been presented here. In contrast to methods based on vulnerability mapping alone, the combination of vulnerability mapping and numerical modeling yields: (1) the vulnerability distribution, not only in the recharge areas but also in the discharge areas, (2) the time dependence of karst groundwater vulnerability, and (3) a quantitative vulnerability measure. Starting with a delineation of recharge and discharge areas on a regional scale, and continuing with the more expensive mapping and numerical modeling on a local scale for selected springs only and the related recharge areas, makes the approach very effective. The costs for mapping and numerical modeling can be justified, for example, in the case of highly discharging springs used for the drinking water supply, or ecologically important springs.

This approach improves existing mapping techniques for vulnerability assessment in other ways beyond those described above. The term 'vulnerability' is generally used in the sense of Vrba and Zaporozec (1994), who defined vulnerability as an intrinsic property of a groundwater system that depends on the sensitivity of that system to human and/or natural impact. Brouyère (2003), however, points out that vulnerability can mean different things: in some cases, a short but heavy contamination might be worse than a long-lasting moderate contamination, in other cases vice versa. Our approach allows different aspects of groundwater vulnerability to be considered on the basis of modeled contaminant breakthrough curves and time series.

Intrinsic vulnerability assessment demands that only the hydrological characteristics of the karst system are taken into account, and not the specific characteristics of a potential contaminant. However, given that karst aquifers exhibit an extremely inhomogeneous, "dual conduit and diffuse" flow system (e.g. Atkinson, 1977), it seems justified to account for a "dual transient and persistent" intrinsic vulnerability. In our study, springs that are highly vulnerable to transient contamination (indicated by the spring protection class P_t1) are not very vulnerable to persistent contamination (indicated by the spring protection class P_p3) and vice versa (c.f., Table 3).

Drinking water management benefits from a quantitative spatial and temporal approach. Combining vulnerability mapping with numerical modeling contributes to a better

understanding of the actual groundwater system and is therefore advantageous if spring water quality is insufficient in spite of a protection zone. The knowledge of how water quality and quantity is generated is a precondition of karst water protection. The consideration of the dimension of time adds a degree of freedom to water protection strategies. Temporally limited land use restrictions in the recharge areas of drinking water sources and water withdrawal management, for example, are possible future applications of temporal approaches. The possibility to compare the vulnerability of different springs from a quantitative point of view provides an objective basis for a regional planning of drinking water supply.

Apart from the needs of drinking water suppliers, the approach is also relevant to environmental considerations. Human activities in the recharge areas endanger the spring water quality and consequently have a direct influence on the ecology of natural spring habitats. Aspects other than spring water quality that depend on hydrological processes may additionally influence spring organisms. Examples are (the variation of) spring discharge, relative contributions to spring discharge from different flow systems, and properties of flow paths linking springs with their catchments. Such aspects can be investigated by combining mapping with modeling techniques. Spring water quality and quantity is not only an important factor for the ecology of the spring itself, but also for the subsequent spring brook, and in succession, of rivers, streams and lakes. Moreover, our approach encourages a possible revitalization of captured springs. The presented methods help to identify springs that are relatively unprotected against fecal contamination due to their hydrologic characteristics. Such springs are of only minor importance to the water supply and, therefore, have high potential for revitalization. Thus concrete recommendations can be made of springs that are to be chosen for revitalization projects.

Strictly speaking, the combined mapping and modeling approach of this study is a special case of a general approach combining mapping and modeling methods for hydrogeologic investigations, applied to vulnerability assessment. The general approach may also be applied to the assessment of natural hazards, risks from waste sites or other geotechnical problems. An actual aspect, for example, concerns the effects of climate change on slope stability. Climate change causes an increase in extreme precipitation events (e.g., Semmler and Jacob, 2004). As a consequence, extreme spring discharges, also at places that are dry under normal conditions, will become more and more frequent. This is especially the case for karst terrains, where groundwater levels are known to rise dramatically after heavy rainfall events (e.g.

Jeannin, 2001). An increase in destructive land slides would be a possible direct consequence. The vast damage that occurred in Switzerland after an extreme rainfall event in August 2005 (FOWG, 2005) may serve as a meaningful example. Our approach is suitable for localizing endangered areas and developing scenarios by the delineation of discharge areas and numerical discharge simulations. Generally, the combined mapping and modeling approach can make a contribution to many geotechnical fields where the knowledge of recharge and discharge areas and knowledge of the response of subsurface flow systems to recharge events under varying conditions are an important prerequisite of detailed investigations.

The data needs of our approach include, in addition to the data evaluated for vulnerability mapping, geological maps to establish the 3D geological model for the delineation of recharge and discharge areas, and time series of meteorological data and hydrographs for the numerical modeling. Geological maps are readily available in good quality for many regions worldwide. The effort required to collect meteorological and hydrograph data is moderate. The comparison of our numerical modeling results obtained from the 26-day investigation and the extended data set covering a period of 461 days clearly shows differences with respect to estimated model parameters and, as a result, also with respect to modeled breakthrough curves. This indicates that long-term recordings give more reliable results than short-term experiments, and that a comparison of different springs should be based on the same data set. Therefore, a commitment to continuously measure the discharge of captured springs is desirable. In many cases, this would represent only a minor burden to drinking water suppliers.

The presented study is a first approach towards a quantitative, spatial and temporal vulnerability assessment. The proposed methods have certain limitations. By applying the ABG approach to the Gempen plateau test site, it was possible to predict the occurrence of more than half of the springs and up to 54% of the hydraulic links confirmed by tracer tests (Butscher and Huggenberger, 2007a). From this it follows that processes, other than those underlying the ABG approach must also be active. Therefore, results have to be validated, at least for those springs and their catchments being in the focus of the investigation. The validation can be done, for example, by tracer tests. There are other points that remain unaddressed in this study. For example, there is currently a certain lack of experience on which thresholds to base the spring protection classes defined here. These thresholds need to

be adapted, in line with the results of further applications. Nevertheless, the spring protection classes used in this study are based on objectively quantifiable values.

'Volumetric' models, where flow systems are globally represented by volumetric compartments, involve a simplification of flow processes. On the one hand, unsaturated flow must be neglected. Flow through the unsaturated zone in mature karst systems, however, is in most cases very fast compared to the time scale of approximately one month at which our numerical modeling was conducted. On the other hand, the transport of substances simulated by volumetric models is not based on the actual processes such as advection. Nevertheless, the typical dual "conduit and diffuse" characteristic of karst systems is adequately included in the numerical model, and parameters that are relevant for the system's vulnerability, such as residence times and storage capacities, are also given adequate consideration. Haitjema (1995) showed for diffuse-source pollution (e.g., from the application of agricultural chemicals or liquid manure to cropland) that the cumulative residence time distribution of ideal catchments is exponential. This is exactly the case for the linear storage used in our volumetric model. By contrast, the residence time distribution of point-source pollution (e.g., from leaking storage tanks or industrial sites) will depend on many local factors. Therefore, the numerical modeling approach of this study is well suited to assess diffuse-source pollution, whereas the assessment of point-source pollution remains critical. The vulnerability to point-source pollution, however, is addressed by the vulnerability mapping in the catchment area.

Distributed modeling techniques, such as MODFLOW (Harbaugh & McDonald, 1996), are based on the actual flow processes and consider local variations of aquifer parameters, but have other limitations in karst areas. When applied to real aquifers, these approaches require extensive data sets (like hydraulic heads and hydraulic conductivities) for both model setup and calibration. Such data are extremely rare in karst areas and are costly to obtain. Additionally, such data are difficult to interpret, because even neighboring observation wells may not be hydraulically connected in karst areas. Moreover, distributed models accounting for the special situation in karst areas nearly always have to combine a continuum with a discrete channel approach ('hybrid' models, e.g. Liedl et al., 2003). This is difficult to implement for real karst aquifers due to the unknown geometry of the conduit network. For that reason, such hybrid models are more used to investigating principle karst processes than to quantifying the actual flow and transport of substances in a certain study area (Sauter et al., 2006). Hence, despite their limitations, we consider the application of volumetric models to

vulnerability assessment in karst areas just as appropriate as distributed modeling approaches. In the context of balancing the pros and cons of different modeling approaches for vulnerability assessment in karst areas, it would be a helpful (but challenging) future project to compare results from models such as presented in this study and distributed models with data from field observations. However, this would require a well-defined test site, where all geometric and hydraulic boundary conditions are accurately known or can be directly observed.

The methods used here have been developed for the special situation of a shallow karst, where groundwater flow patterns are strongly influenced by the aquifer base gradient. An application to karst settings different to those of this study (or even to fractured and porous aquifers) would require an adaptation of the methods. Herold et al. (2000), for example, investigated the influence of tectonic structures on karst groundwater flow patterns in an anticline complex (Weissenbergkette) of the Swiss Folded Jura. In this area, the aquifer base extends beyond the discharge level of the karst system. A conceptual model was proposed, which included fault zones acting as lateral drains perpendicular to the main flow direction. Accounting for this conceptual model, an approach for the identification of recharge and discharge areas could be developed analogous to our ABG approach. Also in this case, and for many other hydrogeological settings, 3D geological modeling can serve as an effective tool providing the structural framework for a conceptual flow model. Thus, the general approach outlined in our study, including the delineation of recharge and discharge areas on a regional scale based on 3D geological modeling, and vulnerability mapping and numerical simulations on a local scale, is suggested to have general application.

IV-5. Conclusions

The combined mapping and modeling approach of this study facilitates a sustainable regional planning of water resources in karst areas by providing a conceptual framework for an integrative vulnerability assessment. The combination of vulnerability mapping and numerical modeling allows (1) the vulnerability distribution, both in the recharge and discharge areas, to be identified, (2) the time dependence of karst groundwater vulnerability to be assessed, and (3) a quantitative basis for vulnerability assessment to be established. Compared to other groundwater modeling techniques, the data requirements are moderate. Apart from drinking water management, ecological and geotechnical problems can also be addressed.

Acknowledgements

References

Atkinson, T. C., 1977. Diffuse flow and conduit flow in limestone terrain in the Mendip Hills, Somerset (Great Britain). J. Hydrol. 35, 93—110.

Auckenthaler, A., Raso, G., Huggenberger, P., 2002. Particle transport in a karst aquifer: Natural and artificial tracer experiments with bacteria, bacteriophages and microspheres. Wat. Sci. Technol. 46 (3), 131—138.

Bakalowicz, M., 2005. Karst Groundwater: a challenge for new resources. Hydrogeol. J. 13 (1), 148—160. doi:10.1007/s10040-004-0402-9.

Bauer, S., Liedl, R., Sauter, M., 2005. Modeling the influence of epikarst evolution on karst aquifer genesis: A time-variant recharge boundary condition for joint karst-epikarst development. Water Resour. Res. 41, W09416. doi:10.1029/2004WR003321.

Bögli, A., 1980. Karst hydrology and physical speleology. Springer, Berlin.

Botosaneau, L. (Ed.), 1998. Studies in crenobiology. The biology of springs and springbrooks. Backhuys Publisher, Leiden.

Brouyère, S., 2003. A quantitative point of view of the concept of vulnerability. - In: Zwahlen, F. (Ed.), Vulnerability and risk mapping for the protection of carbonate (karst) aquifers, COST action 620, Final report. European Comission, Directorat-General XII Science, Research and Development, Brüssel.

Butscher, C., Huggenberger, P., 2007a. Implications for karst hydrology from 3D geological modeling using the aquifer base gradient approach. J. Hydrol. 342 (1-2), 184—198. doi:10.1016/j.jhydrol.2007.05.025.

Butscher, C., Huggenberger, P., 2007b. Intrinsic vulnerability assessment in karst areas: a numerical modeling approach. Submitted to Water Resour. Res., minor revisions requested.

Connell, L. D., van den Daele, G., 2003. A quantitative approach to aquifer vulnerability mapping. J. Hydrol. 276, 71—88.

COST 620, 2003. Vulnerability and risk mapping for the protection of carbonate (karst) aquifers, Final report (COST action 620). European Comission, Directorat-General XII Science, Research and Development, Brüssel.

Daly, D., Dassargues, A., Drew, D., Dunne, S., Goldscheider, N., Neale, S., Popescu, I. C., Zwahlen, F., 2002. Main concepts of the „European approach" to karst-groundwater-vulnerability assessment and mapping. Hydrogeol. J. 10, 340—345.

Doerfliger, N., Jeannin, P.-Y., Zwahlen, F., 1999. Water vulnerability assessment in karst environments: a new method of defining protection areas using a multi-attribute approach and GIS tools (EPIK method). Environ. Geol. 39 (2), 165—176.

Ford, D. C., Williams, P. W., 1989. Karst geomorphology and hydrology. Chapman and Hall, New York.

FOWG, 2005. Bericht über die Hochwasserereignisse 2005 (Report of the flooding event 2005). Federal Office for Water and Geology (FOWG), Bern. Available at http://www.bafu.admin.ch/hydrologie/01834/02041/02043/index.html?lang=de.

Gibert, J., Malard, F., Turquin, M. J., Laurent, R., 2000. Karst ecosystems in the Rhône river basin. In: Wilkens, H., Culver, D. C., Humphreys, W. F. (Eds.), Subterranean ecosystems, 533—558.

Gibert, J., Vervier, P., Malard, F., Laurent, R. & Reygrobellet, J.-L., 1994. Dynamics of communities and ecology of karst ecosystems: example of three karsts in eastern and southern France. In: Gibert, J., Danielopol, D. L., Stanford, J. A. (Eds.), Groundwater ecology, 425—450.

Glazier, D. S., 1991. The fauna of North American temperate and cold springs: Patterns and hypothesis. Freshwater Biology 26, 527—542.

Gogu, R. C., Dassargues, A., 2000. Current trends and future challenges in groundwater vulnerability assessment using overlay and index methods. Environ. Geol. 39 (6), 549—559.

Goldscheider, N., 2002. Hydrogeology and vulnerability of karst systems – examples from the Northern Alps and the Swabian Alb. PhD thesis University of Karlsruhe. Available at http://www.ubka.uni-karlsruhe.de/vvv/2002/bio-geo/3/3.pdf.

Goldscheider, N., 2005. Karst groundwater vulnerability mapping: application of a new method in the Swabian Alb, Germany. Hydrogeol. J. 13, 555—564. doi:10.1007/s10040-003-0291-3.

Haitjema, H. M., 1995. On the residence time distribution in idealized groundwatersheds. J. Hydrol. 172, 127—146.

Harbaugh, A. W., McDonald, M. G., 1996. Programmers documentation for MODFLOW-96 – An update to the US Geological Survey modular finite-difference groundwater model. U. S. Geol. Surv. Open File Rep., 96—486.

Herold, T., Jordan, P., Zwahlen, F., 2000. Influence of tectonic structures on karst flow patterns. Eclogae Geol. Helv. 93, 349—362.

Jeannin, P.-Y., 2001. Modeling flow in phreatic and epiphreatic karst conduits in the Hölloch cave (Muotatal, Switzerland). Water Resour. Res. 37 (2), 191—200.

Kaufmann, G., Braun, J., 2000. Karst aquifer evolution in fractured, porous rocks. Water Resour. Res. 36, 1381—1391.

Kaufmann, G., 2002. Karst aquifer evolution in a changing water table environment. Water Resour. Res. 38 (6). doi:10.1029/2001WR000256.

Liedl, R., Sauter, M., Hückinghaus, D., Clemens, T., Teutsch, G., 2003. Simulation of the development of karst aquifers using a coupled continuum pipe flow model. Water Resour. Res. 39 (3), 1057. doi:10.1029/2001WR001206.

National Research Council, 1993. Groundwater vulnerability assessment, contamination potential under conditions of uncertainty. Committee on Techniques for Assessing Ground Water Vulnerability, Water Science and Technology Board, Commission on Geosciences Environment and Resources. National Academy Press, Washington DC.

Reichert, P., 1994. AQUASIM – A tool for simulation and data analysis of aquatic systems. Wat. Sci. Tech. 30 (2), 21—30.

Ryan, M., Meiman, J., 1996. An Examination of Short-Term Variations in Water Quality at a Karst Spring in Kentucky. Ground Water 34 (1), 23—30. doi:10.1111/j.1745-6584.1996.tb01861.x.

Sauter, M., Kovács, A., Geyer, T., Teutsch, G., 2006. Modellieruing der Hydraulik von Grundwasserleitern – Eine Übersicht (Modeling the hydraulics of aquifers – an overview). Grundwasser 3/2006, 143—156. doi:10.1007/s00767-006-0140-0.

Semmler, T., Jacob, D., 2004. Modeling extreme precipitation events - a climate change simulation for Europe. Global and Planetary Change 44 (1-4), 119—127. doi:10.1016/j.gloplacha.2004.06.008.

Sing, V.P., 1995. Watershed modeling. In: Singh, V. P. (Ed.), Computer models of watershed hydrology. Water Resources Publications, Colorado, pp. 1—22.

Van der Kamp, G., 1995. The hydrology of springs in relation to the biodiversity of spring fauna: a review. Journal of the Kansas Entomological Society 68 (2), 4—17.

Von Fumetti, S., Nagel, P., Scheifhacken, N., Baltes, B., 2006. Factors governing macrozoobenthic assemblages in perennial springs in north-west Switzerland. Hydrobiologia 568, 467—475. doi:10.1007/s10750-006-0227-8.

Vrba, J., Zoporozec, A. (Eds.), 1994. Guidebook on Mapping Groundwater Vulnerability. International Contributions to Hydrogeology (IAH), 16, Hannover.

Weingartner, R., Spreafico, M., Leibundgut, C., 1999. Hydrological Atlas of Switzerland. Federal Office for Water and Geology, Bern.

Appendix: Setup of the numerical model
(from: Butscher and Huggenberger, 2007b)

Schematic illustration
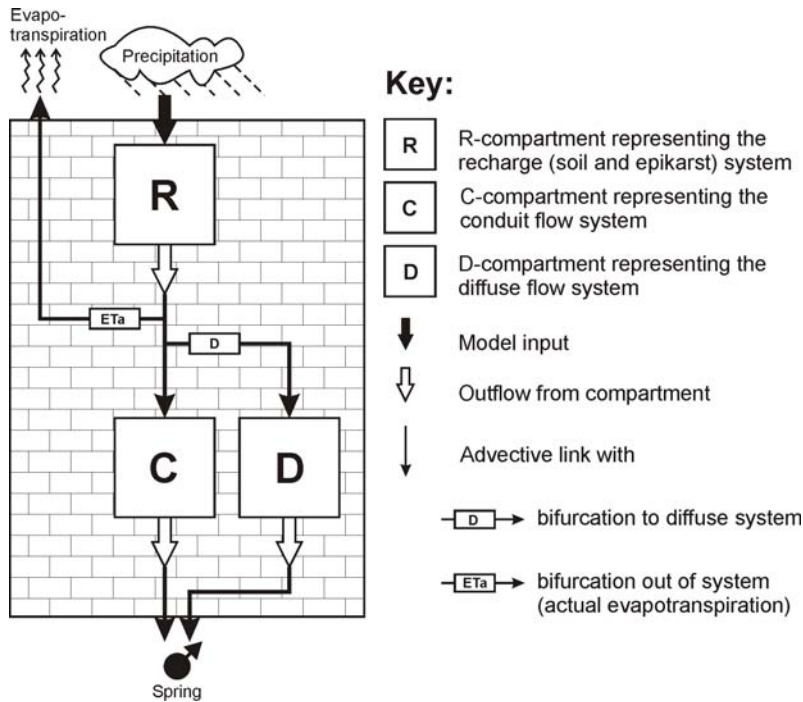
Definition of inflow to model, outflow of compartments, and bifurcating flows

$Q_{bif,D}$ $X_D \cdot Q_{recharge}$

$Q_{bif,ETa}$ if $V_R < V_{ws}$ then $(V_R / V_{ws}) \cdot ETp \cdot A$ else $ETp \cdot A$

Q_{in} $Prec \cdot A$

$Q_{out,C}$ $\alpha_C \cdot V_C$

$Q_{out,D}$ $\alpha_D \cdot V_D$

$Q_{out,R}$ $Q_{bif,ETa} + Q_{recharge}$

$Q_{recharge}$ if $V_R < V_{fc}$ then 0 else $\alpha_R \cdot (V_R - V_{fc})$

Notation

A	Extent of recharge area, (m^2)
ETp	Potential evapotranspiration, (m/d)
$Prec$	Precipitation, (m/d)
$Q_{bif,D}$	Bifurcating flow to compartment D (fraction of groundwater recharge to diffuse system), (m^3/d)
$Q_{bif,ETa}$	Bifurcating flow (actual evapotranspiration) out of model system, (m^3/d)
Q_{in}	Input flow to model, (m^3/d)
$Q_{out,C}$	Outflow of compartment C (conduit system), (m^3/d)
$Q_{out,D}$	Outflow of compartment D (diffuse system), (m^3/d)
$Q_{out,R}$	Outflow of compartment R (recharge system), (m^3/d)
$Q_{recharge}$	Groundwater recharge, (m^3/d)
V_C	Actual volume of compartment C (conduit system), (m^3)
V_D	Actual volume of compartment D (diffuse system), (m^3)
V_{fc}	Threshold volume for groundwater recharge ("field capacity"), (m^3)
V_R	Actual volume of compartment R (recharge system), (m^3)
V_{ws}	Threshold volume for limiting ETp to actual Evapotranspiration ("water stress"), (m^3)
X_D	Coefficient determining fraction of groundwater recharge to diffuse system ($0 \leq X_D \leq 1$), (-)
α_C	Outflow coefficient of compartment C (conduit system), (1/d)
α_D	Outflow coefficient of compartment D (diffuse system), (1/d)
α_R	Outflow coefficient of compartment R (recharge system), (1/d)

V. Zusammenfassung und Schlussfolgerungen

Die im Rahmen der vorliegenden Dissertation durchgeführten Untersuchungen können in drei Themenschwerpunkte gegliedert werden. Die Kapitel II—IV widmen sich je einem dieser Schwerpunkte. Entsprechend werden nachfolgend die Schlussfolgerungen anhand dieser Struktur diskutiert.

In einem ersten Schritt dieser Arbeit wurde eine Methode entwickelt, die es ermöglicht, die Lage und Ausdehnung von Quellgebieten und ihren Einzugsgebieten in Karstgebieten zu ermitteln und die Fliesspfade im Untergrund zu charakterisieren („ABG approach", Kapitel II). Die Methode basiert auf einer 3D Modellierung des geologischen Untergrunds. Aus dem 3D geologischen Modell ergibt sich der strukturelle Rahmen für ein hydrologisches Modell. Mit Hilfe des hydrologischen Modells konnten im Untersuchungsgebiet mehr als die Hälfte der Quellstandorte und bis zu 54 % der hydraulischen Verbindungen, die von Markierversuchen bekannt waren, vorhergesagt werden. Die Methode benötigt keine aufwändigen Datensätze und liefert die konzeptionelle Basis für fundierte Feldexperimente. Sie ist besonders bei einer Anwendung in grossen und komplexen Karstgebieten ein effizientes Planungswerkzeug für regional ausgerichtete Schutzkonzepte.

In einem zweiten Schritt wurde für eine ausgesuchte Quelle die Reaktion der Schüttung auf Niederschlagsereignisse numerisch modelliert (Kapitel III). Es wurden Vorschläge gemacht, wie die kalibrierten Modelle genutzt werden können, die Vulnerabilität des Quellwassers zu quantifizieren. Für die Quantifizierung der Vulnerabilität wurden zwei Kriterien herangezogen: der Vulnerabilitätsindex VI, welcher die Beiträge von schnellen und langsamen Fliesssystemen zur Quellschüttung beschreibt, und die Vulnerabilitätskonzentration C_V, welche die Belastung des Quellwassers mit Schadstoffen repräsentiert. Dadurch konnte insbesondere die zeitliche Änderung der Vulnerabilität berücksichtigt werden. Ausserdem ermöglicht der Ansatz, verschiedene Quellen in Bezug auf ihre Gefährdung zu vergleichen.

Als dritter Schritt wurde ein integrativer Ansatz zur räumlichen und zeitlichen Beurteilung der Vulnerabilität in Karstgebieten vorgestellt, der auf einer Kombination der hier entwickelten Methoden mit bestehenden Kartiermethoden beruht (Kapitel IV). Dabei werden zuerst die Quell- und Einzugsgebiete auf Basis der 3D geologischen Modellierung bestimmt. In den

Einzugsgebieten, die für eine Trinkwasserversorgung oder für den Naturschutz eine besondere Bedeutung haben, wird dann die Vulnerabilität auf Basis von Multikriterienmethoden (z. B. EPIK, Doerfliger und Zwahlen, 1998) kartiert. Gleichzeitig wird für die dazugehörenden Quellen das unterirdische Fliessgeschehen mit numerischen Modellen simuliert. Die Ergebnisse der einzelnen Methoden können durch kombinierte Vulnerabilitätskarten und -zeitreihen dargestellt werden. Die wichtigsten Vorteile gegenüber Methoden, die ausschliesslich auf einer Kartierung der Vulnerabilität beruhen, sind folgende: (1) Die räumliche Verteilung der Vulnerabilität kann nicht nur für Einzugsgebiete, sondern auch für Quellgebiete angegeben werden; (2) Die zeitliche Änderung der Vulnerabilität kann beurteilt werden; und (3) die Quantifizierung der Vulnerabilität anhand von objektiven Kriterien erlaubt ein Vergleich von Quellen untereinander.

Der integrative Ansatz bietet noch weitere Vorteile. Vulnerabilität wird im allgemeinen entsprechend der Definition von Vrba und Zaporozec (1994) verstanden als „… an intrinsic property of a groundwater system that depends on the sensitivity of that system to human and/or natural impact". Brouyère (2003) weist hingegen darauf hin, dass Vulnerabilität Verschiedenes bedeuten kann: Eine kurzfristige starke Belastung einer Quelle kann schlimmer sein als eine langfristige mässige Belastung – oder umgekehrt. Die vorgestellten Methoden erlauben eine differenzierte und problemorientierte Beurteilung der Situation, indem objektive Kriterien für die Fragen nach dem „Wie stark?" und „Wie lang?" definiert werden. Durch die Modellierung des Fliessgeschehens wird eine verbesserte Kenntnis der hydrologisch-hydrogeologischen Prozesse erarbeitet. Dies ist ein grosser Vorteil, wenn Quellfassungen trotz einer Schutzzonenausscheidung eine ungenügende Wasserqualität aufweisen. Die Berücksichtigung zeitlicher Aspekte erweitert Strategien zum Grundwasserschutz um eine Dimension und eröffnet dadurch neue Wege beim Auftreten von Nutzungskonflikten in den Quelleinzugsgebieten. Beispielsweise können Auflagen in den Schutzzonen für die Landnutzer zu Zeiten geringer Vulnerabilität gelockert werden (Bewirtschaftungs-Management) oder das Trinkwasser kann zu Zeiten erhöhter Vulnerabilität an den Quellfassungen verworfen werden (Entnahme-Management). Voraussetzung ist eine genaue Kenntnis der stattfindenden Fliessprozesse und der daraus resultierenden Dynamik bezüglich der Trinkwasserqualität. Ein weiterer Vorteil dieser Vorgehensweise ist, dass die Gefährdung nicht pauschal, sondern in Bezug auf individuelle Quelle angegeben werden kann, auch wenn diese sich ihr Einzugsgebiet mit anderen Quellen teilen. Eine mögliche Aufgabe besonders gefährdeter Trinkwasserquellen kann neue Spielräume bei der Abwägung

von Schutzmassnahmen in den Einzugsgebieten eröffnen. Ausserdem schafft die Möglichkeit, die Vulnerabilität an verschiedenen Quellen quantitativ zu vergleichen, eine objektive Basis für die Regionalplanung.

Der vorliegende Ansatz beginnt mit einer Abgrenzung der Einzugs- und Quellgebiete und Charakterisierung der Fliesswege auf regionaler Ebene und setzt sich anschliessend mit Untersuchungen auf lokaler Ebene für Quellen und ihre Einzugsgebiete fort, die für die Wasserversorgung oder den Naturschutz eine grosse Bedeutung haben. Der Aufwand für die Kartierung, Feldversuche und Modellierung ist für bedeutsame Quellen vertretbar. Genaue Systemkenntnisse können beispielsweise eine gezielte Wahl und Dimensionierung einer Trinkwasseraufbereitungsstufe erleichtern. Abgesehen von den Daten, die für eine Kartierung der Vulnerabilität erhoben werden müssen, beinhalten die erforderlichen Daten einerseits geologische Karten zum Aufbau des 3D geologischen Modells, und andererseits eine kontinuierliche Aufzeichnung der Quellschüttung und meteorologischer Daten zur numerischen Modellierung. Geologische Karten sind häufig in guter Qualität verfügbar. Der Aufwand für die Aufzeichnung der meteorologischen Daten und der Quellschüttung ist moderat. Die Untersuchungen haben gezeigt, dass langfristige Aufzeichnungen (grösser ein Jahr) verlässlichere Ergebnisse erbringen als kurzfristige Experimente. Ausserdem ist für einen regionalen Vergleich der Ergebnisse ein einheitlicher Datensatz erforderlich. Eine Verpflichtung der öffentlichen Trinkwasserversorgung, die Schüttung der einzelnen genutzten Quellfassungen kontinuierlich zu messen, wäre aus Sicht der Qualitätssicherung wünschenswert und würde in vielen Fällen nur eine relativ geringe finanzielle Belastung bedeuten.

Bisher werden Schutzzonen in Karstgebieten meist ausgeschieden, ohne die genaue Lage und Grösse der Einzugsgebiete zu kennen. Um den Schutz der Trinkwasserquellen zu gewährleisten, werden häufig zu grosse Schutzzonen ausgewiesen. Landnutzern, die durch die Schutzbestimmungen Nachteile hinnehmen müssen, kann der Sinn der Schutzzonen aber nur schwer vermittelt werden, wenn nur vage Kenntnisse über die Herkunft des Quellwassers vorhanden sind. Dies gilt insbesondere, wenn trotz der Einschränkungen bei der Landnutzung die Rohwasserqualität nicht immer einwandfrei ist. In der Praxis kann dies zu Problemen bei der Umsetzung von Gewässerschutzmassnahmen führen. Als Folge wird die Ausscheidung von Schutzzonen dann nicht nur durch die hydrologischen, sondern auch durch politische Rahmenbedingungen beeinflusst, oder gar nicht umgesetzt. Mit der vorliegenden Arbeit

wurde ein neuer Weg aufgezeigt, der eine differenzierte Ausscheidung von Schutzzonen ermöglicht. Die Ergebnisse können anschliessend mit Markierversuchen gezielt überprüft werden. Das 3D geologisches Modell und die numerische Simulation des Fliessgeschehens helfen ausserdem, die geologischen Randbedingungen für Entscheidungsträger und Landnutzer zu visualisieren und somit die Akzeptanz für politische Entscheidungen zu erhöhen.

Der vorgestellte Ansatz ist nicht ausschliesslich für die Belange der Trinkwasserversorgung zugeschnitten, sondern hat auch für die Belange des Naturschutzes eine Bedeutung. Die Qualität des Quellwassers hat möglicherweise einen direkten Einfluss auf die Ökologie von Quellhabitaten (z. B. Glazier, 1991). Ausserdem können die hydrologischen Prozesse auch auf andere Weise einen Einfluss auf Quellorganismen haben. Beispiele sind die Variation der Quellschüttung, das Temperaturverhalten des Quellwassers, relative Beiträge aus verschiedenen Fliesssystemen zur Quellschüttung und geometrische Eigenschaften der Fliesswege, die die Quellen mit ihrem Einzugsgebiet verbinden (Gibert et al., 1997; Von Fumetti et al. 2006). Diese Aspekte können mit den vorgestellten Methoden untersucht werden. Die Qualität und Quantität des Quellwassers ist nicht nur für die Ökologie der Quellen selbst von Bedeutung, sondern auch für die der unterhalb folgenden Quellbäche, Flüsse und Seen. Aus dem quantitativen Vergleich der Gefährdung der Trinkwasserqualität verschiedener Quellen ergibt sich zudem ein Potenzial für eine mögliche Revitalisierung von Quellen, die infolge einer hohen Vulnerabilität eine geringere Bedeutung für die Wasserversorgung haben (Baltes et al. 2005). Mit den vorgestellten Methoden können Quellen bestimmt werden, die aufgrund ihrer hydrologischen Eigenschaften und der Vulnerabilität in ihrem Einzugsgebiet relativ ungeschützt vor einer möglichen Verschmutzung sind, und solche, für die ein hoher natürlicher Schutz gegeben ist. Die ermittelten Daten und Ergebnisse liefern somit auch Kriterien, mit denen das Revitalisierungs-Potenzial verschiedener Quellen beurteilt werden kann. So können konkrete Vorschläge für Quellen gemacht werden, die sich für eine Revitalisierung eignen. Dem gegenüber stehen Quellen, die eine grosse Bedeutung für die Trinkwasserversorgung haben und entsprechend ihrer Vulnerabilität vor Verunreinigungen geschützt werden müssen.

Quellaustritte können einen starken Einfluss auf die Stabilität von Hanglagen ausüben. Aus diesem Grund wären nach einer Vorauswahl von Quellen als mögliche Standorte für eine Revitalisierung weitere Abklärungen mit den Landnutzern notwendig. Es ist davon

auszugehen, dass eine Revitalisierung von Quellen Auswirkungen auf Forst und Strassenstabilität haben kann. Auf konkrete geotechnische Untersuchungen wurde im Rahmen der Dissertation jedoch verzichtet, da solche objektspezifisch in der Praxis anzusiedeln wären. Die hier vorliegenden hydrologischen Grundlageninformationen genügen den Anforderungen für entsprechende Untersuchungen. In der Praxis stehen solche Daten nur in den seltensten Fällen in dieser Qualität zur Verfügung.

Die Kombination einer Kartierung mit einer Modellierung könnte auch für andere geotechnische Anwendungen nützlich sein. Der prognostizierte Klimawandel kann zu einer Häufung solcher extremen Wettersituation führen, wie sie im August 2005 in der Zentralschweiz stattfanden (z. B. Semmler und Jakob, 2004). Damals hatten extreme Quellabflüsse, auch in Hanglagen, die unter normalen Bedingungen stabil sind, zerstörerische Bergrutsche zur Folge (BWG, 2005). Der vorliegende Ansatz eignet sich zur Lokalisierung von gefährdeten Gebieten und zur Szenarienentwicklung durch die Abgrenzung der Quellgebiete und die numerische Simulation des Abflussgeschehens.

Literatur:

Baltes, B., Suter, D., Küry, D., Von Fumetti, S., Butscher, C. und Nagel, P., 2005. Integrative concepts for a sustainable use of springs. International Sustainability Conference (ISC) 2005, 13.-14. Oktober 2005, Basel.

Brouyère, S., 2003. A quantitative point of view of the concept of vulnerability.- In: Zwahlen, F., 2003 (Hrsg.). Vulnerability and risk mapping for the protection of carbonate (karst) aquifers, COST action 620, Final report. - European Comission, Directorat-General XII Science, Research and Development, Brüssel

BWG, 2005: Bericht über die Hochwasserereignisse 2005. Bundesamt für Wasser und Geologie (BWG), Bern.

Doerfliger, N. und Zwahlen, F., 1998. Kartierung der Vulnerabilität in Karstgebieten – Praxishilfe. Bundesamt für Umwelt, Wald und Landschaft (BUWAL), Bern.

Gibert, J., Mathieu J. & Fournier F. (Hrsg.), 1997. Groundwater - Surface Water Ecotones: Biological and Hydrological Interactions and Management Options, Cambridge University Press, Cambridge

Semmler, T. und Jacob, D., 2004. Modeling extreme precipitation events—a climate change simulation for Europe. Global and Planetary Change 44 (1-4), 119—127. doi:10.1016/j.gloplacha.2004.06.008

Von Fumetti, S., Nagel, P., Scheifhacken, N. und Baltes, B., 2006. Factors governing macrozoobenthic assemblages in perennial springs in north-west Switzerland. Hydrobiologia 568, 467-475, doi 10.1007/s10750-006-0227-8

Vrba, J. und Zoporozec, A. (Hrsg.), 1994. Guidebook on Mapping Groundwater Vulnerability. International Contributions to Hydrogeology (IAH) 16, Hannover.

Curriculum Vitae

Christoph Butscher

Geboren am 02. April 1972 in Tettnang, Deutschland

Ausbildung:

1978 – 1982	Grundschule in Tettnang
1982 – 1991	Gymnasium in Tettnang, Abitur (allgemeine Hochschulreife)
1993 – 1996	Universität Tübingen, Studium Geologie
1996 – 1997	Universität Oslo, Studium Geologie
1997 – 2000	Universität Tübingen, Studium Geologie, Diplomarbeit: Zur Genese eines Amphibolit-Gneis-Komplexes aus dem Präkambrium Südnorwegens (Betreuer: Prof. J. Löschke, Prof. M. Satir)
2003 – 2007	Universität Basel, PhD Studium am Geologisch-Paläontologischen Institut, vorliegende Dissertation (Betreuer: Prof. P. Huggenberger)

Berufliche Tätigkeit:

2000 – 2002	Wissenschaftlicher Angestellter am Landesamt für Geologie, Rohstoffe und Bergbau Baden-Württemberg (LGRB) in Freiburg
seit 2006	Wissenschaftlicher Mitarbeiter des Geologisch-Paläontologischen Instituts der Universität Basel, Abteilung Angewandte und Umweltgeologie („Kantonsgeologie")